

Functional Renormalization Analytically Continued

Janosh Riebesell

December 14, 2017

Master thesis carried out at the [ITP Heidelberg](#). Supervised by

[Stefan Flörchinger](#), [Michael Scherer](#) and [Christof Wetterich](#).

Submitted to Heidelberg University's department of physics and astronomy.

We discuss a method to analytically continue functional renormalization group equations from imaginary Matsubara frequencies to the real frequency axis as developed in [1]. In this formalism, we investigate the analytic structure of the flowing action and the propagator for a theory of scalar fields with $O(N)$ symmetry. We go on to show how it is possible to derive and solve flow equations for real-time properties such as particle decay widths. The treatment is fully Lorentz-invariant and enables an improved, self-consistent derivative expansion in Minkowski space.

Contents

1. Introduction	2	5. Matsubara Summation	32
2. Theoretical Foundations	3	5.1. Propagator Decomposition	32
2.1. Wetterich Equation	4	5.2. Effective Potential	33
2.2. Average Action	8	5.3. Propagator	38
2.3. Regulator	8	6. Momentum Integration	42
2.4. Truncations	10	6.1. Effective Potential	42
2.5. Potential Flow	12	6.2. Propagator	45
3. Functional Renormalization in Minkowski Space	16	7. Numerical Results	46
3.1. Methodology	17	8. Conclusions and Outlook	48
3.2. Matsubara Formalism	18	A. Propagator	49
3.3. Analytic Structure	19	A.1. Analytic Structure	49
4. Analytic Continuation of Flow Equations	20	A.2. Decomposition	50
4.1. Truncation	21	B. Numerical Implementation	53
4.2. Regulator	23	B.1. Auxiliary functions	53
4.3. Feynman Rules	24	B.2. Threshold Functions	54
4.4. Potential Flow	25	B.3. Flow equations	55
4.5. Propagator Flow	26		

1. Introduction

Field-theoretic infinities first arose in Lorentz's work [2] on classical electrodynamics of point particles in the early 20th century. Over the ensuing decades, divergencies proved so persistent and prevalent all across quantum field theory (QFT) that physicists were forced to develop elaborate machinery to extract sensible predictions out of a minefield of singularities. This line of research resulted in the methods of renormalization and regularization. For years the community saw these as objectionable means by which to work around an inability to develop a more well-behaved description of reality. By mid-century, it had reached a point where many physicists thought QFT had to be discarded outright since so many of its predictions aborted in infinities.

Over the course of the 1970s, this view underwent a dramatic shift. In 1971 Wilson published a seminal paper [3] on what is now known as the Wilsonian interpretation of renormalization. According to Wilson, infinities in field theory are merely the result of feeding a fundamentally flawed assumption – the pretense of knowing the fundamental laws of physics down to arbitrarily small distance scales – into the otherwise functioning machinery of QFT. Instead, Wilson argued, we are ignorant of the correct microscopic degrees of freedom and the laws governing their dynamics. Hence we should view our models of reality as no more than effective descriptions of nature that remain approximately valid down to some cutoff scale at which new physics emerges.

The ensuing change of perspective was so far-reaching that nowadays QFT is heralded as the most successful achievement of theoretical physics to date. Renormalization and regularization are generally accepted as essential tools that allow us to predict nature on experimentally accessible scales even though our models breakdown at smaller distances.

And yet despite its profound impact on our understanding of modern physics, the Wilsonian renormalization group largely failed to manifest itself in actual applications. Over the first 20 years, it remained a mostly formal construct until the unceasing strive for a capable and versatile approach to non-perturbative problems in QFT culminated in Wetterich's 1993 functional formulation of renormalization [4]. This has since proven a workable handle for applying Wilson's renormalization group to practical computations and specific models.

These days applications range from cold gases [5–11] and critical phenomena [12–22] to quantum chromodynamics [23–27] and quantum gravity [28–41]. The functional renormalization group (FRG) has proven especially successful in scenarios that are difficult to treat with other methods such as massless degrees of freedom induced by spontaneous symmetry breaking (Higgs mechanism) or the question of asymptotic safety in quantum gravity. It now stands among the most powerful tools to solve non-perturbative problems in modern physics.

However, certain shortcomings remain. So far, the formalism has been explored mostly in Euclidean space where it describes either static, classical statistical field theories or quantum fields in the imaginary-time formalism. Besides avoiding the path-integral's notorious real-time sign problem, Euclidean space offers the important practical advantage that most propagators and higher correlation functions exhibit but a single isolated singularity at vanishing momentum [1].

This state of affairs leaves something to be desired, however. Real-time physics takes place in Minkowski, not Euclidean space. We therefore expect the FRG's spectrum of applications to benefit immensely from an extension to this new domain. After all, real-time correlation functions hold the key to dynamical observables such as the spectral function which contains information about resonances, the mass spectrum and transport coefficients of a theory [42].

Initial attempts at gathering real-time information from the FRG kept the formalism confined to Euclidean space, used its machinery to compute imaginary-time observables at the macroscopic scale $k = 0$ and resorted to numerical techniques such as Padé approximants or the maximum entropy method to perform the analytic continuation to Minkowski space based on limited numerical Euclidean data. Not only does this constitute an ill-defined problem, these approaches also entail a bias about the continuation and require highly accurate Euclidean data. As a result, this approach suffers from a systematic as well as a numerical constraint [42]. The reconstruction problem can only be overcome by a real-time formulation of the theory.

There is no fundamental obstruction that prevents us from extending the FRG to Minkowski space [1]. However, in practice a number of problems arise. Because the Lorentz-invariant four-momentum square $p^2 = -p_0^2 + \mathbf{p}^2$ is no longer positive semi-definite, the question arises which modes actually correspond to the infrared and which to the ultraviolet. This renders the problem of how to construct an appropriate regulator function non-trivial, particularly if Lorentz invariance is to be preserved. Also, the Euclidean space flowing action Γ_k can be shown to approach the microscopic action S for large cutoff scales which serves as a convenient initial condition for the Wetterich equation. This is not necessarily the case in Minkowski space.

In this work, we give a detailed introduction to an approach developed in [1] with which to overcome these difficulties and calculate dynamical properties from real-time functional renormalization. The formalism uses a linear response framework where the analytic continuation from imaginary Matsubara frequencies to real frequencies is carried out on the level of the flow equations rather than on the final result at $k = 0$, since the former are available in analytic form while the latter can only be attained numerically. This procedure is then applied to the scalar $O(N)$ model.

We proceed as follows. Sec. 2 recounts the basics of Wetterich's functional formulation of renormalization. Sec. 3 focuses on its peculiarities in Minkowski space. The analytic continuation of flow equations is carried out in sec. 4. Secs. 5 and 6 respectively present the Matsubara summation and momentum integration performed in terms of conveniently defined threshold functions. Finally, sec. 7 holds numerical results and sec. 8 states our conclusions.

2. Theoretical Foundations

In 1973, Wegner and Houghton [43] were the first to combine Wilson's intuitive understanding of renormalization with the functional methods of quantum field theory. Over the following two decades, this initially rather formal marriage was developed further [44] and rendered viable for practical applications in 1993 by Wetterich's discovery of an exact evolution equation [45] for the so-called flowing action Γ_k . It serves as the central object in FRG to determine the properties of a theory, including its excitation spectrum, symmetries, dynamics and conserved quantities. Wetterich's surprisingly intuitive functional differential equation for Γ_k demonstrated that the scale dependence of the flowing action is generated solely by one-loop fluctuations of the regularized propagator.

Γ_k is constructed from the microscopic action S by adding to it an infrared regulator R_k with associated renormalization scale k . This is where scale dependence enters the formalism. The modification bestows upon Γ_k the remarkable property of continuously interpolating between the microscopic action $S = \lim_{k \rightarrow \Lambda} \Gamma_k$ at high energies (Λ is some ultraviolet cutoff that regularizes the theory) and the quantum effective action $\Gamma = \lim_{k \rightarrow 0} \Gamma_k$ at macroscopic scales – a process known as transition to complexity. True to the spirit of Wilson's original formulation of renormalization, R_k implements during this procedure a smooth decoupling of high-momentum modes while also acting as an infrared regulator in theories with massless particles – a major advantage when dealing with spontaneous symmetry breaking in the $O(N)$ model.

This section briefly introduces the most important aspects of Euclidean space functional renormalization. Setting out from the Feynman path integral, sec. 2.1 derives Wetterich's equation for a system of scalar fields ϕ_a , $a \in \{1, \dots, N\}$. Secs. 2.2 and 2.3 list important properties of the flowing action Γ_k and the regulator R_k . Sec. 2.4 presents different truncation schemes that make practical applications of this formalism possible. Finally, in sec. 2.5 we construct an exact flow equation for the effective potential U_k – the most important quantity when it comes to equilibrium physics such as the ground state and the low-lying mass spectrum.

2.1. Wetterich Equation

We discuss the derivation of Wetterich's functional renormalization group equation following [12, 45]. The partition function for a theory of N scalar fields $\phi_a(x)$, $a \in \{1, \dots, N\}$ in d Euclidean dimensions with microscopic action $S[\phi]$ in the presence of the source $J_a(x)$ reads

$$Z[J] = \int \mathcal{D}\phi e^{-S[\phi] + J \cdot \phi}, \quad (1)$$

We specify the action together with some ultraviolet reference scale Λ much larger than all other physical scales [46]. (Λ will be the scale at which we initialize our flow equations.) The scalar product sums over field components and integrates over all space

$$J \cdot \phi = \int_x J_a(x) \phi_a(x) = \int_p \tilde{J}_a(p) \tilde{\phi}_a(-p), \quad (2)$$

where

$$\int_x = \int_{\mathbb{R}^d} d^d x, \quad \int_p = \int_{\mathbb{R}^d} \frac{d^d p}{(2\pi)^d}, \quad (3)$$

and $\tilde{\phi}_a(-p) = \tilde{\phi}_a^*(p)$ for real scalar fields. To save on notation, we won't continue to indicate spacetime dependence nor Fourier transforms $\tilde{\phi}$ explicitly and take ϕ and J index-free as vectors in N -dimensional field space.

Expectation values and correlation functions are obtained from $Z[J]$ through functional differentiation,

$$\varphi = \langle \phi \rangle = \frac{1}{Z} \frac{\delta Z}{\delta J} = \frac{1}{Z} \int \mathcal{D}\phi \phi e^{-S[\phi] + J \cdot \phi}, \quad (4)$$

$$\langle \phi^n \rangle = \frac{1}{Z} \frac{\delta^n Z}{\delta^n J} = \frac{1}{Z} \int \mathcal{D}\phi \phi^n e^{-S[\phi] + J \cdot \phi}, \quad (5)$$

earning $Z[J]$ the name generating functional. A more efficient description is possible in terms of only the connected correlation functions. These in turn are generated by the Schwinger functional

$$W[J] = \ln Z[J]. \quad (6)$$

For instance, the connected two point correlator - a.k.a. the propagator - is given by

$$\begin{aligned} G &= \frac{\delta^2 W[J]}{\delta^2 J} = \frac{\delta}{\delta J} \left(\frac{1}{Z} \frac{\delta Z}{\delta J} \right) \\ &= \frac{1}{Z} \frac{\delta^2 Z}{\delta^2 J} - \frac{1}{Z^2} \frac{\delta Z}{\delta J} \frac{\delta Z}{\delta J} \\ &= \langle \phi \phi \rangle - \varphi \varphi \equiv \langle \phi \phi \rangle_c. \end{aligned} \quad (7)$$

$G_{ab}(x, y)$ is an $N \times N$ matrix correlating the field ϕ_a at spacetime point x with ϕ_b at y .

We now modify the Schwinger functional by introducing a renormalization scale-dependent cutoff term ΔS_k that vanishes in the infrared,

$$W_k[J] = \ln Z_k[J] = \ln \int \mathcal{D}\phi e^{-S[\phi] + J \cdot \phi - \Delta S_k[\phi]}, \quad (8)$$

where the renormalization scale k has units of inverse length and can be intuitively understood to specify at which scale we probe a theory. Small k correspond to large distances, large k to small distances. $\Delta S_k[\phi]$ is a quadratic functional of the field ϕ

$$\Delta S_k[\phi] = \frac{1}{2} \phi \cdot R_k \cdot \phi = \frac{1}{2} \int_{x,y} \phi_a(x) R_{k,ab}(x, y) \phi_b(y). \quad (9)$$

with R_k acting as a momentum-dependent mass. We will see that R_k serves both as an infrared *and* ultraviolet regulator in our description. For an $O(N)$ -symmetric scalar theory, it is diagonal both in momentum space and with respect to field indices,

$$R_{k,ab}(x, y) = \delta_{ab} \delta(x - y) R_k(-\partial_x^2). \quad (10)$$

Since the scale dependence of $W_k[J]$ stems solely from ΔS_k , it's k -derivative (at fixed source J) is

$$\begin{aligned} \partial_k W_k[J]|_J &\stackrel{(8)}{=} -\frac{1}{Z_k} \int \mathcal{D}\phi (\partial_k \Delta S_k[\phi]) e^{-S[\phi] + J \cdot \phi - \Delta S_k[\phi]} \\ &= -\frac{1}{2} \langle \phi \cdot \partial_k R_k \cdot \phi \rangle \stackrel{(7)}{=} -\frac{1}{2} (\langle \phi \cdot \phi \rangle_c + \varphi \cdot \varphi) \cdot \partial_k R_k. \end{aligned} \quad (11)$$

For the connected part $\langle \phi \cdot \phi \rangle_c$ we can insert the functional derivative (7),

$$\langle \phi \cdot \phi \rangle_c \equiv W_k^{(2)} = \frac{\delta^2 W_k}{\delta^2 J} = \frac{\delta \varphi}{\delta J} \quad (12)$$

to rewrite (11) as Polchinski's equation [44],

$$\partial_k W_k[J]|_J = -\frac{1}{2} \text{Tr}[W_k^{(2)} \partial_k R_k] - \frac{1}{2} \varphi \cdot (\partial_k R_k) \cdot \varphi, \quad (13)$$

where Tr integrates over position (or momentum¹) space and sums over the field indices a, b ,

$$\text{Tr}[(\partial_k R_k) W_k^{(2)}] = \int_{x,y} W_{k,ab}^{(2)}(x, y) \partial_k R_{k,ab}(x, y). \quad (14)$$

We can construct the flowing action $\Gamma_k[\varphi]$ from the modified Schwinger functional by subtracting from its Legendre transform

$$\tilde{\Gamma}_k[\varphi] = \sup_J (J \cdot \varphi - W_k[J]) \quad \text{where } \varphi = \frac{\delta W_k}{\delta J}, \quad (15)$$

the same cutoff term we added to W_k ,

$$\Gamma_k[\varphi] = \tilde{\Gamma}_k[\varphi] - \Delta S_k[\varphi]. \quad (16)$$

$\Gamma_k[\varphi]$ is also known as the average action [46] because it provides an effective description of physics at distance scales $\gtrsim k^{-1}$ for fields $\varphi_a = \langle \phi_a \rangle$ averaged over a volume k^{-d} . Moreover, it enables a formulation of quantum theory even more economic than the Schwinger functional. In perturbation theory, it acts as the generating functional for only the one-particle irreducible correlation functions, while still encoding all properties of the underlying quantum fields.

Upon functional differentiation with respect to the average field φ_a , the Legendre transform $\tilde{\Gamma}_k$ yields the (scale-dependent) field equation

$$\frac{\delta}{\delta \varphi} \tilde{\Gamma}_k = J_k. \quad (17)$$

Comparing with (12), we identify

$$\tilde{\Gamma}_k^{(2)} = \frac{\delta^2 \tilde{\Gamma}_k}{\delta^2 \varphi} = \frac{\delta J_k}{\delta \varphi} \quad (18)$$

as the inverse propagator,

$$\left(\tilde{\Gamma}_k^{(2)} \cdot W_k^{(2)} \right)_{ab}(x, y) = \int_z \frac{\delta J_c(z)}{\delta \varphi_a(x)} \frac{\delta \varphi_b(y)}{\delta J_c(z)} = \frac{\delta \varphi_b(y)}{\delta \varphi_a(x)} = \delta_{ab} \delta(x - y). \quad (19)$$

¹In momentum space $\text{Tr} = \sum_a \int d^d p / (2\pi)^d$, as appropriate for the unit matrix $\mathbf{1} = (2\pi)^d \delta_{ab} \delta(p - q)$.

Thus

$$W_k^{(2)} = (\tilde{\Gamma}_k^{(2)})^{-1} = (\Gamma_k^{(2)} + R_k)^{-1}. \quad (20)$$

The k -derivative of $\tilde{\Gamma}_k$ (at fixed average field) reads

$$\partial_k \tilde{\Gamma}_k|_\varphi \stackrel{(15)}{=} \left(\varphi - \frac{\delta W_k}{\delta J} \right) \partial_k J - \partial_k W_k|_J = -\partial_k W_k|_J. \quad (21)$$

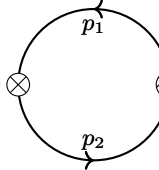
At fixed φ , J becomes scale-dependent, accounting for the second term in (21). The third is due to the scale dependence of R_k in W_k while J is held fixed. Inserting (21) into the k -derivative of (16) gives

$$\partial_k \Gamma_k[\varphi] = -\partial_k W_k|_J - \frac{1}{2} \varphi \cdot (\partial_k R_k) \cdot \varphi. \quad (22)$$

Using (13) and (20), we arrive at Wetterich's equation

$$\partial_k \Gamma_k[\varphi] \stackrel{(13)}{=} \frac{1}{2} \text{Tr} [W_k^{(2)} \partial_k R_k] \stackrel{(20)}{=} \frac{1}{2} \text{Tr} [(\Gamma_k^{(2)} + R_k)^{-1} \partial_k R_k]. \quad (23)$$

(23) is a non-linear functional integro-differential equation of one-loop structure that determines the scale-dependence of the flowing action Γ_k in terms of fluctuations of the fully-dressed regularized propagator $[\Gamma_k^{(2)} + R_k]^{-1}$. (23) admits a simple diagrammatic representation as a one-loop equation,

$$\partial_k \Gamma_k = \frac{1}{2} \sum_{i,j=1}^N \int_{p_1, p_2} \partial_k R_{k,ij}(p_1, p_2) \otimes \text{loop} \left[[\Gamma_k^{(2)} + R_k]_{ji}^{-1}(p_2, p_1) \right], \quad (24)$$


(Since $\partial_k R_{k,ab}(p, q) = \partial_k R_k(p) (2\pi)^d \delta_{ab} \delta(p - q)$, the trace in (23) effectively sums over just one index i and integrates over one loop momentum p , as stated in footnote 1.) This one-loop structure is important when it comes to practical calculations: only one integral has to be computed. In a rotationally invariant setting, it is even one-dimensional. Compared to perturbation theory where we have to sum a potentially non-convergent series of diagrams in which each n -loop diagram requires us to compute n integrals, this amounts to a considerable reduction in complexity [47].

It is worth taking a moment to appreciate the significance of (23). Had we simply applied perturbation theory to the microscopic action S , we would have obtained a structurally very similar equation. Indeed, up to one loop, the perturbative expansion of Γ_k reads

$$\Gamma_k[\varphi]|_{1\text{-loop}} = S[\varphi] + \frac{1}{2} \text{Tr} \ln(S^{(2)}[\varphi] + R_k), \quad (25)$$

which upon differentiation with respect to k yields

$$\partial_k \Gamma_k[\varphi]|_{1\text{-loop}} = \frac{1}{2} \text{Tr} [(S^{(2)}[\varphi] + R_k)^{-1} \partial_k R_k]. \quad (26)$$

Despite looking almost identical to (23), replacing $S^{(2)}[\varphi]$ with the fully dressed 2-point function $\Gamma_k^{(2)}$ turns the perturbative one-loop expression (26) into an exact identity that incorporates effects of arbitrarily high loop order as well as genuinely non-perturbative effects [12]! Further noteworthy features of (23) include [12, 13].

1. Exact flow equations for arbitrarily high n -point functions follow from (23) by functional differentiation. For instance, the 2-point function is given by

$$\begin{aligned} \partial_k \Gamma_k^{(2)} &= \partial_k \frac{\delta^2 \Gamma_k}{\delta^2 \phi} = -\frac{1}{2} \text{Tr} \left[\partial_k R_k \frac{\delta}{\delta \phi} \left([\Gamma_k^{(2)} + R_k]^{-1} \Gamma_k^{(3)} [\Gamma_k^{(2)} + R_k]^{-1} \right) \right] \\ &= \frac{1}{2} \text{Tr} \left[\partial_k R_k [\Gamma_k^{(2)} + R_k]^{-1} \Gamma_k^{(3)} [\Gamma_k^{(2)} + R_k]^{-1} \Gamma_k^{(3)} [\Gamma_k^{(2)} + R_k]^{-1} \right. \\ &\quad \left. + [\Gamma_k^{(2)} + R_k]^{-1} \Gamma_k^{(3)} \partial_k R_k [\Gamma_k^{(2)} + R_k]^{-1} \Gamma_k^{(3)} [\Gamma_k^{(2)} + R_k]^{-1} \right. \\ &\quad \left. - \partial_k R_k [\Gamma_k^{(2)} + R_k]^{-1} \Gamma_k^{(4)} [\Gamma_k^{(2)} + R_k]^{-1} \right]. \end{aligned} \quad (27)$$

Represented diagrammatically (27) reads

$$\partial_k \Gamma_k^{(2)} = \frac{1}{2} \text{Tr} \left(\begin{array}{c} \text{Diagram 1} \\ + \text{Diagram 2} \\ - \text{Diagram 3} \end{array} \right). \quad (28)$$

This alludes to a general property of flow equations for n -point functions: they form a hierarchy; the flow of $\Gamma_k^{(n)}$ depends on $\Gamma_k^{(n+1)}$ and $\Gamma_k^{(n+2)}$.

2. To obtain a scaling form of the evolution equation, we may replace ∂_k on both sides of (23) by a partial derivative with respect to the logarithmic scale $t = \ln(k/\Lambda)$ (also referred to as RG time),

$$\partial_t = \frac{\partial}{\partial \ln(k/\Lambda)} = \frac{k}{\Lambda} \frac{\partial}{\partial (k/\Lambda)} = k \partial_k. \quad (29)$$

3. The presence of the cutoff function R_k renders the momentum integration in Tr both infrared and ultraviolet finite. In particular, for $p^2 \ll k^2$ R_k serves as an additional mass-like term $R_k \sim k^2$ that prevents the propagator $[\Gamma_k^{(2)} + R_k]^{-1}$ from becoming singular at $p = 0$. This makes the formalism suitable for dealing with theories plagued by infrared divergencies when treated perturbatively. These include scalar theories in $d < 4$ or at non-zero temperature near a second order phase transition as well as non-abelian gauge theories [46]. For instance, (23) can be applied to systems with spontaneously broken $O(N)$ symmetry despite the appearance of massless Goldstone bosons if $N > 1$. Their standard loop expansion is highly infrared divergent, making these massless excitations notoriously difficult to treat with other methods [48].
4. Since $\partial_k R_k(p)$ appears in the numerator of (23), its fast decay for $p^2 \gg k^2$ results in UV finiteness of the momentum integration that is part of the trace Tr . Together with the IR regulating properties of $R_k(p)$ in the denominator, this means that only momenta $p^2 \lesssim k^2$ of the order of or smaller than the renormalization scale contribute substantially to the flow at scale k . The divergent loop diagrams of perturbation theory are thus avoided.

An important consequence is the decoupling of massive modes M at low energies. Once $k^2 \ll M^2$, fluctuations of massive modes are strongly suppressed by $\partial_k R_k(p) \approx 0$. They were integrated out during earlier stages of the flow where $M \approx k < \Lambda$, resulting in renormalized couplings for the low-energy theory. If k is lowered further, there will be essentially no change in Γ_k due to fluctuations of these modes [1]. In this way, the flow equations automatically lead to the emergence of effective theories for the low-energy degrees of freedom [12, 13]!

Unfortunately, this also means that given a low-energy theory, we cannot know whether the underlying fundamental theory (at scales larger than M) involves massive excitations or not. Below the scale M there would remain no signal of such a mode.

5. The crucial requirement for practical application of (23) to non-perturbative systems is the availability of sufficiently simple and yet physically relevant truncation schemes. Determining which terms in an expansion of Γ_k can safely be discarded and which operators must be kept in order to capture important behavior requires sophisticated physical insight into a model.²

In this context the close resemblance of (23) to a perturbative expression turns out to be of great use. We can benefit from the fact that for many situations of interest the propagator $(\Gamma_k^{(2)})^{-1}$ is approximately known, allowing us to devise a simple form for $\Gamma_k^{(2)}$ that depends on only a handful of scale-dependent parameters (typically masses, couplings, decay widths and wave function renormalizations) while still describing the relevant physics. (The success of the entire method ultimately depends on a clever guess for the exact propagator, which in turn

²Of course, if we make use of prior knowledge obtained with other methods during this process our formalism loses its claim to being a first-principles-only approach – at least in practical applications.

can depend on the proper choice of degrees of freedom [46].) We can then project the flow (23) of Γ_k onto these parameters and obtain a closed and finite set of ordinary coupled non-linear differential equations that is much easier to solve than the flow of Γ_k itself.

- (23) is equivalent to Wilson's exact RG equation [3] which describes how the Wilsonian effective action S_Λ^W changes with an ultraviolet cutoff Λ . As we saw in its derivation, Polchinski's continuum version of Wilson's equation is even related to (23) by a simple Legendre transform, a suitable field redefinition and the association $\Lambda = k$. Although the formal relation is simple, the practical calculation of S_k^W from Γ_k (and vice versa) can be quite involved.

2.2. Average Action

The average action Γ_k has a number of properties worth mentioning [12, 13].

- In perturbation theory, $\Gamma = \lim_{k \rightarrow 0} \Gamma_k$ acts as the generating functional of one-particle irreducible correlation functions. Once Γ is known, a theory is basically "solved". Since it is the result of integrating out fluctuations on *all* momentum scales $0 < k < \Lambda$, it contains effective couplings; physical masses, charges and wave function renormalizations can simply be read off. It also means the effective action is exact at tree level! Instead of having to manage an infinite (often times divergent) series of Feynman diagrams to calculate some physical observable (such as a scattering cross section) it suffices to evaluate tree-level Feynman diagrams [1].
- If the microscopic action S is invariant under some group G and we construct Γ_k using an IR cutoff that respects this symmetry, Γ_k inherits G -invariance from S for all k (assuming the absence of quantum anomalies). In particular, it relays this symmetry to the effective action Γ at $k = 0$. For example, this is true for translation and rotation invariance if R_k depends only on the distance $(x - y)$ in position space or p^2 in momentum space.
- The most general form of Γ_k is given by an infinite series of *all* field combinations compatible with the given symmetries. Since each term comes with its own scale-dependent coupling (see sec. 2.4), Γ_k in theory contains infinitely many running couplings, making a well-chosen truncation procedure essential.
- Physical quantities should be independent of the choice of cutoff R_k . Scheme independence of final results is a good check for approximations. However, Γ_Λ 's position in and Γ_k 's flow through theory space *are* scheme-dependent.
- Despite their similarities, there is a conceptual difference to the Wilsonian effective action [3]. S_Λ^W describes a set of different actions (parameterized by Λ) for a single model. In contrast, Γ_k acts as effective action for a set of models; for any scale k , Γ_k is related to the generating functional of 1PI n -point functions for a model with a different action $S_k = S + \Delta S_k$. The Wilsonian effective action does not generate the 1PI Green functions.

This completes the picture we have of the flowing action: in its transition to complexity, Γ_k continuously interpolates from the microscopic action at small scales to the effective action at the macroscopic level. It moves through an infinite-dimensional theory space, its path determined by the initial condition S and the choice of regulator R_k . Theory space is spanned by the set of all symmetry-compatible operators, e.g. ϕ^2 , ϕ^4 , $(\partial\phi)^2$, etc. in the case of $O(N)$ -invariant scalar fields ϕ_a . (In fig. 1 the operators are represented by their couplings $\{\lambda_i\}_{i \in \mathbb{N}}$.) Of course, for a practical treatment to remain manageable requires the truncation of Γ_k to but a handful of operators.

2.3. Regulator

Despite being just a mathematical tool without physical meaning, R_k is a central object in this formulation of quantum field theory. To bestow upon Γ_k the property of interpolating between S

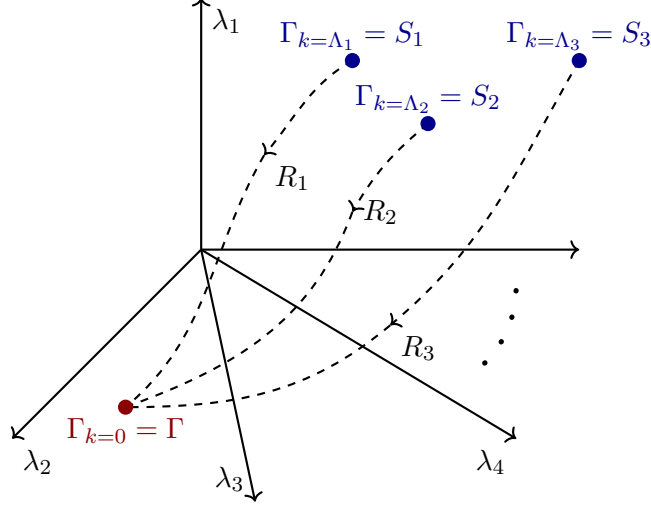


Figure 1: Flow of Γ_k through infinite-dimensional theory space for different regulators R_i . The bare actions S_i obey the same symmetries and thus flow to the same quantum effective action Γ .

at $k = \Lambda$ and Γ at $k = 0$, it must satisfy

$$R_k(p) \rightarrow \begin{cases} k^2 & \text{for } p \rightarrow 0, \\ 0 & \text{for } p \rightarrow \infty, \\ 0 & \text{for } k \rightarrow 0, \\ \infty & \text{for } k \rightarrow \Lambda, \end{cases} \quad (30)$$

where p denotes the internal loop momentum on the r.h.s. of the flow equation.

- $R_k(p) \rightarrow k^2 > 0$ for $p \rightarrow 0$ prevents the propagator $[\Gamma_k^{(2)} + R_k]^{-1}$ from becoming singular at $p = 0$ and thus regularizes the theory in the infrared.
- $R_k(p) \rightarrow 0$ for $p \rightarrow \infty$ ensures a fast decay of $\partial_k R_k$ at high loop-momenta, thus rendering the one-loop flow equation ultraviolet finite.
- $R_k(p) \xrightarrow{k \rightarrow 0} 0$ ensures that the flowing action Γ_k approaches the effective action Γ at macroscopic scales,

$$\lim_{k \rightarrow 0} \Gamma_k[\varphi] \stackrel{(16)}{=} \lim_{k \rightarrow 0} \left(\tilde{\Gamma}_k[\varphi] - \frac{1}{2} \varphi \cdot R_k \cdot \varphi \right) \stackrel{(15)}{=} \sup_J (J \cdot \varphi - W[J]) = \Gamma[\varphi]. \quad (31)$$

- $R_k(p) \xrightarrow{k \rightarrow \Lambda} \infty$ ensures that Γ_k flows towards the microscopic action S for $k \rightarrow \Lambda$. (This is where the necessity to work with a modified Legendre transform becomes apparent.) We resort again to the functional integral formalism,

$$\begin{aligned} e^{-\Gamma_k[\varphi]} &= \exp\left(-\sup_J (J \cdot \varphi - W_k[J]) + \frac{1}{2} \varphi \cdot R_k \cdot \varphi\right) \\ &\stackrel{(8)}{=} \int \mathcal{D}\phi \exp\left(-S[\phi] + J \cdot \phi - \frac{1}{2} \phi \cdot R_k \cdot \phi - J \cdot \varphi + \frac{1}{2} \varphi \cdot R_k \cdot \varphi\right) \\ &= \int \mathcal{D}\phi \exp\left(-S[\varphi + \phi] - \frac{1}{2} \phi \cdot R_k \cdot \phi + \frac{\delta\Gamma_k}{\delta\varphi} \cdot \phi\right), \end{aligned} \quad (32)$$

where in the last step we shifted the field $\phi \rightarrow \varphi + \phi$, used that $R_{k,ab} \propto \delta_{ab}$ is symmetric so that $\varphi \cdot R_k \cdot \phi = \phi \cdot R_k \cdot \varphi$, and inserted

$$\frac{\delta\Gamma_k}{\delta\varphi} \cdot \phi \stackrel{(16)}{=} J \cdot \phi - \varphi \cdot R_k \cdot \phi. \quad (33)$$

In the microscopic limit $\lim_{k \rightarrow \Lambda} R_k$ diverges and the factor $e^{-\frac{1}{2}\phi \cdot R_k \cdot \phi}$ approaches the limit representation of the functional delta distribution³ [12],

$$\delta[\phi] \sim \lim_{k \rightarrow \Lambda} e^{-\frac{1}{2}\phi \cdot R_k \cdot \phi}, \quad (34)$$

allowing us to evaluate the path integral in (32),

$$\lim_{k \rightarrow \Lambda} e^{-\Gamma_k[\varphi]} = \int \mathcal{D}\phi \delta[\phi] e^{-S[\varphi+\phi] + \frac{\delta\Gamma_k}{\delta\varphi} \cdot \phi} = e^{-S[\varphi]}. \quad (35)$$

Thus

$$\lim_{k \rightarrow \Lambda} \Gamma_k[\varphi] = S[\varphi]. \quad (36)$$

(36) is a useful result since it serves as an initial condition for the flow equation (23). However, the property $\Gamma_\Lambda = S$ is not essential since we may as well use Γ_Λ to parametrize the short distance behavior [12]. When taking Γ_k from Λ to larger distances, universality ensures that (up to a few relevant renormalized couplings) the precise form of Γ_Λ is irrelevant in any case. Using Γ_Λ instead of S can even become necessary in cases where no physical cutoff is present or where a UV cutoff would be in conflict with symmetries as in the case of gauge theories.

2.4. Truncations

Solving a functional differential equation like the Wetterich equation (23) exactly is all but impossible. Fortunately, we can descend from the functional formulation into an infinite system of coupled ordinary differential equations by projecting (23) to the infinite number of couplings $\{\lambda_i | i \in \mathbb{N}\}$ appearing in the most general form of Γ_k [12, 13, 46]. Of course, an exact solution of this infinite system is still impossible [46]. To make an explicit treatment feasible, we have to heavily restrict the space of action functionals to a finite number of dimensions, meaning we can allow only a handful of relevant couplings in Γ_k .

This is where (sometimes hard to control) approximations have to be made. Assuming $\Gamma_k[\varphi]$ is invariant under global $O(N)$ transformations, we have several expansion schemes at our disposal.

Derivative expansion The most common way to arrive at a sufficiently simple form of $\Gamma_k[\varphi]$ is to write it as a sum of a few low-order $O(N)$ invariants with order determined by the number of field derivatives $\partial^\mu \varphi_a$. The simplest $O(N)$ -invariant $\rho = \frac{1}{2}\phi_a \phi_a$ contains no derivatives and appears at order zero in this classification. By allowing $U_k(\rho)$ to be an arbitrary polynomial of ρ , the effective potential covers this order completely.

Of course, $\Gamma_k[\varphi]$ is also constrained by spacetime symmetries. In particular, in a relativistic setting it has to be Lorentz invariant. But ∂_μ is a Lorentz vector and so for Γ_k to include Lorentz invariant dynamics, ∂_μ needs to be contracted. Unlike gauge fields A^μ , scalar fields don't carry spacetime indices. Neither do they furnish spinor representations of Clifford algebras with spacetime-indexed generators γ^μ , like fermions do. Therefore, the only way to include a derivative in $\Gamma_k[\varphi]$ in a Lorentz-invariant fashion is by contracting it with another ∂_μ . Thus, first-order $O(N)$ -invariant of scalar fields must already contain two spacetime derivatives. There are two $O(N)$ -invariants we can construct in this way,⁴

$$\partial_\mu \varphi_a \partial^\mu \varphi_a \quad \text{and} \quad \partial_\mu \rho \partial^\mu \rho. \quad (37)$$

By the product rule, acting with derivatives on powers of the fields higher than φ_a and ρ just gives sums of these two building blocks. We will, however, include wave function renormalizations $Z_k(\rho)$ and $Y_k(\rho)$ as prefactors to (37) and these may contain arbitrary order-zero invariants.

³The usual normalization includes a prefactor $\delta[\phi] = \lim_{k \rightarrow \Lambda} \sqrt{R_k/(2\pi)} e^{-\frac{1}{2}\phi \cdot R_k \cdot \phi}$ which we swept under the rug since it results only in a (divergent) additive constant $-\frac{1}{2} \ln[R_\Lambda/(2\pi)]$ to S that doesn't affect the dynamics.

⁴By partial integration under the action with vanishing boundary terms, (37) is equivalent to $\varphi_a \partial^2 \varphi_a$ and $\rho \partial^2 \rho$.

Since we mean to truncate our expansion early, we'll stop here. Putting everything together, we get a flowing action of the form [12]

$$\Gamma_k[\varphi] = \int_x \left[U_k(\rho) + \frac{1}{2} Z_k \partial_\mu \varphi_a \partial^\mu \varphi_a + \frac{1}{4} Y_k \partial_\mu \rho \partial^\mu \rho + \mathcal{O}(\partial^4) \right]. \quad (38)$$

with $Z_\Lambda = Y_\Lambda = 1$. (38) is known as the *derivative expansion*. We can slightly enhance (38) by generalizing Z_k and Y_k to functions of momentum [1, 13],

$$\Gamma_k[\varphi] = \int_x \left[U_k(\rho) + \frac{1}{2} \partial_\mu \varphi_a Z_k(-\partial^2) \partial^\mu \varphi_a + \frac{1}{4} \partial_\mu \rho Y_k(-\partial^2) \partial^\mu \rho + \mathcal{O}(\partial^4) \right], \quad (39)$$

(39) has the advantage that it allows to resolve the propagator's *full* momentum dependence. The effective potential $U_k(\rho)$ can further be expanded into a Taylor series around the location of its minimum,

$$U_k(\rho) = \frac{\lambda}{2} [\rho - \rho_0(k)]^2 + \frac{\mu}{6} [\rho - \rho_0(k)]^3 + \dots \quad (40)$$

$\lambda(k) = \partial_\rho^2 U_k(\rho_0)$ and $\mu(k) = \partial_\rho^3 U_k(\rho_0)$ are scale-dependent couplings that each span a dimension of theory space. The lowest order in the derivative expansion, known as the local potential approximation, is obtained by setting $Z_k = 1$, $Y_k = 0$ so that Γ_k only includes the effective potential and a standard kinetic term,

$$\Gamma_k[\varphi] = \int_x \left[U_k(\rho) + \frac{1}{2} \partial_\mu \varphi_a \partial^\mu \varphi_a \right]. \quad (41)$$

So far the derivative expansion has proven most successful in practical applications of the flow equation (23). The reason it works so well at capturing relevant physics while still reducing Γ_k to but a handful of scale-dependent parameters is quite intuitive. Transformed into Fourier space, (39) becomes an expansion in powers of loop-momenta p around the scale k which converges rapidly thanks to the separation of momentum scales in the flow equation provided by the fast decay of $\partial_k R_k$ for large $p^2 \gg k^2$ (see item 4 on page 7). Only momenta $p^2 \leq k^2$ contribute substantially to the flow and these are captured well by low powers of p .

This is why in practice we usually neglect terms higher than quadratic in the momenta. In particular, we tend to work with momentum-independent Z_k, Y_k as in (38) since the main effect of this extra momentum-dependence is to provide an infrared cutoff scale of order p^2 which is already provided by $R_k(p)$.

Vertex expansion We can also expand Γ_k in terms of n -point functions around some constant field φ_c [12, 13]. This approach known as *vertex expansion* yields

$$\Gamma_k[\varphi] = \sum_{n=0}^{\infty} \frac{1}{n!} \left(\prod_{j=0}^n \int_{x_j} [\varphi(x_j) - \varphi_c] \right) \Gamma_k^{(n)}(x_1, \dots, x_n). \quad (42)$$

As mentioned in item 1 on page 6, flow equations for $\Gamma_k^{(n)}$ follow from functional differentiation of (23). (42) makes particularly clear why.

Canonical dimension expansion A third option very similar to the derivative expansion is to expand in terms of $O(N)$ -invariants around some constant background field ρ_c and classify terms not by the number of derivatives but based on their *canonical dimension*,

$$\begin{aligned} \Gamma_k[\varphi] = \int_x \left\{ & U_k(\rho_c) + U'_k(\rho_c)(\rho - \rho_c) + \frac{1}{2} U''_k(\rho_c)(\rho - \rho_c)^2 + \dots \right. \\ & - \frac{1}{2} \left(Z_k(\rho_c) + Z'_k(\rho_c)(\rho - \rho_c) + \frac{1}{2} Z''_k(\rho_c)(\rho - \rho_c)^2 + \dots \right) \partial_\mu \varphi_a \partial^\mu \varphi_a \\ & + \frac{1}{2} \left(\dot{Z}_k(\rho_c) + \dot{Z}'_k(\rho_c)(\rho - \rho_c) + \dots \right) \varphi_a (\partial_\mu \partial^\mu)^2 \varphi_a \\ & \left. - \frac{1}{4} Y_k(\rho_c) \rho \partial_\mu \partial^\mu \rho \right\}. \end{aligned} \quad (43)$$

Here, primes denote derivatives with respect to ρ and dots with respect to the scale $t = \ln(k/\Lambda)$. The constant field ρ_c is usually chosen as the minimum of effective potential $\rho_0(k)$. If $\rho_0(k) > 0$ the ground state is not $O(N)$ -invariant as can be seen from fig. 2, signaling a theory with spontaneous symmetry breaking. Since $U'_k(\rho_0) = 0$ $\rho_0(k)$ then replaces the coupling $U'_k(\rho_0)$ [12]. In the absence of external sources the value of $\rho_0(k \rightarrow 0)$ determines the order parameter $\varphi_0 = \sqrt{2\rho_0}$.

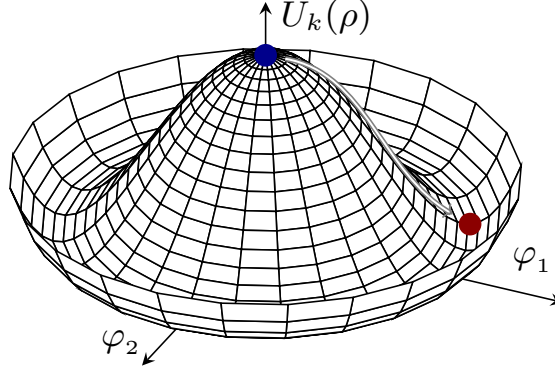


Figure 2: Shape of the effective potential $U_k(\rho)$ in the presence of spontaneous symmetry breaking. Even if a system starts out in the naive $O(N)$ -invariant vacuum (blue dot), quantum fluctuations will quickly push it into the real vacuum (red dot) where $O(N)$ is broken down to $O(N - 1)$.

In all three of the above expansion schemes, the basic strategy is to solve the Wetterich equation in a restricted functional space, not as a series expansion in some small parameter. This is why the formalism can be applied to non-perturbative systems [47].

2.5. Potential Flow

We consider a set of $O(N)$ -invariant scalar fields $\phi_a(x)$ with average action (39). When it comes to the ground state, its preserved or spontaneously broken symmetries and the mass spectrum of excitations, the most important quantity is the effective potential $U_k(\rho)$ [12]. Its scale dependence is two-fold:

- one contribution stems from the scale dependence of the fields $\rho = \frac{1}{2}\varphi_a\varphi_a$, which we renormalize according to

$$\varphi_r = \sqrt{Z_k} \varphi, \quad \rho_r = Z_k \rho, \quad (44)$$

- the other from the scale dependence of $U_k(\rho)$ itself (via the couplings $\lambda_{k,i}$).

The total scale derivative of U_k therefore receives contributions from two terms,

$$\frac{dU_k}{dt} = \frac{\partial U_k}{\partial \rho} \frac{\partial \rho}{\partial t} \Big|_{\rho_r} + \partial_t U_k \Big|_{\rho} = \eta \rho U'_k + \partial_t U_k \Big|_{\rho}, \quad (45)$$

where $\Big|_{\rho_r}$ indicates that ρ_r is held fixed such that $\partial \rho / \partial t \Big|_{\rho_r} = -Z_k^{-2} \rho_r \partial_t Z_k = \eta \rho$. $\eta = -Z_k^{-1} \partial_t Z_k$ denotes the anomalous dimension of the propagator $(\Gamma_k^{(2)})^{-1}$ and $\partial_t U_k \Big|_{\rho}$ contains the effective potential's inherent scale dependence (via the couplings λ_i) at fixed ρ . Wetterich's equation (23) allows us to derive a flow equation for this contribution.

To that end, we relate $U_k(\rho)$ to $\Gamma_k[\varphi]$ by evaluating the latter for a constant background field $\varphi(x) = \varphi_c \forall x$. (φ_c may be any constant field. It is not necessarily related to the minimum of the effective potential $\varphi_0 = \sqrt{2\rho_0}$. However, in actual calculations, we will often choose $\varphi_c = \varphi_0$.) The derivative terms in Γ_k all drop out, leaving us with

$$\Gamma_k \Big|_{\varphi_c} = \int_x U_k(\rho_c) = V_d U_k(\rho_c). \quad (46)$$

with $\rho_c = \frac{1}{2} \varphi_c^2$. Acting on (46) with a scale derivative yields

$$\partial_t U_k|_{\rho_c} = V_d^{-1} \partial_t \Gamma_k|_{\varphi_c} \stackrel{(23)}{=} \frac{1}{2V_d} \text{Tr} \left[\frac{\partial_t R_k}{\Gamma_k^{(2)}|_{\varphi_c} + R_k} \right]. \quad (47)$$

To obtain $\Gamma_k^{(2)}|_{\varphi_c}$ in momentum space, we first expand Γ_k in small fluctuations $\chi_a(x)$ around φ_c . Using $O(N)$ symmetry, we can rotate the fields to have φ_c point in, say, φ_1 -direction,

$$\varphi_a(x) = \varphi_c \delta_{a1} + \chi_a(x) \quad \text{with } \chi_a(x) \ll \varphi_c \quad \forall a, x. \quad (48)$$

Then $\rho = \frac{1}{2} \varphi_c^2 + \varphi_c \chi_1 + \frac{1}{2} \chi_a \chi_a$. Insertion into (39) yields

$$\begin{aligned} \Gamma_k &= \int_x \left[U_k(\rho)|_{\varphi_c} + \frac{\partial U_k(\rho)}{\partial \chi_a} \Big|_{\varphi_c} \chi_a + \frac{1}{2} \frac{\partial^2 U_k(\rho)}{\partial \chi_a \partial \chi_b} \Big|_{\varphi_c} \chi_a \chi_b + \dots \right. \\ &\quad \left. + \frac{1}{2} \partial_\mu \chi_a \left[Z_k(\rho_c, -\partial^2) + (\rho - \rho_c) Z'_k(\rho_c, -\partial^2) + \dots \right] \partial^\mu \chi_a \right. \\ &\quad \left. + \frac{1}{4} \partial_\mu (\varphi_c \chi_1 + \frac{1}{2} \chi_a \chi_a) \left[Y_k(\rho_c, -\partial^2) + (\rho - \rho_c) Y'_k(\rho_c, -\partial^2) + \dots \right] \partial^\mu (\varphi_c \chi_1 + \frac{1}{2} \chi_a \chi_a) \right]. \end{aligned} \quad (49)$$

We are only interested in the part $\Gamma_{k,2}$ that is quadratic in the small fluctuations χ_a . Terms less than quadratic drop out when we perform the functional derivative $\Gamma_k^{(2)} = \delta^2 \Gamma_k / \delta^2 \chi$ and terms higher than quadratic vanish when we evaluate $\Gamma_k^{(2)}|_{\varphi_c}$ for constant background $\chi_a(x) = 0 \quad \forall a, x$.

$$\Gamma_{k,2} = \int_x \left[\frac{1}{2} m_{ab}^2 \chi_a \chi_b + \frac{1}{2} \partial_\mu \chi_a Z_k(\rho_c, -\partial^2) \partial^\mu \chi_a + \frac{1}{4} \varphi_c^2 \partial_\mu \chi_1 Y_k(\rho_c, -\partial^2) \partial^\mu \chi_1 \right], \quad (50)$$

where we defined the mass matrix

$$\begin{aligned} m_{ab}^2 &= \frac{\partial^2 U_k(\rho)}{\partial \chi_a \partial \chi_b} \Big|_{\varphi_c} = \frac{\partial}{\partial \chi_a} \left(\frac{\partial U_k}{\partial \rho} \frac{\partial \rho}{\partial \chi_b} \right) \Big|_{\varphi_c} = \frac{\partial}{\partial \chi_a} \left[U'_k(\rho) (\varphi_c \delta_{b1} + \chi_b) \right] \Big|_{\varphi_c} \\ &= U''_k(\rho) (\varphi_c \delta_{a1} + \chi_a) (\varphi_c \delta_{b1} + \chi_b) + U'_k(\rho) \delta_{ab} \Big|_{\varphi_c} \\ &= 2\rho_c U''_k(\rho_c) \delta_{a1} \delta_{b1} + U'_k(\rho_c) \delta_{ab}. \end{aligned} \quad (51)$$

Expanding $\chi(x)$ into Fourier modes and using the integral representation of the Dirac delta

$$\chi(x) = \int_p \tilde{\chi}(p) e^{ipx}, \quad \int_x e^{i(p-q)x} = (2\pi)^d \delta(p-q), \quad (52)$$

we can transform (50) into momentum space (we won't distinguish between $\chi(x)$ and its Fourier transform $\tilde{\chi}(p)$ in the sequel),

$$\Gamma_{k,2} = \frac{1}{2} \int_p \chi_a(p) \left[m_{ab}^2 + p^2 \left[Z_k(\rho_c, p^2) \delta_{ab} + \rho_c Y_k(\rho_c, p^2) \delta_{a1} \delta_{b1} \right] \right] \chi_b(-p). \quad (53)$$

The 2-point function for constant fields thus reads

$$\begin{aligned} \Gamma_{k,ab}^{(2)}(p, q) \Big|_{\varphi_c} &= \frac{\delta^2 \Gamma_{k,2}}{\delta \chi_a(p) \delta \chi_b(-q)} = \frac{1}{(2\pi)^d} \left[m_{ad}^2 + p^2 \left[Z_k(\rho_c, p^2) \delta_{ad} + \rho_c Y_k(\rho_c, p^2) \delta_{a1} \delta_{d1} \right] \right] \frac{\delta \chi_d(-p)}{\delta \chi_b(-q)} \\ &= \frac{1}{(2\pi)^d} \left[m_{ab}^2 + p^2 \left[Z_k(\rho_c, p^2) \delta_{ab} + \rho_c Y_k(\rho_c, p^2) \delta_{a1} \delta_{b1} \right] \right] \delta(p-q). \end{aligned} \quad (54)$$

Note that the Dirac delta distribution is its own functional inverse,

$$\int d^d k \delta(p-k) \delta(k-q) = \delta(p-q). \quad (55)$$

The operator inverse $[\Gamma_k^{(2)} + R_k]^{-1}$ is therefore simply given by the algebraic inverse,

$$\begin{aligned} & [\Gamma_k^{(2)}(p, q)|_{\varphi_c} + R_k]_{ab}^{-1}(p, q) \\ &= \left[m_{ab}^2 + p^2 \left[Z_k(\rho_c, p^2) \delta_{ab} + \rho_c Y_k(\rho_c, p^2) \delta_{a1} \delta_{b1} \right] + R_k(p) \delta_{ab} \right]^{-1} (2\pi)^d \delta(p - q) \end{aligned} \quad (56)$$

Executing the trace over field indices, we get

$$\left[\Gamma_k^{(2)}|_{\varphi_c} + R_k \right]_{aa}^{-1}(p, q) = \left[\frac{1}{M_1} + \frac{N-1}{M_0} \right] (2\pi)^d \delta(p - q), \quad (57)$$

with

$$\begin{aligned} M_0 &= Z_k(\rho_c, p^2) p^2 + U'_k(\rho_c) + R_k(p), \\ M_1 &= [Z_k(\rho_c, p^2) + \rho_c Y_k(\rho_c, p^2)] p^2 + U'_k(\rho_c) + 2\rho_c U''_k(\rho_c) + R_k(p). \end{aligned} \quad (58)$$

Momentum conservation requires $p = q$ inside the closed loop on the r.h.s. of the flow equation (cf. eq. (24)). As can be seen from (52), (57) thus receives a factor $\delta(0) = V_d/(2\pi)^d$ (with $V_d = \text{vol}(\mathbb{R}^d)$ the volume of d -dimensional Euclidean space) that cancels with the volume factor in (47), resulting in the flow equation for the effective potential

$$\partial_t U_k|_{\rho_c} = \frac{1}{2} \int_p \partial_t R_k(p) \left[\frac{1}{M_1} + \frac{N-1}{M_0} \right]. \quad (59)$$

There are three important things to note here.

1. The flow equation for U_k is exact [45, 46] since our truncation (39) of Γ_k contains the most general terms for quadratic fluctuations around a constant field. As explained above, these are the only ones that contribute to $\Gamma_k^{(2)}$ when evaluated at constant background field.
2. Like (23), (59) is a partial differential equation containing derivatives of U_k with respect to the independent variables k and ρ . But unlike (23) it is no longer functional in nature. In most cases (59) is solved by turning it into an (infinite) set of coupled ordinary differential equations with independent variable k [46]. This is achieved by expanding $U_k(\rho)$ into a Taylor series around some constant ρ_c . If we are interested in excitations close to the vacuum, an expansion around $\rho_0(k)$ is appropriate. In the limit $k \rightarrow 0$, $\rho_0(0)$ specifies the macroscopic vacuum and the ρ -derivatives of U_k the renormalized masses and couplings of the theory.
3. The term M_1^{-1} in (59) incorporates fluctuations from the massive radial field φ_1 . It contributes most to the flow at sufficiently high temperatures where φ_1 excitations are not suppressed by their non-zero mass. On the other hand, M_0^{-1} describes fluctuations of the massless Goldstone bosons. It dominates the flow at low temperatures.
4. As it stands, (59) is not closed. To close it requires flow equations for the ρ_c - and p^2 -dependent wave function renormalizations Z_k, Y_k [12]. In the local potential approximation (41) we take

$$Z_k(\rho_c, p^2) = Z_k, \quad Y_k(\rho_c, p^2) = 0, \quad (60)$$

so that the only thing needed to close (59) is the flow equation

$$\partial_t Z_k = -\eta Z_k, \quad (61)$$

or equivalently the anomalous dimension $\eta = -\partial_t \ln(Z_k)$.

Introducing the threshold functions

$$\begin{aligned} \bar{I}_j(Z, m^2, R) &= (\delta_{0j} - j) \int_p \frac{\partial_t R}{(Z p^2 + m^2 + R)^{j+1}} \\ &= \tilde{\partial}_t \int_p \begin{cases} \ln(Z p^2 + m^2 + R) & j = 0, \\ (Z p^2 + m^2 + R)^{-j} & j \geq 1, \end{cases} \end{aligned} \quad (62)$$

where the cutoff derivative $\tilde{\partial}_t = \partial_t|_{\Gamma_k^{(2)}}$ targets only the explicit scale dependence of the regulator, we can write the flow equation (59) as

$$\partial_t U_k|_{\rho_c} = \frac{1}{2} \bar{I}_0(Z_k + \rho_c Y_k, U'_k + 2\rho_c U''_k, R_k) + \frac{1}{2}(N-1) \bar{I}_0(Z_k, U'_k, R_k). \quad (63)$$

The threshold functions (62) have the important property that they decay rapidly for $m^2 \gg Zk^2$ [12, 13]. This implements the decoupling of heavy modes (see item 4 on page 7). They also diverge for some negative value of m^2 which is related to the fact that the effective potential must become convex for $k \rightarrow 0$.

In principle we could attempt to solve (63) as it stands, allowing for a completely general form of $U_k(\rho)$ [1]. This would require solving a two-dimensional partial differential equation numerically. Our investigation is mostly conceptual and qualitative in nature, however, and so we contend ourselves with another restriction to our truncation (and the volume of field space we search for a solution) by Taylor expanding $U_k(\rho)$ around $\rho = \rho_0$ to quartic order in the fields,

$$U_k(\rho) = U_k(\rho_0) + m^2(\rho - \rho_0) + \frac{\lambda}{2}(\rho - \rho_0)^2, \quad (64)$$

with $m^2 = U'_k(\rho_0)$, $\lambda = U''_k(\rho_0)$. In the phase $\rho_0 > 0$ of spontaneously broken $O(N)$, $U'_k(\rho_0)$ vanishes by definition. The term quadratic in the fields is then given by $-\lambda\rho_0\rho$ which implies $m^2 = -2\lambda\rho_0 < 0$. The potential thus takes the form

$$U_k(\rho) = \begin{cases} U_k(0) + m^2\rho + \frac{1}{2}\lambda\rho^2 & \rho_0 = 0, \\ U_k(\rho_0) + \frac{1}{2}\lambda(\rho - \rho_0)^2 & \rho_0 > 0. \end{cases} \quad (65)$$

To derive flow equations for the couplings m^2 , λ and the minimum location ρ_0 , we project these parameters onto the flow of U_k . Neglecting the (subleading) ρ -dependence of Z_k and Y_k ⁵ and using the recursive relation

$$\partial_{m^2} \bar{I}_j = (\delta_{0j} - j) \bar{I}_{j+1}, \quad (66)$$

taking ρ -derivatives of (63) evaluated at $\rho_c = \rho_0$ yields

$$\partial_t U'_k|_{\rho_0} = \frac{1}{2}(3U''_k + 2\rho_0 U_k^{(3)}) \bar{I}_1(Z_k + \rho_0 Y_k, U'_k + 2\rho_0 U''_k, R_k) + \frac{1}{2}(N-1) U''_k \bar{I}_1(Z_k, U'_k, R_k), \quad (67)$$

$$\begin{aligned} \partial_t U''_k|_{\rho_0} = & -\frac{1}{2}(3U''_k + 2\rho_0 U_k^{(3)})^2 \bar{I}_2(Z_k + \rho_0 Y_k, U'_k + 2\rho_0 U''_k, R_k) - \frac{1}{2}(N-1) (U''_k)^2 \bar{I}_2(Z_k, U'_k, R_k) \\ & + \frac{1}{2}(5U_k^{(3)} + 2\rho_0 U_k^{(4)}) \bar{I}_1(Z_k + \rho_0 Y_k, U'_k + 2\rho_0 U''_k, R_k) + \frac{1}{2}(N-1) U_k^{(3)} \bar{I}_1(Z_k, U'_k, R_k). \end{aligned} \quad (68)$$

⁵Terms that would arise from the product rule if we took into account the ρ -dependence of Z_k and Y_k are all related to a scale dependence of the kinetic term. They will hence be negligible for small anomalous dimensions [4].

The flow equations for m^2 and λ follow from (45) together with (67) and (68),

$$\begin{aligned}
\partial_t m^2 &= \frac{\partial}{\partial \rho} \frac{dU_k}{dt} \Big|_{\rho_0=0} = \frac{\partial}{\partial \rho} \left(\eta \rho U'_k + \partial_t U_k \Big|_{\rho_0} \right) \Big|_{\rho_0=0} \\
&= \eta [U'_k + \rho U''_k] + \partial_t U'_k \Big|_{\rho_0=0} \\
&\stackrel{(67)}{=} \eta U'_k(0) + \frac{3}{2} \lambda \bar{I}_1(Z_k, U'_k, R_k) + \frac{1}{2} (N-1) \lambda \bar{I}_1(Z_k, U'_k, R_k) \\
&= \eta m^2 + \frac{\lambda}{2} (N+2) \bar{I}_1(Z_k, m^2, R_k),
\end{aligned} \tag{69}$$

$$\begin{aligned}
\partial_t \lambda &= \frac{\partial^2}{\partial^2 \rho} \frac{dU_k}{dt} \Big|_{\rho_0} = \frac{\partial}{\partial \rho} \left(\eta [U'_k + \rho U''_k] + \partial_t U'_k \Big|_{\rho_0} \right) \Big|_{\rho_0} \\
&= \eta [2U''_k(\rho_0) + \rho_0 U_k^{(3)}(\rho_0)] + \partial_t U'_k(\rho_0) \Big|_{\rho_0} \\
&\stackrel{(68)}{=} 2\eta \lambda - \frac{\lambda^2}{2} \left[9 \bar{I}_2(Z_k + \rho_0 Y_k, 2\rho_0 \lambda, R_k) + (N-1) \bar{I}_2(Z_k, 0, R_k) \right].
\end{aligned} \tag{70}$$

To obtain a flow equation for ρ_0 , we take the total scale derivative of U'_k evaluated at ρ_0 ,

$$0 = \frac{dU'_k(\rho_0)}{dt} = U''_k(\rho_0) \partial_t \rho_0 + \partial_t U'_k(\rho_0) \Big|_{\rho_0}, \tag{71}$$

which vanishes because the ρ -derivative of the effective potential is zero at its minimum. Solving (71) for $\partial_t \rho_0$ and inserting the ρ -derivative of (45), we get

$$\begin{aligned}
\partial_t \rho_0 &= -\frac{1}{\lambda} \partial_t U'_k(\rho_0) \stackrel{(45)}{=} -\frac{1}{\lambda} \left(\eta \rho_0 U''_k(\rho_0) + \partial_t U'_k(\rho_0) \Big|_{\rho_0} \right) \\
&\stackrel{(67)}{=} -\eta \rho_0 - \frac{1}{2} \left[3 \bar{I}_1(Z_k + \rho_0 Y_k, U'_k + 2\rho_0 U''_k, R_k) + (N-1) \bar{I}_1(Z_k, U'_k, R_k) \right].
\end{aligned} \tag{72}$$

This concludes our introductory section on Euclidean functional renormalization. In the next two sections, we will analytically continue flow equations to extend the formalism to Minkowski space.

3. Functional Renormalization in Minkowski Space

So far, the functional renormalization group in its formulation due to Wetterich [4] has been applied mainly in Euclidean space to either static, classical statistical field theories (where the fields depend on spatial position only) or quantum field theories in the Matsubara formalism where time and frequency become imaginary [1].

While significant progress has been made with this setup over the past 20 years, it is only applicable to static systems and imaginary-time quantities. In nature, actual dynamical processes take place in Minkowski space. It thus stands to reason that our understanding of physics, not to mention the renormalization group itself, particularly where real-time properties such as propagator residues and decay widths are concerned, would greatly benefit from an extension of the formalism to this new domain.

Of course, we expect a number of challenges. Most singular structures become visible only in Minkowski space. (Euclidean space propagators feature singularities too, but only for massless particles at $p = 0$ or at Fermi surfaces [1].) Singularities are difficult to treat numerically, making it convenient to work in Euclidean space where they are fewer. However, singularities in correlation functions are physical and have crucial repercussions on the behavior of the particles they describe. For instance, a pole in the propagator corresponds to a stable particle, a branch cut to a resonance, i.e. an unstable particle.

If we are to fully understand the real-time dynamics of particle propagation and decay on a fundamental level, we must be able to cope with these analytic structures. Fortunately, functional

renormalization has the potential to do that and do it well. In the following we develop an analytic implementation of the FRG that takes poles and branch cuts of the propagator into account in a fully self-consistent manner.

3.1. Methodology

Different strategies for performing the analytic continuation are conceivable [1, 42, 49–58].

1. The most radical approach reconstructs the formalism from the ground up in Minkowski space by analytically continuing the Feynman path integral itself (the starting point of our derivation of the Wetterich equation in sec. 2.1). The advantage of such an approach is its applicability to even far-from-equilibrium dynamics. Unfortunately, we are immediately faced with severe technical complications. Factors of i appear at various places, most importantly in the exponent of the integrand $e^{S_M} = e^{iS_E}$, spoiling its interpretation as a weighting factor. Moreover, this approach requires the technically involved Schwinger-Keldysh closed time contour.
2. A more modest attempt would be to stick to the Euclidean functional integral, work with the formalism as derived in sec. 2 exclusively in Euclidean space and use analytic continuation only on the final result after taking the flow down to $k = 0$. This method has in fact been successfully pursued [59–61]. The advantage of this procedure is that we use the formalism in a setting where it is comparatively transparent and well understood [1].

The disadvantage lies in the analytic continuation itself. It can turn out rather difficult in practice since the Euclidean propagator is known only numerically and only at isolated points along the imaginary axis, the so-called Matsubara frequencies $i\omega_n = 2\pi iTn$, $n \in \mathbb{N}$. Numerical reconstruction based on Padé approximants or the maximum entropy method require information from many points. As a result, the computational effort gets quite large.

Besides this practical issue, there are some systemic shortcomings. First, knowledge about spectral properties does not enable us to improve the renormalization group running. Second, only linear response properties are accessible.

3. A third possibility also keeps the Euclidean space functional integral but performs the analytic continuation already on the flow equations rather than the final result at $k = 0$. From an innovation standpoint, i.e. how much new formalism needs to be developed, it is situated somewhere between options 1 and 2. This is the approach we pursue in our work. It offers a number of advantages [1].
 - i) Because the flow equations for objects such as the effective potential or the propagator are available in analytic form, we can do the analytic continuation by hand instead of having to resort to involved numerical techniques.
 - ii) Real-time properties such as quasi-particle decay widths can be inserted in a self-consistent manner on the r.h.s. of flow equations. This should notably improve the performance of truncations. Particularly properties not directly related to the propagator (such as thermodynamic quantities) are expected to gain enhanced accuracy.
 - iii) All the usual space-time symmetries, i.e. translational as well as Lorentz (or Galilei) invariance are manifest. (A convenient choice of the infrared regulator due to Flörschinger [1] will nevertheless allow us to perform the Matsubara summation in loop expressions analytically, leading to well behaved expressions on the right hand side of flow equations where at most an integral over spatial momenta remains to be done numerically.)
 - iv) Compared to the Schwinger-Keldysh contour, this method is significantly less involved.
 - v) Since we derive all of our flow equations in Euclidean space where functional renormalization is best understood and has progressed the farthest, we can benefit from existing

expertise. For example, it is known how the flowing action approaches the microscopic action for large cutoff scales (this is not obvious in Minkowski space due to the indefiniteness of $p^2 = -p_0^2 + \mathbf{p}^2 \gtrless 0$) or how to construct useful regulators.

The biggest drawback, on the other hand, is that (like option 2) this approach is based on linear response theory. It is hence restricted to close-to-equilibrium physics. Even though it can be applied to weakly non-linear regimes [62], strongly non-linear responses as they dominate far from equilibrium are beyond its scope.

3.2. Matsubara Formalism

In the Matsubara or imaginary time formalism, quantum fields at non-zero temperature live on a generalized torus $\mathcal{M}_{d+1} = S^1 \times \mathbb{R}^d$ with circumference $\beta = 1/T$ in the imaginary time direction $\tau = -it$. We will refer to this topology as Matsubara space. To understand why time becomes imaginary, compact and periodic at non-zero temperature, we recall some basic concepts of statistical mechanics [63]. An equilibrium ensemble at temperature $T = 1/\beta$ can be described by its partition function

$$Z(\beta) = \text{Tr } \rho(\beta) = \text{Tr } e^{-\beta\mathcal{H}}, \quad (73)$$

where the density operator $\rho(\beta)$ determines the occupation number of every possible state at a given temperature and \mathcal{H} is a Hamiltonian that specifies the type of system we are dealing with. (If $\mathcal{H} = H$, where H is the Hamiltonian that appears in the unitary time evolution operator $U = e^{-iHt}$, the ensemble is canonical, i.e. it has a fixed particle number but variable energy due to heat exchange with a bath. If instead $\mathcal{H} = H - \mu N$ with N the number operator and μ the chemical potential, the ensemble is grand canonical and can exchange energy with a bath as well as particles with a reservoir.)

The important observables in a statistical setting are ensemble averages $\langle \mathcal{O} \rangle_\beta$ defined as

$$\langle \mathcal{O} \rangle_\beta = \frac{1}{Z(\beta)} \text{Tr } \mathcal{O} e^{-\beta\mathcal{H}}. \quad (74)$$

for any measurable quantity \mathcal{O} . Cyclicity of the trace renders such averages periodic under imaginary time evolution,

$$\begin{aligned} \langle \mathcal{O}(t) \rangle_\beta &= \frac{1}{Z(\beta)} \text{Tr } e^{-\beta\mathcal{H}} \mathcal{O}(t) e^{\beta\mathcal{H}} e^{-\beta\mathcal{H}} \\ &= \frac{1}{Z(\beta)} \text{Tr } e^{-\beta\mathcal{H}} \mathcal{O}(t + i\beta) = \langle \mathcal{O}(t + i\beta) \rangle_\beta. \end{aligned} \quad (75)$$

This is known as the Kubo-Martin-Schwinger relation. It is a result of the fact that $e^{-\beta\mathcal{H}}$ acts as a time evolution operator on the compact imaginary time axis $0 \leq \tau = -it \leq \beta$ with the extent of time determined by the temperature $T = \beta^{-1}$.

The Matsubara formalism is based on the idea (originally due to Bloch [64] but first implemented perturbatively by Matsubara [65]) that ensemble averages like (74) may be written as expectation values in a Euclidean signature quantum field theory. The trace requires that the bosonic (fermionic) fields of such a theory be (anti-)periodic in the imaginary time direction,

$$\phi(\tau, \mathbf{x}) = \pm \phi(\tau + \beta, \mathbf{x}). \quad (76)$$

In momentum space, this leads to the replacement of continuous frequencies by discrete imaginary Matsubara frequencies $i\omega_n = 2\pi inT$.

The Matsubara formalism has proven useful in studying the behavior of quantum field theories at non-zero temperature [66]. It has been generalized to theories with gauge invariance and was essential in the study of a conjectured deconfining phase transition of Yang-Mills theory [25].

3.3. Analytic Structure

As stated above, our approach is to derive flow equations for n -point functions $\Gamma_k^{(n)}$ in Euclidean space. This yields analytic expressions for $\partial_k \Gamma_k^{(n)}$ at points $i\omega_n$ on the imaginary axis which we can analytically continue to extend them to the entire complex frequency plane with the exception of possible poles and branch cuts along the real axis [1]. This last assertion constitutes a severe restriction to the analytic structure of n -point functions and needs to be justified. We will shed light on how it originates for the example of the 2-point function $\Gamma^{(2)} \sim G^{-1}$. Its analytic structure is of particular importance since real-time properties of the propagator $G(p)$ are the main point of interest in this work. Nonetheless, analogous arguments apply also for $n > 2$.

As we saw in (54), $\Gamma^{(2)}$ is of the form

$$\Gamma^{(2)}(p, q) = \frac{\delta^2 \Gamma[\varphi]}{\delta\varphi(p) \delta\varphi(-q)} = (2\pi)^d \delta(p - q) G^{-1}(p), \quad (77)$$

with $G(p)$ the Euclidean propagator in momentum space. Enforcing upon $G(p)$ restrictions deriving from Poincaré invariance, unitarity and causality⁶ we obtain the Källen-Lehmann spectral representation [67]

$$G(p) = \int_0^\infty d\mu^2 \frac{\rho(\mu^2)}{p^2 + \mu^2}, \quad (78)$$

with real and non-negative spectral weight $\rho(\mu^2) \geq 0$ normalized according to

$$\int_0^\infty \rho(\mu^2) d\mu^2 \stackrel{!}{=} 1. \quad (79)$$

(78) is interesting for several reasons. First, from a field theoretical standpoint, it decomposes the interacting propagator into a weighted sum of free propagators. Second and more relevant to our analysis, it allows for a very instructive investigation of the analytic structure of $G(p)$.

In Euclidean space $p^2 = p_0^2 + \mathbf{p}^2 \geq 0$ is positive semi-definite such that the integrand in (78) is completely regular, rendering $G(p)$ both real and positive for all p . In Minkowski space, on the other hand, $p^2 = -p_0^2 + \mathbf{p}^2 \geq 0$ is indefinite. For $p^2 < 0$, $G(p)$ features singularities on the real frequency axis located at⁷

$$p_0 = \pm \sqrt{\mathbf{p}^2 + \mu^2}. \quad (80)$$

Since μ^2 is integrated over, (80) actually signals a continuum of singularities, i.e. a branch cut

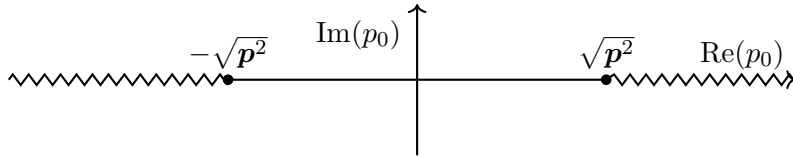


Figure 3: Propagator branch cuts along the real frequency axis extending from $\pm|\mathbf{p}|$ out to $\pm\infty$

spanning from $\pm|\mathbf{p}|$ out to infinity in both directions along the real p_0 -axis as depicted in fig. 3. It is typical for $\rho(\mu^2)$ to contain both pole and branch cut contributions from single-particle and bound states, and multi-particle states with continuous energy spectra, respectively. By

⁶Causality requires that the commutator $[\phi(x), \phi(y)]$ vanishes for spacelike separation $(x - y)^2 > 0$.

⁷Although we integrate over μ^2 in (78), we are interested in the location of these poles in p_0 -space rather than μ -space. This is because to solve flow equations, we have to integrate expressions containing $G(p)$ with respect to spatial momentum and frequency. To perform the p_0 -integration (or Matsubara summation at $T > 0$), we then need to specify an integration contour in the complex frequency plane that avoids the poles. We can either slightly deform the contour away from the real axis at $p_0 = \pm\sqrt{\mathbf{p}^2 + \mu^2}$ or add infinitesimal $\pm i\epsilon$ -terms in the denominator to shift the poles away from the real axis. See app. A.1 for details.

the Sokhotski-Plemelj theorem, (78) can be written as (a detailed derivation was relegated to app. A.1)

$$G(p) = \mathcal{P} \left(\int_0^\infty d\mu^2 \frac{\rho(\mu^2)}{p^2 + \mu^2} \right) + i\pi \operatorname{sign}(\operatorname{Re} p_0 \operatorname{Im} p_0) \rho(-p^2), \quad (81)$$

where \mathcal{P} denotes the Cauchy principal value. (81) reveals the branch cut structure in $G(p)$. Since $\operatorname{sign}(\operatorname{Im} p_0)$ abruptly changes sign when crossing the real axis, $G(p)$ features a cut along the real frequency axis at all p_0 for which $\rho(-p^2) \neq 0$. (81) also shows that $G(p)$ is analytic away from the real axis. (Since $\rho(-p^2) = 0 \forall p^2 < 0$, i.e. for all $p_0^2 - \mathbf{p}^2 \leq p_0^2 < 0 \Leftrightarrow p_0 \in i\mathbb{R}$, there is no branch cut on the imaginary axis). An important consequence is that also the inverse propagator $G^{-1} \sim \Gamma^{(2)}$ has all its poles, zero-crossings and branch cuts on the real axis as well.

Inverting (81), we find that close to the real axis, $\operatorname{Im}(p_0) \approx 0$, the inverse propagator $P(p) = G^{-1}(p)$ is of the form [1]

$$P(p) = P_1(p^2) - is(p_0) P_2(p^2), \quad (82)$$

with $s(p_0) = \operatorname{sign}(\operatorname{Re} p_0 \operatorname{Im} p_0)$ and

$$\begin{aligned} P_1(p^2) &= \frac{\operatorname{Re} G(p)}{[\operatorname{Re} G(p)]^2 + [\operatorname{Im} G(p)]^2}, & P_2(p^2) &= \frac{\operatorname{Im} G(p)}{[\operatorname{Re} G(p)]^2 + [\operatorname{Im} G(p)]^2}, \\ \operatorname{Re} G(p) &= \mathcal{P} \left(\int_0^\infty d\mu^2 \frac{\rho(\mu^2)}{p^2 + \mu^2} \right), & \operatorname{Im} G(p) &= \pi \rho(-p^2). \end{aligned} \quad (83)$$

Close to a point $p^2 = -p_0^2 + \mathbf{p}^2 = -m^2/z$ where $P_1(p^2)$ vanishes (corresponding to a pole in the propagator and thus to a particle), we can expand P_1 and P_2 as

$$P_1(p^2) = Z(z p^2 + m^2) + \dots, \quad P_2(p^2) = Z \gamma^2(p^2) + \dots, \quad (84)$$

(with Z, z, m^2 and γ^2 scale-dependent real and positive quantities) such that the propagator takes the form

$$G(p) = P^{-1}(p) = \frac{1}{Z} \frac{z p^2 + m^2 + is(p_0) \gamma^2}{(z p^2 + m^2)^2 + \gamma^4}. \quad (85)$$

(85) describes an unstable particle whose decay is governed by the Breit-Wigner distribution. $\sqrt{Z} z p^2$ is the center-of-mass energy that produces the resonance, $\sqrt{Z} m^2$ the mass of the resonance and $\Gamma = \gamma^2/m$ the decay width (width of the distribution at half-maximum). Γ is the inverse of the mean lifetime $\tau = 1/\Gamma$. In the limit of vanishing decay width, $\Gamma \rightarrow 0$, the resonance shows up as a delta peak in the spectral function $\rho(p^2)$ and the particle becomes stable. Since this is exactly the type of real-time physics we are interested in, we will continue to employ an inverse propagator of the form (82) and the expansion (84) throughout this work.

Before continuing, we explain why we deem it sufficient to know the form of $P(p)$ only close to the real axis $\operatorname{Im}(p_0) \approx 0$. Of course in principle the analytic structure of $(P_k + R_k)^{-1}$ as a function of complex frequency $p_0 \in i\mathbb{R}$ depends also on the shape of $P(p)$ away from the real axis. However, especially for small k , high-energy fluctuations due to virtual particles are strongly suppressed and we expect the propagator $G(p)$ to be dominated by on-shell excitations corresponding to the poles and branch cuts on the real frequency axis. It should be viewed as part of our truncation that possible deviations from this structure at higher scales are neglected. Based on this reasoning, we use (82) and (84) not only close to the real axis but everywhere in the p_0 -plane. The coefficients Z, m^2 and γ^2 are nonetheless determined by their value at the singularity $p^2 = -m^2/z$ on the real line where $\operatorname{Re}(P(p))$ vanishes.

4. Analytic Continuation of Flow Equations

The analytic continuation proceeds differently for different parts of the flowing action. Since the effective potential U_k is momentum-independent, its analytic continuation is trivial. The

propagator $G(p)$ and higher-order correlation functions, on the other hand, *are* momentum-dependent. Their flow equations are obtained by expanding the flow of Γ_k around a constant background field φ_c that fluctuates with a small momentum-dependent part, $\varphi_a(p) = \varphi_c \delta_{a1} + \chi_a(p)$, $\chi_a(p) \ll \varphi_c \forall a, p$. In this case, we actually have to work to perform the analytic continuation. Once $G(p)$ is extended to the entire complex plane, however, we have easy access to its real-time properties such as the decay width $\Gamma = \gamma^2/m$ by simply evaluating it for $p_0 \in \mathbb{R}$.

Working in Minkowski space has some advantages when it comes to devising truncations [1]. By performing the derivative expansion as a Taylor series around on-shell excitations, i.e. around frequencies and momenta corresponding to a pole or branch cut of the propagator, we expect the convergence of the expansion to improve. After all, loop expressions on the r.h.s. of flow equations (as well as on-shell properties of the effective action) are strongly dominated by such singular structures. Compared to an expansion around vanishing frequency in Euclidean space, higher-order terms of the derivative expansion in Minkowski space should therefore be much more strongly suppressed. In most situations, we expect the essential physics to already be well-described by the lowest-order terms.

This has important consequences. In particular, in many situations it may allow us to use an algebraic (as opposed to exponential or Litim-type) regulator R_k even though it exhibits a much milder decay in the ultraviolet. A simple algebraic form of R_k has two major advantages. First, we may construct R_k in Euclidean space and analytically continue it towards the real frequency afterwards. Second, it enables us to decompose the propagator $(P_k + R_k)^{-1}$ in such a way as to perform the summation over Matsubara frequencies analytically!

In this section we assemble the formalism needed to solve flow equations in Minkowski space. First, in sec. 4.1 we modify the truncation (39) of Γ_k so as to cope with additional singular structures that arise in Minkowski space. Sec. 4.2 introduces the above-mentioned class of regulators. In sec. 4.3 we go on to derive the momentum-space Feynman rules for that particular combination of truncation and regulator. With those tools in place, we construct flow equations for parameters of the effective potential and the propagator in secs. 4.4 and 4.5, respectively.

4.1. Truncation

We consider again the $O(N)$ -invariant scalar field theory of section sec. 2.5, now in $d+1$ dimensions with time added to the d Euclidean dimensions of space. As we saw in sec. 2.5, the spectrum of excitations in the phase with spontaneously broken $O(N)$ consists of a massive radial field φ_1 and $N-1$ massless Goldstone bosons.

Due to the term $\sim \varphi_1 \varphi_a^2$ ($a \neq 1$) in Γ_k (more precisely in U_k), the radial mode can decay into two Goldstone excitations during real-time evolution. This gives rise to a non-vanishing decay width γ_1^2 for the radial mode which makes it a quasi-particle with finite lifetime. The ordered phase $\rho_0 \neq 0$ thus corresponds to a non-zero density of quasi-particles (which we expect to disperse if we increase the temperature and vacate the ground state).

Except for this new decay channel, the system is very similar to the one treated in sec. 2.5. We can therefore employ a similar truncation written in terms of unrenormalized fields $\bar{\varphi}_a(x)$ as⁸

$$\Gamma_k[\varphi] = \oint_x \left[\bar{U}_k(\bar{\rho}) + \frac{1}{2} \bar{\varphi}_a Q_k(-\partial^2) \bar{\varphi}_a + \frac{1}{4} \bar{\rho} S_k(-\partial^2) \bar{\rho} \right], \quad (86)$$

where the sum over $a \in \{1, \dots, N\}$ is implied and we introduced the shorthand notation

$$\oint_x = \int_0^\beta d\tau \int_{\mathbb{R}^d} d^d x \quad (87)$$

to denote integration over Matsubara space $\mathcal{M}_{d+1} = S^1 \times \mathbb{R}^d$. (\mathcal{M}_{d+1} is a $d+1$ -dimensional generalized torus spanned by the Cartesian product of d Euclidean dimensions of space \mathbb{R}^d and a

⁸Up to this point, φ and ρ denoted unrenormalized quantities. We now change notation $\varphi \rightarrow \bar{\varphi}$, $\rho \rightarrow \bar{\rho}$.

circle S_1 of temperature-dependent circumference $\beta = 1/T$ for the cyclic dimension of imaginary time $\tau = it$.) In momentum space this corresponds to

$$\oint_p = T \sum_{p_0} \int_p = T \sum_{p_0} \int_{\mathbb{R}^d} \frac{d^d \mathbf{p}}{(2\pi)^d}, \quad (88)$$

where \sum_{p_0} sums over the discrete imaginary Matsubara frequencies $p_0 \in \{i\omega_n = 2\pi i T n | n \in \mathbb{Z}\}$.

In (86) we made the crucial assumption that the momentum-dependent parts of the inverse propagator $Q_k(p^2)$ and $S_k(p^2)$ are of the same analytic structure as the inverse propagator (82) expanded as in (84) [1]. Removing the momentum-independent mass from (84), this amounts to

$$Q_k(p) = Z_k(p^2) p^2 - is(p_0) \gamma_k^2(p^2), \quad S_k(p) = Y_k(p^2) p^2 - is(p_0) \delta_k^2(p^2). \quad (89)$$

Note that we are neglecting here possible alterations in the analytic structure of the scale-dependent propagator due to the frequency dependence of the regulator $R_k(p)$ used to construct Γ_k . Since $R_k(p) \rightarrow 0$ for $k \rightarrow 0$, any such alterations will disappear at $k = 0$. However, they will be present at non-zero k and might even have non-negligible effects at intermediate stages of the flow. It should be viewed as part of our truncation that we disregard these modifications here.

The functions $\gamma_k^2(p^2)$, $\delta_k^2(p^2)$ determine the size of the jump at the branch cut discontinuity in fig. 3. Since $G(p)$ is completely regular for $p^2 > 0$, $\gamma_k^2(p^2)$ and $\delta_k^2(p^2)$ are non-zero only for $p^2 < 0$. Physically, this ensures causality of the decay process since it requires time-like, i.e. negative p^2 .

To derive the flow equation for $U_k(\rho)$, we again expand Γ_k around a constant background,

$$\bar{\varphi}_a(x) = \bar{\varphi}_c \delta_{a1} + \bar{\chi}_a(x), \quad \bar{\rho}_c = \frac{1}{2} \bar{\varphi}_c^2. \quad (90)$$

Only the part $\Gamma_{k,2}$ that is quadratic in the fluctuating fields $\bar{\chi}_a(x)$ contributes to the flow of $U_k(\rho)$. In momentum space it reads

$$\Gamma_{k,2} = \frac{1}{2} \sum_p \bar{\chi}_a(p) \left[\delta_{ab} (Q_k(p^2) + \bar{U}'_k(\bar{\rho}_c)) + \delta_{a1} \delta_{b1} (\bar{\rho}_c S_k(p^2) + 2\bar{\rho}_c \bar{U}''_k(\bar{\rho}_c)) \right] \bar{\chi}_b(-p). \quad (91)$$

Just like in (84), we further expand (91) around zero-crossings of

$$\text{Re} \left[Q_k(p) + \bar{\rho}_c S_k(p) + \bar{U}'_k(\bar{\rho}_c) + 2\bar{\rho}_c \bar{U}''_k(\bar{\rho}_c) \right] \quad \text{and} \quad \text{Re} \left[Q_k(p) + \bar{U}'_k(\bar{\rho}_c) \right], \quad (92)$$

corresponding to the point on the real frequency axis where the propagators $G_1(p)$ and $G_a(p)$ ($a \neq 1$) become singular. These are the on-shell excitations of the radial field and the Goldstone bosons, respectively. Strictly speaking, the location of the zero-crossings depend on the value of the background field $\bar{\rho}_c$. For the regimes we will study, however, it suffices to expand (92) around some $p^2 = -m^2$ such that the expressions (92) vanish at the minimum ρ_0 . Since

$$m_{ab}^2 = \bar{U}'_k(\bar{\rho}_0) \delta_{ab} + 2\rho_0 \bar{U}''_k(\bar{\rho}_0) \delta_{a1} \delta_{b1} \quad \text{with} \quad \bar{U}'_k(\bar{\rho}_0) = 0, \quad (93)$$

the Goldstone bosons ($a = b > 1$) are massless at the minimum $\bar{\rho}_0$. This puts their expansion point at $p = 0$. The discontinuity along the real frequency axis vanishes here, $\gamma^2(0) = 0$, so that

$$Q_k(p) = Z_k(0) p^2, \quad (\text{for } a = b > 1). \quad (94)$$

The massive radial field ($a = b = 1$) we expand around $p^2 = -m_1^2 = -[2\bar{\rho}_0 \bar{U}''_k(\bar{\rho}_0)]^2$, where $\gamma^2(-m_1^2)$ is non-zero such that

$$Q_k(p) + \bar{\rho}_0 S_k(p) = [Z_k(-m_1^2) + \bar{\rho}_0 Y_k(-m_1^2)] p^2 - is(p_0) [\gamma_k^2(-m_1^2) + \bar{\rho}_0 \delta_k^2(-m_1^2)], \quad (95)$$

Introducing the abbreviations

$$Z_1 = \frac{1}{Z_k} [Z_k(-m_1^2) + \bar{\rho}_0 Y_k(-m_1^2)], \quad \gamma_1^2 = \frac{1}{Z_k} [\gamma_k^2(-m_1^2) + \bar{\rho}_0 \delta_k^2(-m_1^2)], \quad (96)$$

where we set $Z_k = Z_k(0)$, an expression analogous to (91) but in terms of renormalized fields

$$\varphi_a = \sqrt{Z_k} \bar{\varphi}_a, \quad \rho = Z_k \bar{\rho}, \quad \bar{U}_k(\bar{\rho}) = U_k(\rho), \quad (97)$$

can be written as

$$\Gamma_{k,2} = \frac{1}{2} \sum_p \chi_a(p) \left\{ \delta_{ab} [p^2 + U'_k(\rho_c)] + \delta_{a1} \delta_{b1} [(Z_1 - 1)p^2 - is(p_0) \gamma_1^2 + 2\rho_c U''_k(\rho_c)] \right\} \chi_b(-p), \quad (98)$$

where we pulled a factor Z_k out of every term and absorbed it into the fluctuating fields $\chi_a = \sqrt{Z_k} \bar{\chi}_a$. By evaluating (98) for $\rho_c = \rho_0$, we can directly read off the radial mode's renormalized mass and decay width,

$$m_1 = \sqrt{2\rho_0 U''_k(\rho_0)/Z_1}, \quad \Gamma_1 = \gamma_1^2 / (Z_1 m_1) = \gamma_1^2 / \sqrt{2\rho_0 U''_k(\rho_0) Z_1} \quad (99)$$

4.2. Regulator

Our next goal is to find a regulator R_k that allows for analytic continuation of $(P_k + R_k)^{-1}$ in truncations where close to the real frequency axis, $\text{Im}(p_0) \approx 0$, P_k is well approximated by (82) expanded according to (84), i.e.

$$P = Z \left[z p^2 + m^2 - is(p_0) \gamma^2 \right]. \quad (100)$$

The problem we face is that given the indefiniteness of $p^2 = -p_0^2 + \mathbf{p}^2$ in Minkowski space, it is unclear which modes correspond to the infrared and which to the ultraviolet part of the spectrum. Some high frequency $p_0 \approx \Lambda$ could join with an equally large momentum $|\mathbf{p}| \approx \Lambda$ to produce a vanishing p^2 . Yet R_k still needs to suppress fluctuations from these modes during late stages of the flow (i.e. at small k) if the derivative expansion is to have any chance at convergence. This might not seem like such a difficult problem until we recall that we cannot split up p^2 and simply implement the decay for high p_0 and high \mathbf{p} separately if we wish to keep rotational and Lorentz invariance. At this point it is still unclear which requirements R_k must fulfill in order to act as an effective infrared and ultraviolet regulator in Minkowski space.

In Euclidean space by contrast, $p^2 \geq 0$ establishes an unambiguous order relation for all modes in the spectrum. Constructing a regulator with the desired properties becomes a simple matter. Our approach will therefore be to construct a regulator in Euclidean space and use analytic continuation to extend it to Minkowski space. There are some caveats to this method, however. A function that is smooth and regular on the imaginary frequency axis may nevertheless feature poles and discontinuities in other regions of the complex plane. In fact, it stands to reason that this is even unavoidable if we require R_k to decay rapidly for large imaginary values of p_0 . We thus expect analytic continuation to be difficult for most choices of R_k that have proven useful in Euclidean space. For that reason, we adopt here a special class of regulators due to Flörchinger [1] which is particularly suited to analytic continuation,

$$R_k(p) = \frac{Z k^2}{\sum_{j=0}^{\infty} c_j \left(\frac{p^2}{k^2}\right)^j} = \frac{Z k^2}{c_0 + c_1 \frac{p^2}{k^2} + c_2 \left(\frac{p^2}{k^2}\right)^2 + \dots}. \quad (101)$$

The coefficient Z can be chosen for convenience. We will identify it with the wave function renormalization Z_k but it could be any real, positive function of k .

When only a few coefficients c_j are non-zero, (101) has a comparatively mild algebraic decay in the ultraviolet. We still expect it to provide adequate separation of momentum modes due to the improved convergence of the derivative expansion in Minkowski space. (101) has all desired properties for Euclidean argument $p_0^2 + \mathbf{p}^2 \geq 0$ if the coefficients c_j are real and positive. Regularization of the ultraviolet improves if some c_j with large j are non-zero. On the other hand,

calculations simplify if only a few c_j with small j are non-zero. The simplest, non-trivial choice is $c_0 = 1$, $c_1 = c > 0$, $c_j = 0 \forall j > 1$. Then

$$R_k(p) = \frac{Z k^2}{1 + c \frac{p^2}{k^2}}, \quad \partial_t R_k(p) = k \partial_k R_k(p) = \frac{2k^2 Z + k^2 \partial_t Z}{1 + c \frac{p^2}{k^2}} + \frac{2c Z p^2}{(1 + c \frac{p^2}{k^2})^2}. \quad (102)$$

This will be our setup in the sequel.

4.3. Feynman Rules

In the truncation (98) the (unrenormalized) propagator $\bar{G}_k = [\bar{\Gamma}_k^{(2)} + R_k]^{-1}$ reads

$$\begin{aligned} \varphi_a &\xrightarrow{p_1} \text{---} \textcircled{\text{---}} \text{---} \xrightarrow{p_2} \varphi_b \quad (p_1 = p_2) \\ &= [\bar{\Gamma}_k^{(2)} + R_k]_{ab}^{-1}(p_1, p_2)|_{\varphi_c} = \left[\frac{\delta^2 \Gamma_k[\varphi]}{\delta \bar{\chi}_a(p_1) \delta \bar{\chi}_b(-p_2)} \Big|_{\varphi_c} + R_k(p_1) (2\pi)^{d+1} \delta_{ab} \delta(p_1 - p_2) \right]^{-1} \quad (103) \\ &= \frac{\delta(p_1 - p_2)}{(2\pi)^{d+1} Z_k} \begin{cases} [Z_1 p_1^2 - is(p_{0,1}) \gamma_1^2 + U'_k(\rho_c) + 2\rho_c U''_k(\rho_c) + k^2/(1 + c p^2/k^2)]^{-1} & a = b = 1, \\ [p_1^2 + U'_k(\rho_c) + k^2/(1 + c p^2/k^2)]^{-1} & a = b > 1, \end{cases} \end{aligned}$$

where we defined the Matsubara space Dirac delta as

$$\delta(p - q) \equiv \delta_M^{(d+1)}(p - q) = \frac{T}{2\pi} \delta_{m,n} \delta^{(d)}(\mathbf{p} - \mathbf{q}). \quad (104)$$

In the zero-temperature limit, we have $\sum_{n \in \mathbb{Z}} \frac{T}{2\pi} \xrightarrow{T \rightarrow 0} \int_{-\infty}^{\infty} dp_0$ and $\delta_{m,n} \xrightarrow{T \rightarrow 0} \delta(p_0 - q_0)$ so that

$$\lim_{T \rightarrow 0} \delta_M^{(d+1)}(p - q) = \delta(p_0 - q_0) \delta^{(d)}(\mathbf{p} - \mathbf{q}). \quad (105)$$

Since we will evaluate n -point functions for constant fields, we consider again the field configuration

$$\varphi_a(p) = \varphi_c \delta_{a1} + \chi_a(p), \quad \text{with } \chi_a(p) \ll \varphi_c \quad \forall a, p. \quad (106)$$

in which $\delta\varphi_a(p) = \delta\chi_a(p)$ and $\rho = \frac{1}{2} \sum_{a=1}^N (\varphi_c \delta_{a1} + \chi_a(p))^2$. The 3-point function is then given by

$$\begin{aligned} &\varphi_a \xrightarrow{p_1} \text{---} \textcircled{\text{---}} \text{---} \begin{matrix} \nearrow^{p_2} \varphi_b \\ \searrow^{p_3} \varphi_c \end{matrix} \quad \Gamma_{k,abc}^{(3)}(p_1, p_2, p_3) \quad (p_1 + p_2 + p_3 = 0) \\ &\text{assuming momentum-independent vertices} \\ &= \Gamma_{k,abc}^{(3)}(p_1, p_2, p_3)|_{\varphi_c} \stackrel{\downarrow}{=} \sum_p \frac{\delta^3 U_k(\rho)}{\delta \chi_a(p_1) \delta \chi_b(p_2) \delta \chi_c(p_3)} \Big|_{\varphi_c} \quad (107) \\ &= \sum_p \left[U_k''' \frac{\delta \rho}{\delta \chi_a(p_1)} \frac{\delta \rho}{\delta \chi_b(p_2)} \frac{\delta \rho}{\delta \chi_c(p_3)} + U_k'' \frac{\delta^2 \rho}{\delta \chi_a(p_1) \delta \chi_b(p_2)} \frac{\delta \rho}{\delta \chi_c(p_3)} + U_k'' \frac{\delta^2 \rho}{\delta \chi_a(p_1) \delta \chi_c(p_3)} \frac{\delta \rho}{\delta \chi_b(p_2)} \right. \\ &\quad \left. + U_k'' \frac{\delta^2 \rho}{\delta \chi_b(p_2) \delta \chi_c(p_3)} \frac{\delta \rho}{\delta \chi_a(p_1)} + U_k' \frac{\delta^3 \rho}{\delta \chi_a(p_1) \delta \chi_b(p_2) \delta \chi_c(p_3)} \right] \Big|_{\varphi_c} \end{aligned}$$

The functional derivatives in (107) are

$$\left. \frac{\delta \rho(\chi(p))}{\delta \chi_a(p_1)} \right|_{\varphi_c} = [\varphi_c \delta_{a1} + \chi_a(p)] \delta(p - p_1) \Big|_{\varphi_c} = \varphi_c \delta_{a1} \delta(p - p_1), \quad (108)$$

$$\left. \frac{\delta^2 \rho}{\delta \chi_a(p_1) \delta \chi_b(p_2)} \right|_{\varphi_c} = \delta_{ab} \delta(p - p_1) \delta(p - p_2), \quad (109)$$

$$\left. \frac{\delta^3 \rho}{\delta \chi_a(p_1) \delta \chi_b(p_2) \delta \chi_c(p_3)} \right|_{\varphi_c} = 0. \quad (110)$$

The Feynman rule for the 3-point function therefore reads

$$\Gamma_{k,abc}^{(3)}(p_1, p_2, p_3) \Big|_{\varphi_c} = \left[\varphi_c^3 U_k''' \delta_{a1} \delta_{b1} \delta_{c1} + \varphi_c U_k'' (\delta_{a1} \delta_{bc} + \delta_{b1} \delta_{ac} + \delta_{c1} \delta_{ab}) \right] \delta(p_1 + p_2 + p_3). \quad (111)$$

We can immediately read off two non-zero index combinations,

$$\Gamma_{k,abc}^{(3)}(p_1, p_2, p_3) \Big|_{\varphi_c} = \delta(p_1 + p_2 + p_3) \begin{cases} \varphi_c^3 U_k''' + 3\varphi_c U_k'' & a = b = c = 1, \\ \varphi_c U_k'' & a = 1, b = c \neq 1, \\ 0 & \text{else.} \end{cases} \quad (112)$$

Else contains the cases

$$1 \begin{array}{c} \swarrow \\ \bullet \\ \searrow \end{array} \begin{array}{c} 1 \\ a \end{array} = 1 \begin{array}{c} \swarrow \\ \bullet \\ \searrow \end{array} \begin{array}{c} a \\ b \end{array} = a \begin{array}{c} \swarrow \\ \bullet \\ \searrow \end{array} \begin{array}{c} a \\ a \end{array} = a \begin{array}{c} \swarrow \\ \bullet \\ \searrow \end{array} \begin{array}{c} b \\ b \end{array} = a \begin{array}{c} \swarrow \\ \bullet \\ \searrow \end{array} \begin{array}{c} b \\ c \end{array} = 0, \quad \text{with } a \neq b \neq c \in \{2, \dots, N\}. \quad (113)$$

Thus our theory features two kinds of 3-point interactions: one purely radial and one between a radial mode and any two identical Goldstone bosons. All other 3-point correlations vanish (within our approximation). We will see in sec. 4.5 that despite the hierarchy of flow equations (see item 1 on page 6), higher vertices won't be necessary to compute the flow of parameters of the 2-point function under the assumption of momentum-independent vertices.

4.4. Potential Flow

Except for an additional discrete frequency dimension and the presence of the discontinuity γ_1^2 , eqs. (53) and (98) are strikingly similar. We can follow exactly the same steps as in sec. 2.5 to derive the flow of the effective potential. This time around, the result is

$$\partial_t U_k \Big|_{\rho_c} = \frac{1}{2} \sum_p \frac{\partial_t R_k(p)}{Z_k} \left[\frac{1}{\bar{M}_1} + \frac{N-1}{\bar{M}_0} \right], \quad (114)$$

with

$$\bar{M}_1 = Z_1 p^2 - is(p_0) \gamma_1^2 + U_k' + 2\rho_c U_k'' + \frac{R_k}{Z_k}, \quad \bar{M}_0 = p^2 + U_k' + \frac{R_k}{Z_k}. \quad (115)$$

Note that (94) and (95) are expansions around points on the real frequency axis. Thus (114) loses all validity when taken too far from the real axis. In particular, we should not evaluate it for large imaginary values $p_0 = 2\pi i T n$ with $n \gg 1$. Fortunately, performing the Matsubara summation \sum_{p_0} in (114) relies on contour integration methods. Due to the analytic structure of the propagator $G(p)$ discussed in sec. 3.3, this means we only need to evaluate residues and integrals along branch cuts on the real frequency axis (or close to it for $k > 0$) where (114) is valid.

By modifying the threshold functions I_j in eq. (62) for renormalized quasi-particles in $d+1$ dimensions [1, 68],

$$\begin{aligned} I_j(Z, z, m^2, \gamma^2, R) &= (\delta_{j0} - j) \sum_p \frac{1/Z \partial_t R}{(z p^2 + m^2 - is(p_0) \gamma^2 + R/Z)^{j+1}} \\ &= \tilde{\partial}_t \sum_p \begin{cases} \ln(z p^2 + m^2 - is(p_0) \gamma^2 + R/Z) & j = 0, \\ (z p^2 + m^2 - is(p_0) \gamma^2 + R/Z)^{-j} & j \geq 1, \end{cases} \end{aligned} \quad (116)$$

we can rewrite (114) as in (63),

$$\partial_t U_k|_{\rho_c} = \frac{1}{2} I_0(Z_k, Z_1, U'_k + 2\rho_c U''_k, \gamma_1^2, R_k) + \frac{1}{2} (N-1) I_0(Z_k, 1, U'_k, 0, R_k). \quad (117)$$

Neglecting again the (subleading) ρ -dependence of Z_1 and γ_1^2 , the flow equations for the derivatives of $U_k(\rho)$ expanded as in (65) and evaluated at $\rho_c = \rho_0$ read

$$\begin{aligned} \partial_t U'_k|_{\rho_0} &= \frac{1}{2} (3U''_k + 2\rho_0 U_k^{(3)}) I_1(Z_k, Z_1, U'_k + 2\rho_0 U''_k, \gamma_1^2, R_k) \\ &\quad + \frac{1}{2} (N-1) U''_k I_1(Z_k, 1, U'_k, 0, R_k), \end{aligned} \quad (118)$$

$$\begin{aligned} \partial_t U''_k|_{\rho_0} &= -\frac{1}{2} (3U''_k + 2\rho_0 U_k^{(3)})^2 I_2(Z_k, Z_1, U'_k + 2\rho_0 U''_k, \gamma_1^2, R_k) \\ &\quad - \frac{1}{2} (N-1) (U''_k)^2 I_2(Z_k, 1, U'_k, 0, R_k) \\ &\quad + \frac{1}{2} (5U_k^{(3)} + 2\rho_0 U_k^{(4)}) I_1(Z_k, Z_1, U'_k + 2\rho_0 U''_k, \gamma_1^2, R_k) \\ &\quad + \frac{1}{2} (N-1) U_k^{(3)} I_1(Z_k, 1, U'_k, 0, R_k). \end{aligned} \quad (119)$$

from which we obtain by the same steps taken in sec. 2.5 the following flow equations for the mass squared m^2 , the location of the minimum $\rho_0(k)$ and the quartic coupling λ ,

$$\partial_t m^2 = \eta m^2 + \frac{\lambda}{2} (N+2) I_1(Z_k, 1, m^2, 0, R_k), \quad (120)$$

$$\partial_t \rho_0 = -\eta \rho_0 - \frac{1}{2} \left[3 I_1(Z_k, Z_1, 2\rho_0 \lambda, \gamma_1^2, R_k) + (N-1) I_1(Z_k, 1, 0, 0, R_k) \right], \quad (121)$$

$$\partial_t \lambda = 2\eta \lambda - \frac{\lambda^2}{2} \left[9 I_2(Z_k, Z_1, 2\rho_0 \lambda, \gamma_1^2, R_k) + (N-1) I_2(Z_k, 1, 0, 0, R_k) \right]. \quad (122)$$

4.5. Propagator Flow

To close the system of differential equations eqs. (120) to (122), we need three additional flow equations for the remaining scale-dependent parameters Z_k , γ_1^2 and Z_1 that are incorporated self-consistently in our truncation. Our course of action will be to calculate the flow of $\Gamma_k^{(2)}$ and then project it to $\partial_t Z_k$, $\partial_t \gamma_1^2$ and $\partial_t Z_1$.

To derive the unrenormalized 2-point function $\bar{\Gamma}_k^{(2)} = \Gamma_k^{(2)}/Z_k$, we expand Γ_k in powers of $\bar{\chi}_a(p)$, take two functional derivatives with respect to the unrenormalized fluctuating fields $\bar{\chi}_a(p)$ and evaluate the result for constant fields $\varphi(x) = \varphi_c$, i.e. $\chi_a(p) = 0 \ \forall a$, resulting in⁹

$$\begin{aligned} \bar{\Gamma}_{k,ab}^{(2)}(p, q)|_{\varphi_c} &= \frac{\delta^2 \Gamma_{k,2}}{\delta \bar{\chi}_a(p) \delta \bar{\chi}_b(-q)} \\ &\stackrel{(98)}{=} Z_k \left\{ \delta_{ab} \left[p^2 + U'_k(\rho_c) \right] + \delta_{a1} \delta_{b1} \left[(Z_1 - 1) p^2 - is(p_0) \gamma_1^2 + 2\rho_c U''_k(\rho_c) \right] \right\} \frac{\delta(p-q)}{(2\pi)^{d+1}} \end{aligned} \quad (123)$$

The $a = b = 1$ -component governs propagation of the radial mode φ_1 (equal incoming and outgoing momenta ensure momentum conservation),

$$\bar{\Gamma}_{k,11}^{(2)}(q, q)|_{\varphi_c} = \bar{P}_r(q) \frac{T}{(2\pi)^d} \delta(0), \quad (124)$$

where the inverse propagator of the radial mode is given by

$$\bar{P}_r(q) = \bar{G}_r^{-1}(q) = Z_k \left[Z_1 q^2 - is(q_0) \gamma_1^2 + U'_k(\rho) + 2\rho U''_k(\rho) \right]. \quad (125)$$

⁹The two functional derivatives strip away all terms less than quadratic in the fluctuating fields. Setting $\chi_a(p) = 0$ afterwards removes any terms higher than quadratic. So we only need to consider the quadratic fluctuations eq. (98) to obtain the most general form of $\Gamma_k^{(2)}|_{\varphi_c}$ (cf. eqs. (53) and (54))

To project onto Z_1 , we take the q^2 -derivative of (125),

$$Z_1 = \frac{1}{Z_k} \partial_{q^2} \bar{P}_r(q). \quad (126)$$

(Z_1 and γ_1^2 are q -independent within our approximation since we expanded the inverse propagator around the radial mode's on-shell energy $q^2 = -m_1^2$, cf. eq. (96).) The t -derivative of (126) yields

$$\partial_t Z_1 = -\frac{1}{Z_k^2} (\partial_t Z_k) \partial_{q^2} \bar{P}_r(q) + \frac{1}{Z_k} \partial_t \partial_{q^2} \bar{P}_r(q) = \eta Z_1 + \frac{1}{Z_k} \partial_t \partial_{q^2} \bar{P}_r(q). \quad (127)$$

Similarly, we can project onto γ_1^2 [1],

$$\gamma_1 = \frac{1}{Z_k} \text{disc}_{q_0} \bar{P}_r(q) \quad (128)$$

and so

$$\partial_t \gamma_1 = \eta \gamma_1 + \frac{1}{Z_k} \partial_t \text{disc}_{q_0} \bar{P}_r(q), \quad (129)$$

where the discontinuity projector disc_{q_0} is defined as

$$\text{disc}_{q_0} f(x) = \frac{i}{2} \text{sign}(q_0) \lim_{\epsilon \rightarrow 0^+} [f(q_0 + i\epsilon) - f(q_0 - i\epsilon)], \quad (130)$$

Propagation of the Goldstone bosons is governed by components of $\Gamma_k^{(2)}$ with $a = b > 1$,

$$\bar{\Gamma}_{k,22}^{(2)}(q, q) \Big|_{\varphi_c} = \bar{P}_g(q) \frac{T}{(2\pi)^d} \delta(0), \quad (131)$$

with inverse Goldstone propagator

$$\bar{P}_g(q) = \bar{G}_g^{-1}(q) = Z_k [q^2 + U'_k(\rho)]. \quad (132)$$

so that

$$\partial_t Z_k = \partial_t \partial_{q^2} \bar{P}_g(q). \quad (133)$$

The flow equations for Z_1 , γ_1^2 and Z_k can therefore be derived by using Wetterich's equation to determine an algebraic expression for $\partial_t \Gamma_k^{(2)}$ and inserting that into (127), (129) and (133). A step by step prescription for the construction of flow equations for n -point functions goes as follows [13]:

1. Write down all one-loop Feynman diagrams obtained by taking n functional derivatives of (23). These diagrams incorporate all quantum fluctuations contributing to the scale dependence of $\Gamma^{(n)}$. Alternatively, since functional and scale derivatives commute, we can perform the functional derivatives after casting (23) into a form particularly suited for taking derivatives,

$$\partial_t \Gamma_k = \frac{1}{2} \text{Tr} \tilde{\partial}_t \ln(\Gamma_k^{(2)} + R_k) = \tilde{\partial}_t \Gamma_k[\varphi] \Big|_{1\text{-loop}}, \quad (134)$$

with cutoff derivative $\tilde{\partial}_t = \partial_t \Big|_{\Gamma_k^{(2)}}$ and renormalization group-improved one-loop contribution to the flowing action $\Gamma_k[\varphi] \Big|_{1\text{-loop}} = S[\varphi] + \frac{1}{2} \text{Tr} \ln(\Gamma_k^{(2)} + R_k)$ (cf. eq. (25)).

2. Insert n th functional derivatives of Γ_k for all n -point functions with $n \geq 3$. It is important to be aware that such vertices may be momentum-dependent even if they were constant on the classical level (i.e. as functional derivatives of the microscopic action $S = \Gamma_\Lambda$). Unless prohibited by symmetries there will also be contributions from higher vertices that are absent in S . This is a consequence of the partial integration of momentum modes with $q^2 > k^2$ in Γ_k .

3. Insert for all propagator lines the full regularized propagator $G_k = (\Gamma_k^{(2)} + R_k)^{-1}$ (evaluated at fixed field φ_c).
4. If we used (134), reapply the $\tilde{\partial}_t$ -derivative which acts on the integrand of the one-loop momentum integrals. This will increase the number of diagrams since it generates multiple diagrams with identical topology but regulator insertions attached to different internal lines [69]. It also renders momentum integrals both UV and IR finite. The resulting exact flow equation for $\Gamma_k^{(n)}$ is therefore fully regularized.

An example of this procedure, the case $n = 2$ for a scalar theory, was presented in eqs. (27) and (28) using a simplified notation that suppresses momentum arguments and field indices. To gain a more detailed understanding of the type of fluctuations that generate the flow of $\Gamma_k^{(2)}$, we rederive the result here with indices and momenta reinstated. For the one-point function we get¹⁰

$$\begin{aligned}
\partial_t \Gamma_{k,a}^{(1)}(q) &= \frac{\delta}{\delta \varphi_a(q)} \frac{1}{2} \text{Tr} \left[\frac{\partial_t R_k}{\Gamma_k^{(2)} + R_k} \right] = \frac{\delta}{\delta \varphi_a(q)} \frac{1}{2} \sum_{i,j=1}^N \int_{p_1, p_2} \frac{\partial_t R_{k,ij}(p_1, p_2)}{\Gamma_{k,ji}^{(2)}(p_2, p_1) + R_{k,ji}(p_2, p_1)} \\
&= -\frac{1}{2} \sum_{\substack{i,j \\ k,l}}^N \int_{\substack{p_1, p_2 \\ p_3, p_4}} \frac{\partial_t R_{k,ij}(p_1, p_2)}{\Gamma_{k,jk}^{(2)}(p_2, p_3) + R_{k,jk}(p_2, p_3)} \frac{\Gamma_{k,akl}^{(3)}(q, p_3, p_4)}{\Gamma_{k,li}^{(2)}(p_4, p_1) + R_{k,li}(p_4, p_1)}. \tag{135}
\end{aligned}$$

The integrand in (135) corresponds to the diagram

$$\tag{136}$$

The sign as well as the additional index summation over k, l and momentum integration over p_3, p_4 in (135) stem from the functional chain rule,

$$\begin{aligned}
\frac{\delta [\Gamma_{k,bc}^{(2)}(q_2, q_3)]^{-1}}{\delta \varphi_a(q_1)} &= \sum_{i,j=1}^N \int_{p'_1, p'_2} \frac{\delta [\Gamma_{k,bc}^{(2)}(q_2, q_3)]^{-1}}{\delta \Gamma_{k,ij}^{(2)}(p_1, p_2)} \frac{\delta \Gamma_{k,ij}^{(2)}(p_1, p_2)}{\delta \varphi_a(q_1)} \\
&= -\sum_{\substack{i,j \\ k,l}}^N \int_{\substack{p'_1, p'_2 \\ p_3, p_4}} \frac{1}{\Gamma_{k,bk}^{(2)}(q_2, p_3)} \frac{\delta \Gamma_{k,kl}^{(2)}(p_3, p_4)}{\delta \Gamma_{k,ij}^{(2)}(p_1, p_2)} \frac{1}{\Gamma_{k,lc}^{(2)}(p_4, q_3)} \Gamma_{k,aij}^{(3)}(q_1, p_1, p_2) \tag{137} \\
&= -\sum_{i,j=1}^N \int_{p'_1, p'_2} \frac{\Gamma_{k,aij}^{(3)}(q_1, p_1, p_2)}{\Gamma_{k,bi}^{(2)}(q_2, p_1) \Gamma_{k,cj}^{(2)}(p_2, q_3)}.
\end{aligned}$$

¹⁰A primed integration variable indicates that it does not include the factor $T/(2\pi)^d$ as in eq. (88), but rather $\int_{p'} = \sum_{p_0} \int_{\mathbb{R}^d} d^d p$ as appropriate for the functional chain rule.

Taking a further derivative $\delta/\delta\varphi_b(q_2)$ of (135) yields the flow equation for the 2-point function,

$$\partial_t \Gamma_{k,ab}^{(2)}(q_1, q_2) = \frac{1}{2} \sum_{\substack{i,j,k \\ l,m,n}}^N \int \partial_t R_{k,ij}(p_1, p_2) \quad (138)$$

$$\times \left(G_{k,jk}(p_2, p_3) \Gamma_{k,akl}^{(3)}(q_1, p_3, -p_4) G_{k,lm}(p_4, p_5) \Gamma_{k,bmn}^{(3)}(-q_2, p_5, -p_6) G_{k,ni}(p_6, p_1) \quad (139)$$

$$+ G_{k,jm}(p_2, p_5) \Gamma_{k,bmn}^{(3)}(-q_2, p_5, -p_6) G_{k,nk}(p_6, p_3) \Gamma_{k,akl}^{(3)}(q_1, p_3, -p_4) G_{k,li}(p_4, p_1) \quad (140)$$

$$- G_{k,jk}(p_2, p_3) \Gamma_{k,abkl}^{(4)}(q_1, -q_2, p_3, -p_4) G_{k,li}(p_4, p_1) \Big), \quad (141)$$

where

$$(139) = \begin{array}{c} \partial_k R_{k,ij}(p_1, p_2) \\ G_{k,jk}(p_2, p_3) \quad G_{k,ni}(p_6, p_1) \\ \begin{array}{c} \xrightarrow{q_1} \quad \xrightarrow{q_2} \\ \varphi_a \quad \varphi_b \end{array} \\ \Gamma_{k,akl}^{(3)}(q_1, p_3, -p_4) \quad \Gamma_{k,bmn}^{(3)}(-q_2, p_5, -p_6) \\ G_{k,lm}(p_4, p_5) \end{array}, \quad (142)$$

$$(140) = \begin{array}{c} G_{k,nk}(p_6, p_3) \\ \Gamma_{k,akl}^{(3)}(q_1, p_3, -p_4) \quad \Gamma_{k,bmn}^{(3)}(-q_2, p_5, -p_6) \\ \begin{array}{c} \xrightarrow{q_1} \quad \xrightarrow{q_2} \\ \varphi_a \quad \varphi_b \end{array} \\ G_{k,li}(p_4, p_1) \quad G_{k,jm}(p_2, p_5) \\ \partial_k R_{k,ij}(p_1, p_2) \end{array}, \quad (143)$$

$$(141) = \begin{array}{c} \partial_k R_{k,ij}(p_1, p_2) \\ G_{k,jk}(p_2, p_3) \quad G_{k,li}(p_4, p_1) \\ \begin{array}{c} \xrightarrow{q_1} \quad \xrightarrow{q_2} \\ \varphi_a \quad \varphi_b \end{array} \\ \Gamma_{k,abkl}^{(4)}(q_1, -q_2, p_3, -p_4) \end{array}. \quad (144)$$

(Sums over indices and integrals over momenta apply only to diagrams in which they appear, i.e. m, n, p_5 and p_6 are not traced in the third diagram.)

By undoing the cutoff derivative, (138) reduces to

$$\begin{aligned} \partial_t \Gamma_{k,ab}^{(2)}(q_1, q_2) = & \frac{1}{2} \sum_{\substack{i,j \\ k,l}}^N \int \tilde{\partial}_t \left[G_{k,ij}(p_1, p_2) \Gamma_{k,abji}^{(4)}(q_1, -q_2, p_1, -p_2) \right. \\ & \left. - G_{k,ij}(p_1, p_2) \Gamma_{k,akl}^{(3)}(q_1, p_2, -p_3) G_{k,kl}(p_3, p_4) \Gamma_{k,bli}^{(3)}(-q_2, -p_1, p_4) \right] \quad (145) \end{aligned}$$

$$= \frac{1}{2} \sum_{\substack{i,j \\ k,l}}^N \sum_{\substack{p_1,p_2 \\ p_3,p_4}} \tilde{\partial}_t \left(\begin{array}{c} \text{Diagram 1: } G_{k,ij}(p_1, p_2) \text{ loop with } p_1, p_2 \text{ and } \varphi_a, \varphi_b \text{ external lines.} \\ \Gamma_{k,abji}^{(4)}(q_1, -q_2, -p_1, p_2) \end{array} - \begin{array}{c} \text{Diagram 2: } G_{k,ij}(p_1, p_2) \text{ loop with } p_1, p_2, p_3, p_4 \text{ and } \varphi_a, \varphi_b \text{ external lines.} \\ \Gamma_{k,ajk}^{(3)}(q_1, p_2, -p_3) \Gamma_{k,bli}^{(3)}(-q_2, -p_1, p_4) \\ G_{k,kl}(p_3, p_4) \end{array} \right).$$

Despite what we said in item 2 on page 27, we will now make the simplifying assumption of momentum-independent vertices. This has two important consequences.

1. The effective vertices $\Gamma_k^{(n)}$ follow more easily as field derivatives not of the entire effective action Γ_k but only its momentum-independent part, i.e. the effective potential $U_k(\rho)$.
2. Since we are working with amputated diagrams, neglecting the momentum-dependence of vertices renders (144) and the first diagram in (145) q -independent. As a result, it drops out of all flow equations upon projecting with ∂_{q^2} or disc_{q_0} so we don't need to consider it (nor the 4-point function) further.

Using the Feynman rules derived in sec. 4.3, we can assemble an algebraic expression for the r.h.s. of (145). For $a = b = 1$ and $q_1 = q_2 = q$ (as appropriate for quantum fluctuations generating the scale dependence of Z_1 and γ_1^2), the second diagram evaluates to

$$- \frac{1}{2} \sum_{\substack{i,j \\ k,l}}^N \sum_{\substack{p_1,p_2 \\ p_3,p_4}} \begin{array}{c} \text{Diagram 2: } G_{k,ij}(p_1, p_2) \text{ loop with } p_1, p_2, p_3, p_4 \text{ and } \varphi_a, \varphi_b \text{ external lines.} \\ \Gamma_{k,ajk}^{(3)}(q_1, p_2, -p_3) \Gamma_{k,bli}^{(3)}(-q_2, -p_1, p_4) \\ G_{k,kl}(p_3, p_4) \end{array} \quad (a = b = 1, \quad q_1 = q_2 = q) \quad (146)$$

$$= -\frac{1}{2} \left(\varphi_c^3 U_k''' + 3\varphi_c U_k'' \right)^2 \sum_p G_r(p) G_r(q+p) - \frac{1}{2} (N-1) \varphi_c^2 (U_k'')^2 \sum_p G_g(p) G_g(q+p),$$

where G_r and G_g denote the (renormalized) radial and Goldstone propagators,

$$G_r(p) = \frac{1}{Z_1 p^2 + U_k'(\rho_c) + 2\rho_c U_k''(\rho_c) - is(p_0) \gamma_1^2 + R_k(p)/Z_k}, \quad (147)$$

$$G_g(p) = \frac{1}{p^2 + U_k'(\rho_c) + R_k(p)/Z_k}$$

The index summation and momentum integration in (146) were carried out separately, the former yielding

$$\sum_{i,j,k,l=1}^N G_{ij} \left[\varphi_c^3 U_k''' \delta_{11} \delta_{j1} \delta_{k1} + \varphi_c U_k'' \left(\delta_{11} \delta_{jk} + \delta_{j1} \delta_{k1} + \delta_{k1} \delta_{j1} \right) \right]$$

$$\times G_{kl} \left[\varphi_c^3 U_k''' \delta_{11} \delta_{i1} \delta_{l1} + \varphi_c U_k'' \left(\delta_{11} \delta_{il} + \delta_{i1} \delta_{l1} + \delta_{i1} \delta_{l1} \right) \right] \quad (148)$$

$$= \left(\varphi_c^3 U_k''' + 3\varphi_c U_k'' \right)^2 G_r^2 + (N-1) \varphi_c^2 (U_k'')^2 G_g^2,$$

while for the latter, three of the four momentum integrals are trivial,

$$\sum_{\substack{p_1,p_2 \\ p_3,p_4}} \delta(q + p_2 - p_3) G(p_1) \delta(p_1 - p_2) \delta(-q - p_1 + p_4) G(p_3) \delta(p_3 - p_4) = \frac{T \delta(0)}{(2\pi)^d} \sum_p G(p) G(q+p). \quad (149)$$

Notice the $T \delta(0)/(2\pi)^d$ which cancels with the one in eqs. (124) and (131). Thus the flow equations for Z_1 and γ_1 read

$$\left. \begin{aligned} \partial_t Z_1 \\ \partial_t \gamma_1^2 \end{aligned} \right\} = \left\{ \begin{aligned} \eta Z_1 + \partial_{q^2} \\ \eta \gamma_1^2 + \text{disc}_{q_0} \end{aligned} \right\} \frac{1}{Z_k} \tilde{\partial}_t \left[-\frac{1}{2} \left(\varphi_c^3 U_k''' + 3\varphi_c U_k'' \right)^2 \sum_p G_r(p) G_r(q+p) \right. \\ \left. - \frac{1}{2} (N-1) \varphi_c^2 (U_k'')^2 \sum_p G_g(p) G_g(q+p) \right]. \quad (150)$$

Using $\varphi_c = \sqrt{2\rho_c}$, the prefactor of the radial propagator arising from the momentum-independent vertices can be expanded into

$$\frac{1}{2} \left(\varphi_c^3 U_k''' + 3\varphi_c U_k'' \right)^2 = 4\rho_c^3 (U_k''')^2 + 12\rho_c^2 U_k'' U_k''' + 9\rho_c (U_k'')^2. \quad (151)$$

For our choice of a quartic effective potential of the form (65) this reduces to

$$4\rho_c^3 (U_k''')^2 + 12\rho_c^2 U_k'' U_k''' + 9\rho_c (U_k'')^2 = 9\rho_c \lambda^2. \quad (152)$$

Moving on to derive the flow of Z_k , we set $a = b = 2$. The index summation now yields

$$\sum_{i,j,k,l=1}^N G_{ij} \left[\varphi_c^3 U_k''' \delta_{21} \delta_{j1} \delta_{k1} + \varphi_c U_k'' \left(\delta_{21} \delta_{jk} + \delta_{j1} \delta_{k2} + \delta_{k1} \delta_{j1} \right) \right] \\ G_{kl} \left[\varphi_c^3 U_k''' \delta_{11} \delta_{i1} \delta_{l1} + \varphi_c U_k'' \left(\delta_{11} \delta_{il} + \delta_{i1} \delta_{l1} + \delta_{i1} \delta_{l1} \right) \right] \\ = 2\varphi_c^2 (U_k'')^2 G_r G_g. \quad (153)$$

The structure of Dirac deltas remains the same. Thus the flow equation for Z_k is

$$\partial_t Z_k = -\frac{1}{2} \partial_{q^2} \tilde{\partial}_t 2\varphi_c^2 (U_k'')^2 \sum_p G_r(p) G_g(q+p). \quad (154)$$

We now introduce the threshold functions $\tilde{\partial}_t J_{ab}^{ij} = \tilde{\partial}_t \sum_p G_a^i(p) G_b^j(q+p)$, where $a, b \in \{r, g\}$ specify the type of fields running in the loop (radial or Goldstone mode). In our truncation they take the following explicit forms,

$$J_{11}^{ij} = J_{11}^{ij}(q, z_1, z_2, m_1^2, m_2^2, \gamma_1^2, \gamma_2^2, R) \\ = \sum_p \frac{1}{(z_1 p^2 + m_1^2 - is(p_0) \gamma_1^2 + R)^i} \frac{1}{(z_2 (p+q)^2 + m_2^2 - is(p_0 + q_0) \gamma_2^2 + R)^j}, \\ J_{22}^{ij} = J_{22}^{ij}(q, 1, 1, 0, 0, 0, 0, R) = \sum_p \frac{1}{(p^2 + R)^i} \frac{1}{((p+q)^2 + R)^j}, \\ J_{12}^{ij} = J_{12}^{ij}(q, z_1, 1, m_1^2, 0, \gamma_1^2, 0, R) = \sum_p \frac{1}{(z_1 p^2 + m_1^2 - is(p_0) \gamma_1^2 + R)^i} \frac{1}{((p+q)^2 + R)^j}. \quad (155)$$

Using the shorthand notation $J_{ab}^{11} = J_{ab}$, we can write the flow equations (150) and (154) for $\rho_c = \rho_0$ very compactly,

$$\partial_t Z_1 = \eta Z_1 - \partial_{q^2} \tilde{\partial}_t \rho_0 \lambda^2 [9 J_{11} + (N-1) J_{22}], \quad (156)$$

$$\partial_t \gamma_1^2 = \eta \gamma_1^2 - \text{disc}_{q_0} \tilde{\partial}_t \rho_0 \lambda^2 [9 J_{11} + (N-1) J_{22}], \quad (157)$$

$$\partial_t Z_k = -\partial_{q^2} \tilde{\partial}_t 2\rho_0 \lambda^2 J_{12}. \quad (158)$$

To describe on-shell excitations of the radial field, (156) and (157) should be evaluated at the external energy $q^2 = 2\rho_0 \lambda^2 / Z_1$, whereas Goldstone bosons are on-shell for $q^2 = 0$ which is where we evaluate (158). It is worth noting, however, that if we were interested in virtual particles, we would be free to solve the flow equations (156) to (158) for arbitrary q .

5. Matsubara Summation

Our goal in this section is to analytically perform the summation over Matsubara frequencies $i\omega_n$, $n \in \mathbb{Z}$ which for $T > 0$ is part of the trace Tr on the r.h.s. of all flow equations. We will carry out the summation on the level of the threshold functions I_j and $\tilde{\partial}_t J_{ab}^{ij}$. They provide a unified means of formulating flow equations, allowing us to perform the summation once and apply it to multiple flow equations by virtue of the recursive relation (66).

In sec. 5.1 we show how the class of regulators introduced in sec. 4.2 enables us to decompose the regularized propagator $G_k(p) = (P_k + R_k)^{-1}$ into a sum of free propagators [1]. This will be the crucial ingredient that allows us to perform the Matsubara summations in I_j in sec. 5.2 and in J_{ij} in sec. 5.3 analytically.

5.1. Propagator Decomposition

The choices (100) and (102) for the inverse propagator P_k and regulator R_k ,

$$P_k = Z_k \left[z p^2 + m^2 - i s(p_0) \gamma^2 \right], \quad R_k(p) = \frac{Z_k k^2}{1 + c \frac{p^2}{k^2}} \quad (159)$$

enable us to conveniently decompose the regularized propagator $(P_k + R_k)^{-1}$ [1]. A detailed calculation can be found in app. A.2. Here we only quote the final result,

$$\frac{1}{P_k + R_k} = \frac{1}{Z_k} \left(\frac{\beta^+}{p^2 + \alpha^+ k^2} + \frac{\beta^-}{p^2 + \alpha^- k^2} \right), \quad (160)$$

with dimensionless complex scale-dependent coefficients

$$\begin{aligned} \alpha^\pm &= \frac{1}{2} \left(\frac{1}{c} + \frac{\tilde{m}^2}{z} - i s(p_0) \frac{\tilde{\gamma}^2}{z} \right) \pm (A + i s(p_0) B), \\ \beta^\pm &= \frac{1}{2z} \pm (C + i s(p_0) D), \end{aligned} \quad (161)$$

where $\tilde{m}^2 = m^2/k^2$, $\tilde{\gamma}^2 = \gamma^2/k^2$ and

$$A = \frac{1}{2i} \left[\sqrt{\frac{1}{cz} - \frac{1}{4} \left(\frac{1}{c} - \frac{\tilde{m}^2}{z} - \frac{i\tilde{\gamma}^2}{z} \right)^2} - \sqrt{\frac{1}{cz} - \frac{1}{4} \left(\frac{1}{c} - \frac{\tilde{m}^2}{z} + \frac{i\tilde{\gamma}^2}{z} \right)^2} \right], \quad (162)$$

$$B = \frac{1}{2} \left[\sqrt{\frac{1}{cz} - \frac{1}{4} \left(\frac{1}{c} - \frac{\tilde{m}^2}{z} - \frac{i\tilde{\gamma}^2}{z} \right)^2} + \sqrt{\frac{1}{cz} - \frac{1}{4} \left(\frac{1}{c} - \frac{\tilde{m}^2}{z} + \frac{i\tilde{\gamma}^2}{z} \right)^2} \right], \quad (163)$$

$$C = -\frac{A \left(\frac{1}{c} - \frac{\tilde{m}^2}{z} \right) + B \frac{\tilde{\gamma}^2}{z}}{4z(A^2 + B^2)}, \quad D = \frac{B \left(\frac{1}{c} - \frac{\tilde{m}^2}{z} \right) - A \frac{\tilde{\gamma}^2}{z}}{4z(A^2 + B^2)}. \quad (164)$$

(160) closely resembles the sum of two free propagators, which significantly simplifies calculations. Choosing the branch cut of the complex square root along the negative real axis ensures that A , B , C and D are always real. (Even though we set $c_0 = 1$, $c_1 = c > 0$, $c_j = 0 \forall j > 1$ to obtain this result, a similar decomposition is possible for the whole class of regulators (101).)

We showed in sec. 3.3 that the propagator $P_k^{-1}(p)$ may exhibit poles and branch cuts only on the real frequency axis. The same cannot be said for the regularized propagator $(P_k + R_k)^{-1}$. Since R_k brings with it its own analytic structure, $(P_k + R_k)^{-1}$ will in general feature singularities away from the real frequency axis [1]. In our case (160), for $\tilde{\gamma}^2/z - B < 0$ and $s(p_0) = 1$ there are poles at $p_0 = \pm \sqrt{p^2 + \alpha^+ k^2}$. A Källén-Lehmann spectral representation of the form (78) is therefore not possible for $(P_k + R_k)^{-1}$. Although a proof is still pending, this is believed to be a generic feature of cutoff functions that serve as effective UV regulators in Minkowski space [1]. Notably, $(P_k + R_k)^{-1}$ also has a branch cut. However, assuming all integrals along this branch cut are dominated by nearby poles on the different Riemann sheets, it will not inhibit our analytic treatment.

5.2. Effective Potential

We now perform the Matsubara summation for the simplest threshold function I_0 [68]. We can afterwards extend the result to higher-orders I_j with $j \geq 1$ by using the relation (66), $\partial_{m^2} I_j = (\delta_{j0} - j) I_{j+1}$. I_0 was defined as (cf. eq. (116))

$$\begin{aligned} I_0(Z_k, z, m^2, \gamma^2, R_k) &= T \sum_{p_0} \int_{\mathbf{p}} \frac{\partial_t R_k / Z_k}{z p^2 + m^2 - i s(p_0) \gamma^2 + R_k / Z_k} \\ &= \not\sum_p \frac{\partial_t R_k}{P_k + R_k} = \tilde{\partial}_t \not\sum_p \ln(P_k + R_k). \end{aligned} \quad (165)$$

We denote the difference between I_0 evaluated at some intermediate renormalization scale k and in the ultraviolet Λ as ΔI_0 ,¹¹

$$\begin{aligned} \Delta I_0 &= \int_{\Lambda}^k \tilde{d}t I_0 = \not\sum_p [\ln(P_k + R_k) - \ln(P_{\Lambda} + R_{\Lambda})] \\ &= - \not\sum_p \left\{ \ln \frac{1}{Z_k} \left[\frac{\beta^+}{p^2 + \alpha^+ k^2} + \frac{\beta^-}{p^2 + \alpha^- k^2} \right] - \ln \frac{1}{Z_{\Lambda}} \left[\frac{\beta^+}{p^2 + \alpha^+ \Lambda^2} + \frac{\beta^-}{p^2 + \alpha^- \Lambda^2} \right] \right\}, \end{aligned} \quad (166)$$

where we inserted the decomposition (160). The tilde on $\tilde{d}t$ indicates that we integrate with respect to the explicit scale dependence in R_k only. Since the second term in ΔI_0 is k -independent, we can at any time easily recover I_0 by taking the $\tilde{\partial}_t$ derivative of ΔI_0 .

Using $Z_{\Lambda} = 1 \approx Z_k$, $\beta^+ + \beta^- = \frac{1}{z}$ and $\alpha^+ \beta^- + \alpha^- \beta^+ = \frac{1}{cz}$ (see (275)), we can write

$$\begin{aligned} - \ln \left(\frac{\beta^+}{p^2 + \alpha^+ k^2} + \frac{\beta^-}{p^2 + \alpha^- k^2} \right) &= \ln[(p^2 + \alpha^+ k^2)(p^2 + \alpha^- k^2)] \\ &\quad - \ln[\beta^+(p^2 + \alpha^- k^2) + \beta^-(p^2 + \alpha^+ k^2)] \\ &= \ln(p^2 + \alpha^+ k^2) + \ln(p^2 + \alpha^- k^2) - \ln\left(\frac{1}{z} p^2 + \frac{1}{cz} k^2\right), \end{aligned} \quad (167)$$

(and similarly for the Λ -term) so that ΔI_0 can also be written

$$\begin{aligned} \Delta I_0 &= \not\sum_p \left[\ln(p^2 + \alpha^+ k^2) + \ln(p^2 + \alpha^- k^2) - \ln(p^2 + \frac{1}{c} k^2) \right. \\ &\quad \left. - \ln(p^2 + \alpha^+ \Lambda^2) - \ln(p^2 + \alpha^- \Lambda^2) + \ln(p^2 + \frac{1}{c} \Lambda^2) \right], \end{aligned} \quad (168)$$

The terms in (168) can be pairwise combined into integrals,

$$T \sum_{p_0} \ln(p^2 + \alpha^+ k^2) - \ln(p^2 + \alpha^+ \Lambda^2) = \int_{\mathbf{p}^2 + \alpha^+ \Lambda^2}^{\mathbf{p}^2 + \alpha^+ k^2} dx^2 T \sum_{n \in \mathbb{Z}} \frac{1}{\omega_n^2 + x^2}, \quad (169)$$

and similarly for the other four terms. (Recall that $p^2 = -p_0^2 + \mathbf{p}^2$ where $p_0 \in \{i\omega_n = 2\pi i T n | n \in \mathbb{Z}\}$.) The Matsubara summation can then be expressed as the complex contour integral,

$$T \sum_{n \in \mathbb{Z}} \frac{1}{\omega_n^2 + x^2} = \oint_C \frac{dp_0}{2\pi i} \frac{1}{-p_0^2 + x^2} [n_B(p_0) + \frac{1}{2}], \quad (170)$$

where

$$n_B(p_0) = \frac{1}{e^{p_0/T} - 1} \quad (171)$$

is the Bose-Einstein distribution and C is the path shown in fig. 4.

¹¹This step serves as a type of implicit Pauli-Villars regularization with the heavy mass term replaced by the momentum-dependent $R_{\Lambda}(p)$ in the inverse propagator [13].

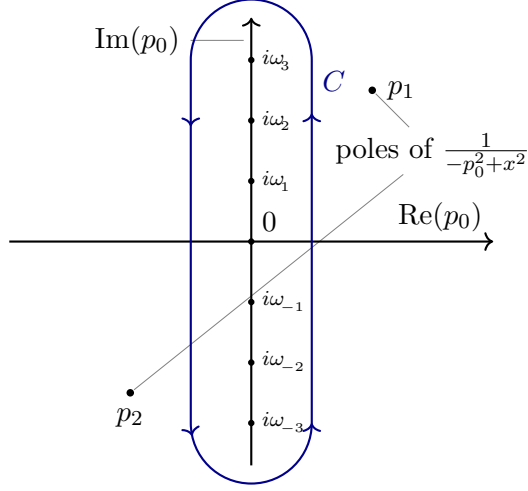


Figure 4: Counterclockwise path C around the imaginary p_0 -axis but excluding poles of $(-p_0^2+x^2)^{-1}$

In (170), we used that $n_B(p_0)$ has only simple poles located at all Matsubara frequencies $i\omega_n$, $n \in \mathbb{Z}$. At $p_0 = i\omega_n = i2\pi Tn$, we have $e^{p_0/T} = e^{2\pi i n} = 1$ and so the denominator in (171) vanishes. Using l'Hôpital's rule, we find that the residue at all poles is the temperature T ,

$$\lim_{p_0 \rightarrow i\omega_n} \frac{p_0 - i\omega_n}{e^{p_0/T} - 1} = \lim_{p_0 \rightarrow i\omega_n} \frac{T}{e^{p_0/T}} = T \quad \forall n \in \mathbb{Z}. \quad (172)$$

The $+\frac{1}{2}$ was merely added to antisymmetrize $n_B(-p_0) + \frac{1}{2} = -[n_B(p_0) + \frac{1}{2}]$. Applying (170) to all terms in ΔI_0 we get

$$\Delta I_0 = \int_p \left(\int_{p^2+\alpha+k^2} + \int_{p^2+\alpha-k^2} + \int_{p^2+k^2/c} \right) dx^2 \oint_C \frac{dp_0}{2\pi i} \frac{n_B(p_0) + \frac{1}{2}}{-p_0^2 + x^2}. \quad (173)$$

We now deform the contour C into a circle and take the radius to infinity. This will enclose the poles of $(-p_0^2+x^2)^{-1}$ scattered throughout the complex plane. Their contribution is removed again by enclosing them in clockwise contours as shown in fig. 5.

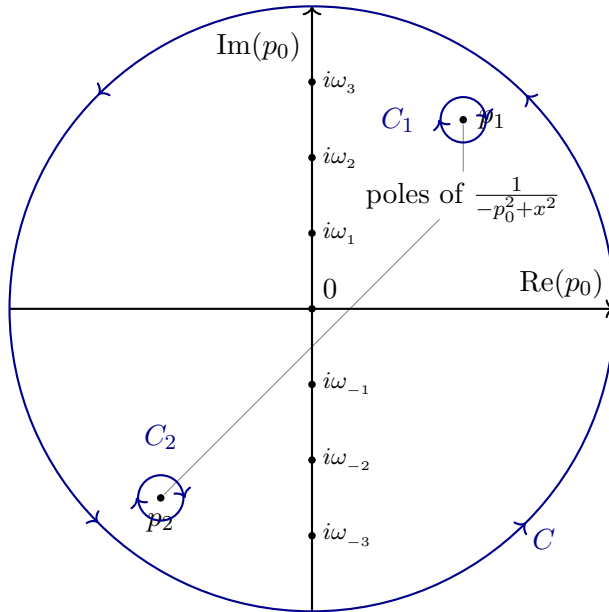


Figure 5: Sum of contours equivalent to C in fig. 4

Since the integrand (170) falls off faster than $1/p_0$, contributions from the circle C at infinity vanish. This contour is thus equivalent to the one in fig. 6 where we discarded C and blew up C_1 and C_2 to enclose the entire p_0 -plane save for the imaginary axis.

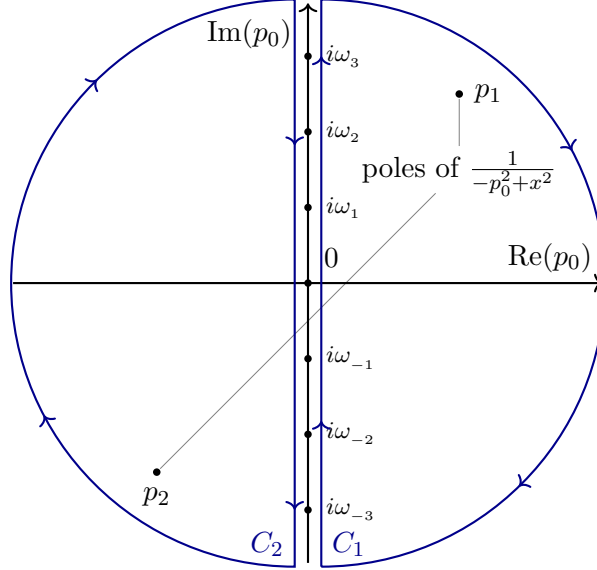


Figure 6: Contour enclosing the entire plane except for the imaginary axis

It is important in this context that α^\pm depends on $s(p_0)$ as this implies $x = x(s(p_0))$. The contour in (170) therefore encloses both poles and branch cuts. If there were only poles, we could simply invoke the residue theorem to turn the infinite sum over Matsubara frequencies (170) into a finite sum over the residues at the poles $p_0 = \pm x$ of $(-p_0^2 + x^2)^{-1}$. This would give

$$T \sum_{n \in \mathbb{Z}} \frac{1}{\omega_n^2 + x^2} = - \sum_{p_0 = \pm x} \text{Res} \frac{n_B(p_0) + \frac{1}{2}}{-p_0^2 + x^2} = - \frac{n_B(-x) - n_B(x)}{2x} = \frac{\coth(x/2T)}{2x}. \quad (174)$$

(The residues appear with a sign due to the clockwise contour.) Evaluating the contribution from the branch cuts, however, requires additional work. Using

$$\frac{1}{-p_0^2 + x^2} = \frac{1}{2x} \left(\frac{1}{p_0 + x} - \frac{1}{p_0 - x} \right) \quad (175)$$

and substituting $dx^2 = 2x dx$, (169) becomes

$$\begin{aligned} & T \sum_{n \in \mathbb{Z}} \ln(p^2 + \alpha^+ k^2) - \ln(p^2 + \alpha^+ \Lambda^2) \\ &= \int_{\sqrt{p^2 + \alpha^+ \Lambda^2}}^{\sqrt{p^2 + \alpha^+ k^2}} dx \oint_{C_1 + C_2} \frac{dp_0}{2\pi i} \left[\frac{1}{p_0 + x} - \frac{1}{p_0 - x} \right] [n_B(p_0) + \frac{1}{2}]. \end{aligned} \quad (176)$$

Note that the integral boundaries receive a square root when substituting $dx^2 \rightarrow dx$.

We can now use the structure of $s(p_0)$ plotted in fig. 7 to split the contour integral into two parts, the first being branch-cut free and the second with branch cut structure manifest.

$$\begin{aligned} (176) &= \frac{1}{2} \int_{C_1 + C_2} \frac{dp_0}{2\pi i} \left[\int_{\sqrt{p^2 + \alpha^+ \Lambda^2}}^{\sqrt{p^2 + \alpha^+ k^2}} + \int_{\sqrt{p^2 + \alpha^+ \Lambda^2}}^{\sqrt{p^2 + \alpha^+ k^2}} \right] dx \left[\frac{1}{p_0 + x} - \frac{1}{p_0 - x} \right] [n_B(p_0) + \frac{1}{2}] \\ &+ \frac{1}{2} \int_{C_1 + C_2} \frac{dp_0}{2\pi i} s(p_0) \left[\int_{\sqrt{p^2 + \alpha^+ \Lambda^2}}^{\sqrt{p^2 + \alpha^+ k^2}} - \int_{\sqrt{p^2 + \alpha^+ \Lambda^2}}^{\sqrt{p^2 + \alpha^+ k^2}} \right] dx \left[\frac{1}{p_0 + x} - \frac{1}{p_0 - x} \right] [n_B(p_0) + \frac{1}{2}]. \end{aligned} \quad (177)$$

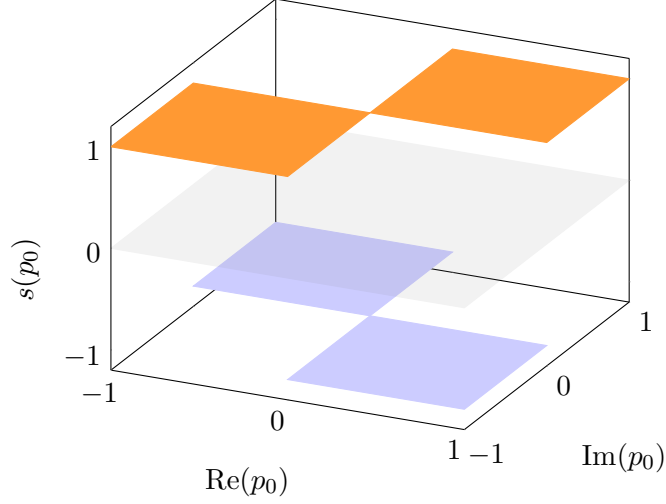


Figure 7: Structure of the sign function $s(p_0) = \text{sign}(\text{Re } p_0 \text{ Im } p_0)$

Observe that in the first and third quadrant of the complex plane where $s(p_0) = 1$, the first and third x -integrals in (177) combine to give (176) while the second and fourth cancel. Conversely, in the second and fourth quadrant $s(p_0) = -1$ and so the first and third x -integrals cancel while the second and fourth sum to (176). This split up is beneficial in two ways. Not only does it reveal the branch cut structure in ΔI_0 , it also separates the x -integration into parts where $s(p_0)$ takes a definite sign as reflected in the shorthand notation $\alpha^{\pm\pm} = \alpha^{\pm}(s(p_0) = \pm 1)$.

We now perform the p_0 -integration in the upper and lower line of (177) separately. The former contains only (simple) poles at $p_0 = \pm x$. The residues can be computed by the limit formula,

$$\text{Res}_{p_0=\mp x} \frac{1}{p_0 \pm x} = \lim_{p_0 \rightarrow \mp x} (p_0 \pm x) \frac{1}{p_0 \pm x} = 1. \quad (178)$$

The first line thus integrates to

$$\left[\int \frac{\sqrt{p^2 + \alpha^{++} k^2}}{\sqrt{p^2 + \alpha^{++} \Lambda^2}} + \int \frac{\sqrt{p^2 + \alpha^{+-} k^2}}{\sqrt{p^2 + \alpha^{+-} \Lambda^2}} \right] dx [n_B(x) + \frac{1}{2}] \quad (179)$$

Due to $s(p_0)$, the integral on the second line encloses a branch cut along the real p_0 -axis in addition to the poles at $p_0 = \pm x$. The contribution from the poles alone is

$$\left[\int \frac{\sqrt{p^2 + \alpha^{++} k^2}}{\sqrt{p^2 + \alpha^{++} \Lambda^2}} - \int \frac{\sqrt{p^2 + \alpha^{+-} k^2}}{\sqrt{p^2 + \alpha^{+-} \Lambda^2}} \right] dx s_I(x) [n_B(x) + \frac{1}{2}], \quad (180)$$

where $s_I(x) = \text{sign}(\text{Im } x)$. To isolate the contribution from the branch cut, we integrate along the

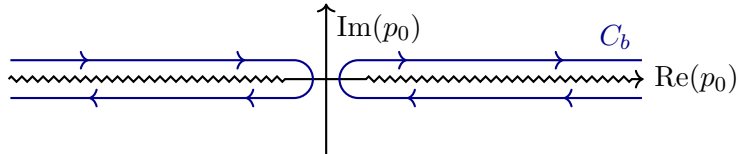


Figure 8: Contour C_b suitable to evaluate only branch cut contributions

contour C_b in fig. 8. C_b amounts to an integral from 0 to ∞ and one from $-\infty$ to 0. We integrate twice along these stretches in opposite directions. Usually the resulting contributions cancel. In

our case, however, $s_I(p_0) = -1$ along the lower lines so we get a factor of 2,

$$\begin{aligned} \int_{C_b} \frac{dp_0}{2\pi i} &= \int_{-\infty}^0 \frac{dp_0}{2\pi i} \underbrace{s_I(p_0 + i\epsilon)}_1 + \int_0^{-\infty} \frac{dp_0}{2\pi i} \underbrace{s_I(p_0 - i\epsilon)}_{-1} \\ &+ \int_0^{\infty} \frac{dp_0}{2\pi i} \underbrace{s_I(p_0 + i\epsilon)}_1 + \int_{\infty}^0 \frac{dp_0}{2\pi i} \underbrace{s_I(p_0 - i\epsilon)}_{-1} = 2 \int_{-\infty}^0 \frac{dp_0}{2\pi i} + 2 \int_0^{\infty} \frac{dp_0}{2\pi i}, \end{aligned} \quad (181)$$

Exchanging bounds on the first integral and substituting $p_0 \rightarrow -p_0$ (which leaves the integrand $(p_0 + x)^{-1} - (p_0 - x)^{-1}$ invariant), the total contribution from the cut is therefore

$$\left[\int_{\sqrt{p^2 + \alpha^{++}\Lambda^2}}^{\sqrt{p^2 + \alpha^{++}k^2}} - \int_{\sqrt{p^2 + \alpha^{+-}\Lambda^2}}^{\sqrt{p^2 + \alpha^{+-}k^2}} \right] dx 2 \int_0^{\infty} \frac{dp_0}{2\pi i} \left[\frac{1}{p_0 + x} - \frac{1}{p_0 - x} \right] \left[n_B(p_0) + \frac{1}{2} \right] \quad (182)$$

Away from the imaginary axis the Bose-Einstein distribution plotted in fig. 9 becomes approximately flat, particularly at sufficiently low temperatures. We assume $|\text{Re}(x)| \gg 0$ (which is satisfied unless $p^2 + \text{Re}(\alpha^{\pm\pm})k^2 < 0$ and $\text{Im}(\alpha^{\pm\pm})k^2 \approx 0$) so that the distribution is approximately constant across the width of the poles in (182). Since p_0 is integrated from 0 to ∞ , these integrals are dominated by the poles at $p_0 = x$ (as opposed to those at $p_0 = -x$) so we make the simplifying replacement $n_B(p_0) \rightarrow n_B(x)$. This allows us to write

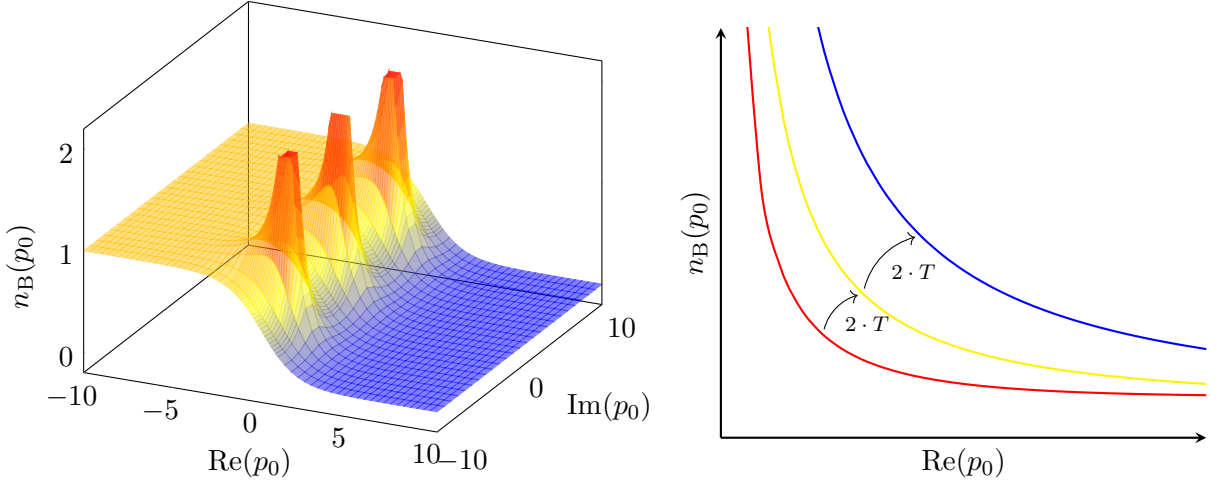


Figure 9: Bose distribution plotted over the complex plane and for different temperatures

$$2 \int_0^{\infty} \frac{dp_0}{2\pi i} \left[\frac{1}{p_0 + x} - \frac{1}{p_0 - x} \right] = \int_{-\infty}^{\infty} \frac{dp_0}{2\pi i} \left[\frac{1}{p_0 + x} - \frac{1}{p_0 - x} \right] = -s_I(x). \quad (183)$$

Plugging this back into (182), we find that it precisely cancels with the contribution (180) from the poles. The result of the Matsubara summation in (176) is therefore simply given by (179). Executing the x -integration we get (179)

$$\begin{aligned} \sum_{p_0} \left[\ln(p^2 + \alpha^+ k^2) - \ln(p^2 + \alpha^+ \Lambda^2) \right] &= \left(\int_{\sqrt{p^2 + \alpha^{++}\Lambda^2}}^{\sqrt{p^2 + \alpha^{++}k^2}} + \int_{\sqrt{p^2 + \alpha^{+-}\Lambda^2}}^{\sqrt{p^2 + \alpha^{+-}k^2}} \right) dx \left[n_B(x) + \frac{1}{2} \right] \\ &= \frac{1}{2} \left[\sqrt{p^2 + \alpha^{++}k^2} - \sqrt{p^2 + \alpha^{++}\Lambda^2} + \sqrt{p^2 + \alpha^{+-}k^2} - \sqrt{p^2 + \alpha^{+-}\Lambda^2} \right] \\ &+ T \left[\ln \left(\frac{e^{\sqrt{p^2 + \alpha^{++}k^2}/T} - 1}{e^{\sqrt{p^2 + \alpha^{++}\Lambda^2}/T} - 1} \right) + \ln \left(\frac{e^{\sqrt{p^2 + \alpha^{+-}k^2}/T} - 1}{e^{\sqrt{p^2 + \alpha^{+-}\Lambda^2}/T} - 1} \right) \right], \end{aligned} \quad (184)$$

where we used

$$\int_a^b \left(\frac{1}{e^{x/T} - 1} + \frac{1}{2} \right) dx = \frac{1}{2}(b - a) + T \ln \left(\frac{e^{b/T} - 1}{e^{a/T} - 1} \right). \quad (185)$$

The second bracket in (184) disappears for $T \rightarrow 0^+$ so the threshold functions split up into a term that carries the entire temperature dependence and a T -independent offset. In total, ΔI_0 after Matsubara summation reads

$$\Delta I_0 = \int_{\mathbf{p}} \sum_{j=1}^{10} w_j \left[\frac{1}{2} \sqrt{\mathbf{p}^2 + \mu_j} + T \ln \left(e^{\sqrt{\mathbf{p}^2 + \mu_j}/T} - 1 \right) \right], \quad (186)$$

where

j	1	2	3	4	5	6	7	8	9	10
μ_j	$\alpha^{++}k^2$	$\alpha^{+-}k^2$	$\alpha^{-+}k^2$	$\alpha^{--}k^2$	$\frac{1}{c}k^2$	$\alpha^{++}\Lambda^2$	$\alpha^{+-}\Lambda^2$	$\alpha^{-+}\Lambda^2$	$\alpha^{--}\Lambda^2$	$\frac{1}{c}\Lambda^2$
w_j	1	1	1	1	-2	-1	-1	-1	-1	2

The terms $\frac{1}{c}k^2$ and $\frac{1}{c}\Lambda^2$ appear with a factor of ± 2 because they are independent of $s(p_0)$. They therefore give the same contribution twice in (177) where we performed the split into $s(p_0) = 1$ and $s(p_0) = -1$. We can recover I_0 by taking the derivative with respect to explicit k -dependence of (186)

$$I_0 = \tilde{\partial}_t \Delta I_0 = \int_{\mathbf{p}} \sum_{j=1}^5 \frac{w_j}{2} \frac{\tilde{\partial}_t \mu_j}{\sqrt{\mathbf{p}^2 + \mu_j}} \left[\frac{1}{2} + \frac{1}{1 - e^{-\sqrt{\mathbf{p}^2 + \mu_j}/T}} \right]. \quad (187)$$

Recall that $\tilde{\partial}_t$ targets only the explicit scale dependence that was introduced into the regularized propagator $(P_k + R_k)^{-1}$ by the regulator $R_k = Z_k k^2 / (1 + c p^2 / k^2)$. The only explicit k -dependence in $\alpha^{\pm\pm}$ is contained in $\tilde{m}^2 = m^2 / k^2$ and $\tilde{\gamma}^2 = \gamma^2 / k^2$. By the chain rule $\tilde{\partial}_t \mu_j$ thus evaluates to

$$\tilde{\partial}_t \mu_j = k \tilde{\partial}_k \mu_j = \begin{cases} 2k^2 \alpha^{\pm\pm} - 2\tilde{m}^2 \partial_{\tilde{m}^2} \alpha^{\pm\pm} - 2\tilde{\gamma}^2 \partial_{\tilde{\gamma}^2} \alpha^{\pm\pm} & j \in \{1, 2, 3, 4\}, \\ 2k^2 / c & j = 5, \end{cases} \quad (188)$$

and zero for $j > 5$. Higher orders follow from I_0 by taking derivatives with respect to \tilde{m}^2 .

5.3. Propagator

We now perform the Matsubara summation for the threshold function $\tilde{\partial}_t J_{ab}$ in terms of which we formulated the flow equations for Z_k , Z_1 , and γ_1^2 . Consider [68]

$$\begin{aligned} J_{11} &= J_{11}(q, z_1, z_2, m_1^2, m_2^2, \gamma_1^2, \gamma_2^2, R) = \not\int_p G_1(p) G_2(p+q) \\ &= \not\int_p \frac{1}{z_1 p^2 + m_1^2 - is(p_0) \gamma_1^2 + R} \frac{1}{z_2 (p+q)^2 + m_2^2 - is(p_0 + q_0) \gamma_2^2 + R}. \end{aligned} \quad (189)$$

The two propagators can be decomposed according to (160),

$$G_1(p) = \frac{\beta_1^+}{-p_0^2 + \mathbf{p}^2 + \alpha_1^+ k^2} + \frac{\beta_1^-}{-p_0^2 + \mathbf{p}^2 + \alpha_1^- k^2}, \quad (190)$$

$$G_2(p+q) = \frac{\beta_2^+}{-(p_0 + q_0)^2 + \mathbf{p}^2 + \alpha_2^+ k^2} + \frac{\beta_2^-}{-(p_0 + q_0)^2 + \mathbf{p}^2 + \alpha_2^- k^2}. \quad (191)$$

We set $\mathbf{q} = 0$ since the external spatial momentum is irrelevant for the Matsubara summation. It affects neither the poles nor the branch cut structure in a qualitative way. We further defined

$$\begin{aligned} \alpha_1^\pm &= \alpha^\pm(m_1^2, \gamma_1^2, s(p_0), z_1, c), & \beta_1^\pm &= \beta^\pm(m_1^2, \gamma_1^2, s(p_0), z_1, c), \\ \alpha_2^\pm &= \alpha^\pm(m_2^2, \gamma_2^2, s(p_0 + q_0), z_2, c), & \beta_2^\pm &= \beta^\pm(m_2^2, \gamma_2^2, s(p_0 + q_0), z_2, c). \end{aligned} \quad (192)$$

Multiplying (190) and (191) we get four terms,

$$\begin{aligned}
J_{11} &= \sum_{i,j \in \pm} \oint_p \frac{\beta_1^i}{-p_0^2 + \mathbf{p}^2 + \alpha_1^i k^2} \frac{\beta_2^j}{-(p_0 + q_0)^2 + \mathbf{p}^2 + \alpha_2^j k^2} \\
&= \sum_{i,j \in \pm} \oint_p \frac{\beta_1^i}{2\sqrt{\mathbf{p}^2 + \alpha_1^i k^2}} \left[\frac{1}{-p_0 + \sqrt{\mathbf{p}^2 + \alpha_1^i k^2}} - \frac{1}{-p_0 - \sqrt{\mathbf{p}^2 + \alpha_1^i k^2}} \right] \\
&\quad \times \frac{\beta_2^j}{2\sqrt{\mathbf{p}^2 + \alpha_2^j k^2}} \left[\frac{1}{-(p_0 + q_0) + \sqrt{\mathbf{p}^2 + \alpha_2^j k^2}} - \frac{1}{-(p_0 + q_0) - \sqrt{\mathbf{p}^2 + \alpha_2^j k^2}} \right].
\end{aligned} \tag{193}$$

In the second step, we used the decomposition (175). (193) has four simple poles at

$$p_0 = \pm \sqrt{\mathbf{p}^2 + \alpha_1^i k^2} \quad \text{and} \quad p_0 = -q_0 \pm \sqrt{\mathbf{p}^2 + \alpha_2^j k^2}, \tag{194}$$

Due to the presence of $s(p_0)$ and $s(p_0 + q_0)$ in $\alpha_{1/2}^\pm$, $\beta_{1/2}^\pm$, the integrand (193) also exhibits branch cuts.¹² To deal with these cuts, we use the structure of $s(p_0)$ to decompose the integrand in a manner very similar to eq. (177) into a sum of four terms $J_{11} = J_1 + J_2 + J_3 + J_4$, each with a different branch cut structure parametrized by one of the following factors,

$$1, \quad s(p_0), \quad s(p_0 + q_0), \quad s(p_0) s(p_0 + q_0). \tag{195}$$

J_1 contains neither $s(p_0)$ nor $s(p_0 + q_0)$ and is thus branch-cut-free. It takes the form

$$\begin{aligned}
J_1 &= \frac{1}{4} \sum_{i,j \in \pm} \sum_{r,s \in \pm} \oint_p \frac{\beta_1^{ir}}{2\sqrt{\mathbf{p}^2 + \alpha_1^{ir} k^2}} \left[\frac{1}{-p_0 + \sqrt{\mathbf{p}^2 + \alpha_1^{ir} k^2}} - \frac{1}{-p_0 - \sqrt{\mathbf{p}^2 + \alpha_1^{ir} k^2}} \right] \\
&\quad \times \frac{\beta_2^{js}}{2\sqrt{\mathbf{p}^2 + \alpha_2^{js} k^2}} \left[\frac{1}{-(p_0 + q_0) + \sqrt{\mathbf{p}^2 + \alpha_2^{js} k^2}} - \frac{1}{-(p_0 + q_0) - \sqrt{\mathbf{p}^2 + \alpha_2^{js} k^2}} \right].
\end{aligned} \tag{196}$$

The J_i with $i > 1$ are identical except for additional factors of

$$J_2 : r s(p_0), \quad J_3 : s s(q_0 + p_0), \quad J_4 : r s(p_0) s(q_0 + p_0), \tag{197}$$

to be placed inside the sum and p_0 -integral. Since J_1 contains no cut, we can immediately carry out the Matsubara summation via contour integration as done previously. This will pick up the residues at the poles in (194), resulting in

$$\begin{aligned}
J_1 &= \frac{1}{4} \sum_{i,j,r,s} \int_{\mathbf{p}} \frac{\beta_1^{ir}}{2\sqrt{\mathbf{p}^2 + \alpha_1^{ir} k^2}} \frac{\beta_2^{js}}{2\sqrt{\mathbf{p}^2 + \alpha_2^{js} k^2}} \\
&\quad \left\{ \left[n_B(\sqrt{\mathbf{p}^2 + \alpha_1^{ir} k^2}) + \frac{1}{2} \right] \right. \\
&\quad \times \left(\frac{1}{-q_0 - \sqrt{\mathbf{p}^2 + \alpha_1^{ir} k^2} + \sqrt{\mathbf{p}^2 + \alpha_2^{js} k^2}} - \frac{1}{-q_0 - \sqrt{\mathbf{p}^2 + \alpha_1^{ir} k^2} - \sqrt{\mathbf{p}^2 + \alpha_2^{js} k^2}} \right. \\
&\quad \left. \left. + \frac{1}{-q_0 + \sqrt{\mathbf{p}^2 + \alpha_1^{ir} k^2} + \sqrt{\mathbf{p}^2 + \alpha_2^{js} k^2}} - \frac{1}{-q_0 + \sqrt{\mathbf{p}^2 + \alpha_1^{ir} k^2} - \sqrt{\mathbf{p}^2 + \alpha_2^{js} k^2}} \right) \right. \\
&\quad \left. + \left[n_B(\sqrt{\mathbf{p}^2 + \alpha_2^{js} k^2}) + \frac{1}{2} \right] \right. \\
&\quad \left. \right\} \quad \begin{array}{l} \text{(contribution from poles at } p_0 = \pm \sqrt{\mathbf{p}^2 + \alpha_1^{ir} k^2}) \\ \\ \\ \text{(contribution from poles at } p_0 = -q_0 \pm \sqrt{\mathbf{p}^2 + \alpha_2^{js} k^2}) \end{array}
\end{aligned} \tag{198}$$

¹²Our notation suggests q_0 and p_0 are real. Keep in mind that p_0, q_0 are analytically continued frequencies. Their original domain, the imaginary axis, was extended to the entire complex plane. This enables $s(p_0)$ and $s(p_0 + q_0)$ to parametrize branch cuts along the real frequency axis.

$$\times \left(\frac{1}{q_0 - \sqrt{\mathbf{p}^2 + \alpha_2^{js} k^2} + \sqrt{\mathbf{p}^2 + \alpha_1^{ir} k^2}} - \frac{1}{q_0 - \sqrt{\mathbf{p}^2 + \alpha_2^{js} k^2} - \sqrt{\mathbf{p}^2 + \alpha_1^{ir} k^2}} \right. \\ \left. + \frac{1}{q_0 + \sqrt{\mathbf{p}^2 + \alpha_2^{js} k^2} + \sqrt{\mathbf{p}^2 + \alpha_1^{ir} k^2}} - \frac{1}{q_0 + \sqrt{\mathbf{p}^2 + \alpha_2^{js} k^2} - \sqrt{\mathbf{p}^2 + \alpha_1^{ir} k^2}} \right) \quad (199)$$

$$= \frac{1}{4} \sum_{i,j,r,s} \int_{\mathbf{p}} \frac{\beta_1^{ir}}{2\sqrt{\mathbf{p}^2 + \alpha_1^{ir} k^2}} \frac{\beta_2^{js}}{2\sqrt{\mathbf{p}^2 + \alpha_2^{js} k^2}} \\ \times \left[\frac{n_B(\sqrt{\mathbf{p}^2 + \alpha_1^{ir} k^2}) + n_B(\sqrt{\mathbf{p}^2 + \alpha_2^{js} k^2}) + 1}{-q_0 + \sqrt{\mathbf{p}^2 + \alpha_1^{ir} k^2} + \sqrt{\mathbf{p}^2 + \alpha_2^{js} k^2}} + \frac{n_B(\sqrt{\mathbf{p}^2 + \alpha_1^{ir} k^2}) - n_B(\sqrt{\mathbf{p}^2 + \alpha_2^{js} k^2})}{-q_0 - \sqrt{\mathbf{p}^2 + \alpha_1^{ir} k^2} + \sqrt{\mathbf{p}^2 + \alpha_2^{js} k^2}} \right. \\ \left. - \frac{n_B(\sqrt{\mathbf{p}^2 + \alpha_1^{ir} k^2}) + n_B(\sqrt{\mathbf{p}^2 + \alpha_2^{js} k^2}) + 1}{-q_0 - \sqrt{\mathbf{p}^2 + \alpha_1^{ir} k^2} - \sqrt{\mathbf{p}^2 + \alpha_2^{js} k^2}} - \frac{n_B(\sqrt{\mathbf{p}^2 + \alpha_1^{ir} k^2}) - n_B(\sqrt{\mathbf{p}^2 + \alpha_2^{js} k^2})}{-q_0 + \sqrt{\mathbf{p}^2 + \alpha_1^{ir} k^2} - \sqrt{\mathbf{p}^2 + \alpha_2^{js} k^2}} \right]. \quad (200)$$

In (198), we used antisymmetry of $n_B(-p_0) + \frac{1}{2} = -[n_B(p_0) + \frac{1}{2}]$ to pull out an overall factor of $[n_B(\sqrt{\mathbf{p}^2 + \alpha_1^{ir} k^2}) + \frac{1}{2}]$ in front of all four terms, even though the last two terms originate from the pole at $p_0 = -\sqrt{\mathbf{p}^2 + \alpha_1^{ir} k^2}$ and therefore initially appear with a factor $[n_B(-\sqrt{\mathbf{p}^2 + \alpha_1^{ir} k^2}) + \frac{1}{2}]$. This gives rise to a relative sign in front of the last two terms which is compensated by another sign in front of $-(-p_0 - \sqrt{\mathbf{p}^2 + \alpha_1^{ir} k^2})^{-1}$. Likewise, in (199) we used $n_B(-p_0 - q_0) + \frac{1}{2} = -[n_B(p_0 + q_0) + \frac{1}{2}]$ which compensates the sign in front of $-[-(p_0 + q_0) - \sqrt{\mathbf{p}^2 + \alpha_2^{js} k^2}]^{-1}$. (200) follows from combining terms in (198) and (199).

The contributions from J_2 and J_3 vanish to good approximation. The reason is again the same cancellation between pole and branch cut contributions demonstrated for ΔI_0 in eqs. (180), (182) and (183). To see this explicitly, consider the integral

$$\int_{C_1+C_2} \frac{dp_0}{2\pi i} s(p_0) f(p_0) \left(\frac{1}{p_0 - E} - \frac{1}{p_0 + E} \right) [n_B(p_0) + \frac{1}{2}], \quad (201)$$

where C_1 and C_2 enclose the entire complex plane save the imaginary axis as shown in fig. 10. The poles at $p_0 = \pm E$ contribute

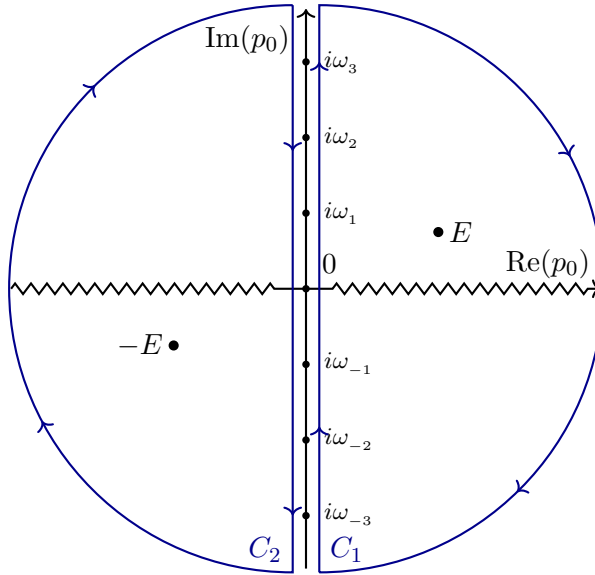


Figure 10: Contour enclosing poles and branch cuts of $J_{2/3}$ but excluding the Matsubara frequencies

$$- s(E) [f(E) + f(-E)] [n_B(E) + \frac{1}{2}], \quad (202)$$

where we used $s(E) = s(-E)$ and $n_B(-E) + \frac{1}{2} = -[n_B(E) + \frac{1}{2}]$. The overall sign comes from the clockwise contour. The branch cut is evaluated by shrinking C_1 and C_2 until all poles scattered throughout the complex plane are excluded. We can target only the contribution from the branch cut by again integrating along C_b in fig. 8. This gives

$$2 \left[\int_0^\infty - \int_{-\infty}^0 \right] \frac{dp_0}{2\pi i} f(p_0) \left(\frac{1}{p_0 - E} - \frac{1}{p_0 + E} \right) [n_B(p_0) + \frac{1}{2}]. \quad (203)$$

The factor of 2 comes from running back and forth along the real axis. The relative sign derives from $s(p_0)$ since $\text{sign}(\text{Re } p_0) < 0$ for the left half of the contour. For sufficiently large $\text{Re}(E)$ the first integral is strongly dominated by the pole at $p_0 = E$ while the second is dominated by $p_0 = -E$. That is because, as shown in fig. 9, $n_B(p_0)$ is approximately constant away from the real axis, especially at low temperatures. If we assume the same property for $f(p_0)$ (in the case of the J_i , this is even true exactly since they contain no p_0 -dependence besides the pole structure and the jump at $\text{Re } p_0 = 0$ due to $s(p_0)$), we can replace

$$[n_B(p_0) + \frac{1}{2}] \rightarrow [n_B(E) + \frac{1}{2}], \quad f(p_0) \rightarrow f(E) \quad (204)$$

in the first integral in (203), and

$$[n_B(p_0) + \frac{1}{2}] \rightarrow [n_B(-E) + \frac{1}{2}] = -[n_B(E) + \frac{1}{2}], \quad f(p_0) \rightarrow f(-E) \quad (205)$$

in the second. This gives

$$2 \left[\int_0^\infty f(E) + \int_{-\infty}^0 f(-E) \right] \frac{dp_0}{2\pi i} \left(\frac{1}{p_0 - E} - \frac{1}{p_0 + E} \right) [n_B(E) + \frac{1}{2}]. \quad (206)$$

Since the integrand is now symmetric with respect to $p_0 \rightarrow -p_0$, we have $2 \int_0^\infty = 2 \int_{-\infty}^0 = \int_{-\infty}^\infty$, and so (206) can be written

$$\int_{-\infty}^\infty \frac{dp_0}{2\pi i} [f(E) + f(-E)] \left(\frac{1}{p_0 - E} - \frac{1}{p_0 + E} \right) [n_B(E) + \frac{1}{2}]. \quad (207)$$

The integral can be closed with a half-circle at infinity and evaluated by means of the residue theorem, resulting in

$$s(E) [f(E) + f(-E)] [n_B(E) + \frac{1}{2}], \quad (208)$$

which precisely cancels the contribution (202) from the poles.

Finally, J_4 is proportional to $\gamma_1^2 \gamma_2^2$. In many cases, this vanishes exactly. For instance, if (at least) one of the particles running in the loop is a stable massless Goldstone boson with vanishing decay width $\Gamma = \gamma^2/m = 0$. Even if $\gamma_1^2 \neq 0 \neq \gamma_2^2$ are not zero for all p , J_4 will only receive contributions from those p for which both $\gamma_1^2(p^2) \neq 0$ and $\gamma_2^2(p^2) \neq 0$. Since $G(p)$ is without discontinuities if p^2 is positive, such p are few. Thus the value of J_4 is expected to be small even in cases where it is non-zero. It will therefore be neglected. In summary, we have approximately $J_{11} \approx J_1$ and the result of the Matsubara summation in J_{11} is simply (200).

Looking more closely at the expression (200) reveals that for $k > 0$, J_1 contains not only a single discontinuity on the real frequency axis but several jumps along lines that are approximately parallel to the real q_0 -axis as shown in fig. 11. The cuts are located at

$$q_0 = \sqrt{\mathbf{p}^2 + \alpha_1^{ir} k^2} + \sqrt{\mathbf{p}^2 + \alpha_2^{js} k^2} \quad \text{and} \quad q_0 = \left| \sqrt{\mathbf{p}^2 + \alpha_1^{ir} k^2} - \sqrt{\mathbf{p}^2 + \alpha_2^{js} k^2} \right|. \quad (209)$$

(Note that we were dealing with branch cuts in the p_0 -plane when we decomposed J_{11} into $J_1 + J_2 + J_3 + J_4$ and said that J_1 is branch cut-free. Now, we are looking at J_1 's branch cut structure in the q_0 -plane.)

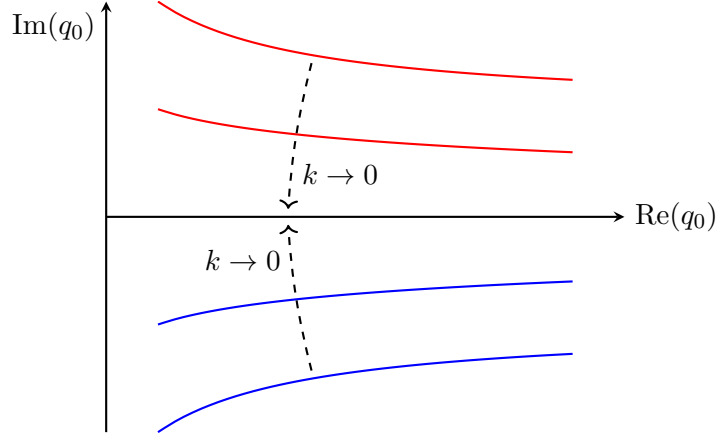


Figure 11: Branch cut structure of J_1 in the q_0 -plane

The cuts approach the real q_0 -axis with decreasing k where they merge for $k \rightarrow 0$. Instead of taking into account the complete analytic structure of J_1 , we approximate the regularized propagator as having only a single cut on the real q_0 -axis. To simplify the calculation, we sum the contributions from the different discontinuities at real q_0 even if they are shifted away from the real axis for $k \neq 0$. For $k \rightarrow 0$ this simplification converges on the correct result and for $k > 0$ it yields a reasonable approximation.

We project the cuts to the real q_0 -axis by replacing in (200)

$$\alpha_1^{ir} \rightarrow \text{Re } \alpha_1^{ir}, \quad \alpha_2^{js} \rightarrow \text{Re } \alpha_2^{js}. \quad (210)$$

This gives

$$\begin{aligned} \text{disc}_{q_0} J_1 = & \frac{1}{4} \sum_{i,j,r,s} \int_{\mathbf{p}} \frac{\beta_1^{ir}}{2\sqrt{\mathbf{p}^2 + \alpha_1^{ir} k^2}} \frac{\beta_2^{js}}{2\sqrt{\mathbf{p}^2 + \alpha_2^{js} k^2}} \left\{ \left[n_B(\sqrt{\mathbf{p}^2 + \alpha_1^{ir} k^2}) + n_B(\sqrt{\mathbf{p}^2 + \alpha_2^{js} k^2}) \right] \right. \\ & \times \text{sign}(\text{Re } \alpha_1^{ir} - \text{Re } \alpha_2^{js}) \pi \delta\left(q_0 - \left| \sqrt{\mathbf{p}^2 + \text{Re } \alpha_1^{ir} k^2} - \sqrt{\mathbf{p}^2 + \text{Re } \alpha_2^{js} k^2} \right| \right) \\ & \left. + \left[n_B(\sqrt{\mathbf{p}^2 + \alpha_1^{ir} k^2}) + n_B(\sqrt{\mathbf{p}^2 + \alpha_2^{js} k^2}) + 1 \right] \pi \delta\left(q_0 - \sqrt{\mathbf{p}^2 + \text{Re } \alpha_1^{ir} k^2} - \sqrt{\mathbf{p}^2 + \text{Re } \alpha_2^{js} k^2} \right) \right\}. \end{aligned} \quad (211)$$

6. Momentum Integration

6.1. Effective Potential

Since the integrand (186) of ΔI_0 depends only on the magnitude of \mathbf{p} , the d -dimensional momentum integration is best carried out in spherical coordinates with trivial angular integration [68],

$$\int_{\mathbf{p}} = \int_{\mathbb{R}^d} \frac{d^d \mathbf{p}}{(2\pi)^d} = S_d \int_0^\infty \frac{dp}{(2\pi)^d} p^{d-1}, \quad S_d = \frac{2\pi^{d/2}}{\Gamma(\frac{d}{2})}, \quad (212)$$

where S_d denotes the surface area of the d -dimensional unit sphere and $p = |\mathbf{p}|$ is no longer the 4-momentum but the spatial momentum magnitude. The temperature-dependent part of the \mathbf{p} -integral in (186) will be evaluated numerically. Considering only the T -independent part, we can proceed analytically.

$$\int d\mathbf{p} p^{d-1} \frac{1}{2} \sqrt{p^2 + \mu_j} = \begin{cases} \frac{1}{16} [p \sqrt{p^2 + \mu_j} (2p^2 + \mu_j) - \mu_j^2 \ln(p + \sqrt{p^2 + \mu_j})] & d = 3, \\ \frac{1}{6} [p^2 + \mu_j]^{3/2} & d = 2, \\ \frac{1}{4} [p \sqrt{p^2 + \mu_j} + \mu_j \ln(p + \sqrt{p^2 + \mu_j})] & d = 1. \end{cases} \quad (213)$$

Approximating (213) for $d = 3$ at the upper integration boundary where $p^2 \gg \mu_j$ gives

$$\begin{aligned} & \frac{1}{16} [p \sqrt{p^2 + \mu_j} (2p^2 + \mu_j) - \mu_j^2 \ln(p + \sqrt{p^2 + \mu_j})] \\ &= \frac{1}{16} \left[2p^4 \sqrt{1 + \frac{\mu_j}{p^2}} \left(1 + \frac{\mu_j}{2p^2}\right) - \mu_j^2 \ln \left(p + p \underbrace{\sqrt{1 + \frac{\mu_j}{p^2}}}_{\approx 1} \right) \right] \\ &\approx \frac{p^4}{8} \left(1 + \frac{\mu_j}{2p^2}\right) \left(1 + \frac{\mu_j}{2p^2}\right) - \frac{\mu_j^2}{16} \ln(2p) \approx \frac{p^4}{8} + \frac{\mu_j p^2}{8} + \frac{\mu_j^2}{32} - \frac{\mu_j^2}{16} \ln(2p), \end{aligned} \quad (214)$$

where we used $(1+x)^n \approx 1+nx$ for $x \ll 1$. In $d = 2$, the same boundary contributes

$$\frac{1}{6} (p^2 + \mu_j)^{3/2} = \frac{p^3}{6} \left(1 + \frac{\mu_j}{p^2}\right)^{3/2} \approx \frac{p^3}{6} + \frac{\mu_j p}{4}, \quad (215)$$

and in $d = 1$

$$\frac{1}{4} [p \sqrt{p^2 + \mu_j} + \mu_j \ln(p + \sqrt{p^2 + \mu_j})] \approx \frac{p^2}{4} + \frac{\mu_j}{8} + \frac{\mu_j}{4} \ln(2p). \quad (216)$$

Since $w_j = -w_{j+5}$ all the leading terms in (214) to (216) without a factor of μ_j cancel under the sum over j . Terms containing μ_j cancel as well up to a shift of the effective potential. To see why, consider

$$\alpha^{++} k^2 \alpha^{+-} k^2 + \alpha^{-+} k^2 \alpha^{--} k^2 = \frac{2m^2}{z} + \frac{2k^2}{c}, \quad (217)$$

and similarly for the $(k \rightarrow \Lambda)$ -term. Using the definition (276), we can calculate

$$\begin{aligned} & (\alpha^{++})^2 + (\alpha^{+-})^2 + (\alpha^{-+})^2 + (\alpha^{--})^2 \\ &= \left[\frac{1}{2} \left(\frac{1}{c} + \frac{\tilde{m}^2}{z} - i \frac{\tilde{\gamma}^2}{z} \right) + (A + iB) \right]^2 + \left[\frac{1}{2} \left(\frac{1}{c} + \frac{\tilde{m}^2}{z} + i \frac{\tilde{\gamma}^2}{z} \right) + (A - iB) \right]^2 \\ &+ \left[\frac{1}{2} \left(\frac{1}{c} + \frac{\tilde{m}^2}{z} - i \frac{\tilde{\gamma}^2}{z} \right) - (A + B) \right]^2 + \left[\frac{1}{2} \left(\frac{1}{c} + \frac{\tilde{m}^2}{z} + i \frac{\tilde{\gamma}^2}{z} \right) - (A - B) \right]^2 \\ &= \left(\frac{1}{c} + \frac{\tilde{m}^2}{z} \right)^2 - \frac{\tilde{\gamma}^4}{z^2} + 4(A^2 - B^2) \stackrel{(279)}{=} -\frac{4}{cz} + 2 \left(\frac{1}{c^2} + \frac{\tilde{m}^4}{z^2} - \frac{\tilde{\gamma}^4}{z^2} \right), \end{aligned} \quad (218)$$

where in the last step we used $4(A^2 - B^2) = -\frac{4}{cz} + \left(\frac{1}{c} - \frac{\tilde{m}^2}{z}\right)^2 - \frac{\tilde{\gamma}^4}{z^2}$. In combination one finds

$$\sum_{j=1}^{10} w_j \mu_j^2 = \frac{4}{cz} (\Lambda^4 - k^4). \quad (219)$$

This can be neglected since it is independent of \tilde{m}^2 and $\tilde{\gamma}^2$ and therefore only amounts to a temperature-independent shift of the effective potential, immaterial for most practical purposes. Thus, for $d \in \{1, 2, 3\}$, the contribution from the upper boundary of the momentum integration vanishes. The lower boundary, on the other hand, is non-zero and contributes with a minus sign,

$$\begin{aligned} & -\frac{1}{16} [p \sqrt{p^2 + \mu_j} (2p^2 + \mu_j) - \mu_j^2 \ln(p + \sqrt{p^2 + \mu_j})] \xrightarrow{p \rightarrow 0} \frac{1}{32} \mu_j^2 \ln(\mu_j), & d = 3, \\ & -\frac{1}{6} [p^2 + \mu_j]^{3/2} \xrightarrow{p \rightarrow 0} -\frac{1}{6} \mu_j^{3/2}, & d = 2, \\ & -\frac{1}{4} [p \sqrt{p^2 + \mu_j} + \mu_j \ln(p + \sqrt{p^2 + \mu_j})] \xrightarrow{p \rightarrow 0} -\frac{1}{8} \mu_j \ln(\mu_j), & d = 1, \end{aligned} \quad (220)$$

and in combination for ΔI_0 ,

$$\Delta I_0 = \frac{S_d}{(2\pi)^d} \sum_{j=1}^{10} w_j \begin{cases} \frac{1}{32} \mu_j^2 \ln(\mu_j) & d = 3, \\ -\frac{1}{6} \mu_j^{3/2} & d = 2, \\ -\frac{1}{8} \mu_j \ln(\mu_j) & d = 1. \end{cases} \quad (221)$$

The prefactor is

$$\frac{S_d}{(2\pi)^d} = \frac{1}{(2\pi)^d} \frac{2\pi^{d/2}}{\Gamma(\frac{d}{2})} = \begin{cases} \frac{1}{2\pi^2} & d = 3, \\ \frac{1}{2\pi} & d = 2, \\ \frac{1}{\pi} & d = 1. \end{cases} \quad (222)$$

We thus get the following explicit expressions for the dimensionless threshold functions $\tilde{I}_j = k^{2j-d-1}I_j$ for different values of d [68].

$d + 1 = 4$ Dropping again the shift of the effective potential (219), $\Delta\tilde{I}_0$ takes the form

$$\Delta\tilde{I}_0 = k^{-4} \Delta I_0 = k^{-4} \left[\frac{m^4 - \gamma^4}{32\pi^2 z^2} \ln(k^2/\Lambda^2) + \mathcal{K}_4^k k^4 - \mathcal{K}_4^\Lambda \Lambda^4 \right], \quad (223)$$

$$\tilde{I}_0 = k^{-4} \tilde{\partial}_t \Delta I_0 = \frac{\tilde{m}^4 - \tilde{\gamma}^4}{16\pi^2 z^2} + \left(4 - 2\tilde{m}^2 \partial_{\tilde{m}^2} - 2\tilde{\gamma}^2 \partial_{\tilde{\gamma}^2} \right) \mathcal{K}_4, \quad (224)$$

Recall that $\tilde{\partial}_t = k \tilde{\partial}_k$ only targets explicit k -dependence of R_k in ΔI_0 . The kernel \mathcal{K}_3^k is defined as

$$\begin{aligned} \mathcal{K}_4 &= \frac{1}{64\pi^2} \sum_{j=1}^4 w_j \mu_j^2 \ln(\mu_j) \\ &= \frac{1}{64\pi^2} \left[(\alpha^{++})^2 \ln(\alpha^{++}) + (\alpha^{+-})^2 \ln(\alpha^{+-}) + (\alpha^{-+})^2 \ln(\alpha^{-+}) + (\alpha^{--})^2 \ln(\alpha^{--}) \right]. \end{aligned} \quad (225)$$

Higher orders can be generated by taking derivatives with respect to $\tilde{m}^2 = m^2/k^2$.

$$\tilde{I}_1 = \partial_{\tilde{m}^2} \tilde{I}_0 = \frac{\tilde{m}^2}{8\pi^2 z^2} + \left(2\partial_{\tilde{m}^2} - 2\tilde{m}^2 \partial_{\tilde{m}^2}^2 - 2\tilde{\gamma}^2 \partial_{\tilde{m}^2} \partial_{\tilde{\gamma}^2} \right) \mathcal{K}_4, \quad (226)$$

$$\tilde{I}_2 = -\partial_{\tilde{m}^2} \tilde{I}_1 = -\frac{1}{8\pi^2 z^2} + \left(2\tilde{m}^2 \partial_{\tilde{m}^2}^3 + 2\tilde{\gamma}^2 \partial_{\tilde{m}^2}^2 \partial_{\tilde{\gamma}^2} \right) \mathcal{K}_4, \quad (227)$$

$$\tilde{I}_3 = -\frac{1}{2} \partial_{\tilde{m}^2} \tilde{I}_2 = -\frac{1}{2} \left(2\partial_{\tilde{m}^2}^3 + 2\tilde{m}^2 \partial_{\tilde{m}^2}^4 + 2\tilde{\gamma}^2 \partial_{\tilde{m}^2}^3 \partial_{\tilde{\gamma}^2} \right) \mathcal{K}_4, \quad (228)$$

$$\tilde{I}_4 = -\frac{1}{3} \partial_{\tilde{m}^2} \tilde{I}_3 = \frac{1}{6} \left(4\partial_{\tilde{m}^2}^4 + 2\tilde{m}^2 \partial_{\tilde{m}^2}^5 + 2\tilde{\gamma}^2 \partial_{\tilde{m}^2}^4 \partial_{\tilde{\gamma}^2} \right) \mathcal{K}_4. \quad (229)$$

$d + 1 = 3$ In two spatial dimensions,

$$\mathcal{K}_3 = -\frac{1}{12\pi} \sum_{j=1}^4 w_j \mu_j^{3/2} = -\frac{1}{12\pi} \left[(\alpha^{++})^{3/2} + (\alpha^{+-})^{3/2} + (\alpha^{-+})^{3/2} + (\alpha^{--})^{3/2} \right] \quad (230)$$

in terms of which the threshold functions read

$$\Delta\tilde{I}_0 = k^{-3} \left(\mathcal{K}_3^k k^3 - \mathcal{K}_3^\Lambda \Lambda^3 \right), \quad (231)$$

$$\tilde{I}_0 = k^{-3} \tilde{\partial}_t \Delta I_0 = \left(3 - 2\tilde{m}^2 \partial_{\tilde{m}^2} - 2\tilde{\gamma}^2 \partial_{\tilde{\gamma}^2} \right) \mathcal{K}_3, \quad (232)$$

$$\tilde{I}_1 = \partial_{\tilde{m}^2} \tilde{I}_0 = \left(\partial_{\tilde{m}^2} - 2\tilde{m}^2 \partial_{\tilde{m}^2}^2 - 2\tilde{\gamma}^2 \partial_{\tilde{m}^2} \partial_{\tilde{\gamma}^2} \right) \mathcal{K}_3, \quad (233)$$

$$\tilde{I}_2 = -\partial_{\tilde{m}^2} \tilde{I}_1 = \left(\partial_{\tilde{m}^2}^2 + 2\tilde{m}^2 \partial_{\tilde{m}^2}^3 + 2\tilde{\gamma}^2 \partial_{\tilde{m}^2}^2 \partial_{\tilde{\gamma}^2} \right) \mathcal{K}_3, \quad (234)$$

$$\tilde{I}_3 = -\frac{1}{2} \partial_{\tilde{m}^2} \tilde{I}_2 = -\frac{1}{2} \left(3\partial_{\tilde{m}^2}^3 + 2\tilde{m}^2 \partial_{\tilde{m}^2}^4 + 2\tilde{\gamma}^2 \partial_{\tilde{m}^2}^3 \partial_{\tilde{\gamma}^2} \right) \mathcal{K}_3, \quad (235)$$

$$\tilde{I}_4 = -\frac{1}{3} \partial_{\tilde{m}^2} \tilde{I}_3 = \frac{1}{6} \left(5\partial_{\tilde{m}^2}^4 + 2\tilde{m}^2 \partial_{\tilde{m}^2}^5 + 2\tilde{\gamma}^2 \partial_{\tilde{m}^2}^4 \partial_{\tilde{\gamma}^2} \right) \mathcal{K}_3. \quad (236)$$

$d + 1 = 2$ For a single dimension of space, the threshold functions take the form

$$\Delta \tilde{I}_0 = k^{-2} \left[-\frac{m^2}{4\pi z} \ln(k^2/\Lambda^2) + \mathcal{K}_2^k k^2 - \mathcal{K}_2^\Lambda \Lambda^2 \right], \quad (237)$$

$$\tilde{I}_0 = k^{-2} \tilde{\partial}_t \Delta I_0 = -\frac{m^2}{2zk^2} + \left(2 - 2\tilde{m}^2 \partial_{\tilde{m}^2} - 2\tilde{\gamma}^2 \partial_{\tilde{\gamma}^2} \right) \mathcal{K}_2, \quad (238)$$

$$\tilde{I}_1 = -\partial_{\tilde{m}^2} \tilde{I}_0 = \frac{1}{2z} + \left(2\tilde{m}^2 \partial_{\tilde{m}^2}^2 + 2\tilde{\gamma}^2 \partial_{\tilde{m}^2} \partial_{\tilde{\gamma}^2} \right) \mathcal{K}_2, \quad (239)$$

$$\tilde{I}_2 = -\partial_{\tilde{m}^2} \tilde{I}_1 = -\left(2\partial_{\tilde{m}^2}^2 + 2\tilde{m}^2 \partial_{\tilde{m}^2}^3 + 2\tilde{\gamma}^2 \partial_{\tilde{m}^2}^2 \partial_{\tilde{\gamma}^2} \right) \mathcal{K}_2, \quad (240)$$

$$\tilde{I}_3 = -\frac{1}{2} \partial_{\tilde{m}^2} \tilde{I}_2 = \frac{1}{2} \left(4\partial_{\tilde{m}^2}^3 + 2\tilde{m}^2 \partial_{\tilde{m}^2}^4 + 2\tilde{\gamma}^2 \partial_{\tilde{m}^2}^3 \partial_{\tilde{\gamma}^2} \right) \mathcal{K}_2, \quad (241)$$

$$\tilde{I}_4 = -\frac{1}{3} \partial_{\tilde{m}^2} \tilde{I}_3 = -\frac{1}{6} \left(6\partial_{\tilde{m}^2}^4 + 2\tilde{m}^2 \partial_{\tilde{m}^2}^5 + 2\tilde{\gamma}^2 \partial_{\tilde{m}^2}^4 \partial_{\tilde{\gamma}^2} \right) \mathcal{K}_2, \quad (242)$$

where

$$\begin{aligned} \mathcal{K}_2 &= -\frac{1}{8\pi} \sum_{j=1}^4 w_j \mu_j \ln(\mu_j) \\ &= -\frac{1}{8\pi} \left[\alpha^{++} \ln(\alpha^{++}) + \alpha^{+-} \ln(\alpha^{+-}) + \alpha^{-+} \ln(\alpha^{-+}) + \alpha^{--} \ln(\alpha^{--}) \right]. \end{aligned} \quad (243)$$

$d + 1 = 1$ Even the case of a time dimension all by itself with zero dimensions of space has experimental relevance (for instance in the context of quantum dots coupled to reservoirs [1]). The threshold functions in this case become

$$\Delta \tilde{I}_0 = k^{-1} [\mathcal{K}_1^k k - \mathcal{K}_1^\Lambda \Lambda], \quad (244)$$

$$\tilde{I}_0 = k^{-1} \tilde{\partial}_t \Delta I_0 = (1 - 2\tilde{m}^2 \partial_{\tilde{m}^2} - 2\tilde{\gamma}^2 \partial_{\tilde{\gamma}^2}) \mathcal{K}_1, \quad (245)$$

$$\tilde{I}_1 = -\partial_{\tilde{m}^2} \tilde{I}_0 = (\partial_{\tilde{m}^2} + 2\tilde{m}^2 \partial_{\tilde{m}^2}^2 + 2\tilde{\gamma}^2 \partial_{\tilde{m}^2} \partial_{\tilde{\gamma}^2}) \mathcal{K}_1, \quad (246)$$

$$\tilde{I}_2 = -\partial_{\tilde{m}^2} \tilde{I}_1 = -(3\partial_{\tilde{m}^2}^2 + 2\tilde{m}^2 \partial_{\tilde{m}^2}^3 + 2\tilde{\gamma}^2 \partial_{\tilde{m}^2}^2 \partial_{\tilde{\gamma}^2}) \mathcal{K}_1, \quad (247)$$

$$\tilde{I}_3 = -\frac{1}{2} \partial_{\tilde{m}^2} \tilde{I}_2 = \frac{1}{2} (5\partial_{\tilde{m}^2}^3 + 2\tilde{m}^2 \partial_{\tilde{m}^2}^4 + 2\tilde{\gamma}^2 \partial_{\tilde{m}^2}^3 \partial_{\tilde{\gamma}^2}) \mathcal{K}_1, \quad (248)$$

$$\tilde{I}_4 = -\frac{1}{3} \partial_{\tilde{m}^2} \tilde{I}_3 = -\frac{1}{6} (7\partial_{\tilde{m}^2}^4 + 2\tilde{m}^2 \partial_{\tilde{m}^2}^5 + 2\tilde{\gamma}^2 \partial_{\tilde{m}^2}^4 \partial_{\tilde{\gamma}^2}) \mathcal{K}_1, \quad (249)$$

with

$$\mathcal{K}_1 = \frac{1}{2} \sum_{j=1}^4 w_j \sqrt{\mu_j} = \frac{1}{2} \left[\sqrt{\alpha^{++}} + \sqrt{\alpha^{+-}} + \sqrt{\alpha^{-+}} + \sqrt{\alpha^{--}} \right]. \quad (250)$$

6.2. Propagator

Like I_j , J only depends on the magnitude of \mathbf{p} , so we again use spherical coordinates in the form

$$\int_{\mathbf{p}} = \frac{2\pi^{\frac{d}{2}}}{\Gamma(\frac{d}{2})} \frac{1}{2} \int_0^\infty \frac{dp^2}{(2\pi)^d} (\mathbf{p}^2)^{\frac{d-2}{2}}, \quad (251)$$

with $dp^2 = 2p dp$. Integrating the first Dirac delta in (211) gives [68]

$$q_0 = \sqrt{\mathbf{p}^2 + \text{Re } \alpha_1^{ir} k^2} + \sqrt{\mathbf{p}^2 + \text{Re } \alpha_2^{js} k^2} \quad (252)$$

which we can solve for \mathbf{p}^2 to get

$$\mathbf{p}^2 = \frac{1}{4q_0^2} \left[q_0^4 - 2q_0^2 (\text{Re } \alpha_1^{ir} + \text{Re } \alpha_2^{js}) k^2 + (\text{Re } \alpha_1^{ir} - \text{Re } \alpha_2^{js})^2 k^4 \right]. \quad (253)$$

Since (252) is a simple root of $f(\mathbf{p}^2) = q_0 - \sqrt{\mathbf{p}^2 + \text{Re } \alpha_1^{ir} k^2} - \sqrt{\mathbf{p}^2 + \text{Re } \alpha_2^{js} k^2}$, the prefactor arising from the Dirac delta $\delta(f(\mathbf{p}^2)) = \frac{1}{|f'(\mathbf{p}^2)|} \delta(\mathbf{p}^2 - q_0^2)$ is

$$\begin{aligned} \frac{1}{|f'(\mathbf{p}^2)|} &= \left(\frac{1}{2\sqrt{\mathbf{p}^2 + \text{Re } \alpha_1^{ir} k^2}} + \frac{1}{2\sqrt{\mathbf{p}^2 + \text{Re } \alpha_2^{js} k^2}} \right)^{-1} \\ &= \frac{2}{q_0} \sqrt{\mathbf{p}^2 + \text{Re } \alpha_1^{ir} k^2} \sqrt{\mathbf{p}^2 + \text{Re } \alpha_2^{js} k^2}, \end{aligned} \quad (254)$$

and only contributes for $q_0 > \sqrt{\mathbf{p}^2 + \text{Re } \alpha_1^{ir} k^2} + \sqrt{\mathbf{p}^2 + \text{Re } \alpha_2^{js} k^2}$, i.e. for

$$\theta\left(q_0 - \sqrt{\mathbf{p}^2 + \text{Re } \alpha_1^{ir} k^2} - \sqrt{\mathbf{p}^2 + \text{Re } \alpha_2^{js} k^2}\right) = 1, \quad (255)$$

where θ denotes the Heaviside step function. The second Dirac delta gives for e.g. $\text{Re } \alpha_1^{ir} > \text{Re } \alpha_2^{js}$

$$q_0 = \sqrt{\mathbf{p}^2 + \text{Re } \alpha_1^{ir} k^2} - \sqrt{\mathbf{p}^2 + \text{Re } \alpha_2^{js} k^2}. \quad (256)$$

It contributes only for $0 = q_0 = |\sqrt{\mathbf{p}^2 + \text{Re } \alpha_1^{ir} k^2} - \sqrt{\mathbf{p}^2 + \text{Re } \alpha_2^{js} k^2}|$.

Interestingly, the corresponding solution for \mathbf{p}^2 is the same as in (253) and so is the prefactor $|f'(\mathbf{p}^2)|^{-1}$. (The ranges are such that they are distinct except when one of the α s vanishes.)

In summary, we find after momentum integration

$$\begin{aligned} \text{disc } J &= -\frac{1}{4} \sum_{i,j,r,s} \frac{\pi^{\frac{d}{2}}}{\Gamma(\frac{d}{2})} \frac{(\mathbf{p}^2)^{\frac{d-2}{2}}}{(2\pi)^d} \frac{\sqrt{\mathbf{p}^2 + \text{Re } \alpha_1^{ir} k^2}}{\sqrt{\mathbf{p}^2 + \alpha_1^{ir} k^2}} \frac{\sqrt{\mathbf{p}^2 + \text{Re } \alpha_2^{js} k^2}}{\sqrt{\mathbf{p}^2 + \alpha_2^{js} k^2}} \frac{\pi \beta_1^{ir} \beta_2^{js}}{2q_0} \\ &\times \left[\left[1 + n_{\text{B}}\left(\sqrt{\mathbf{p}^2 + \alpha_1^{ir} k^2}\right) + n_{\text{B}}\left(\sqrt{\mathbf{p}^2 + \alpha_2^{js} k^2}\right) \right] \theta\left(q_0 - \sqrt{\mathbf{p}^2 + \text{Re } \alpha_1^{ir} k^2} - \sqrt{\mathbf{p}^2 + \text{Re } \alpha_2^{js} k^2}\right) \right. \\ &\quad + \left[n_{\text{B}}\left(\sqrt{\mathbf{p}^2 + \alpha_1^{ir} k^2}\right) - n_{\text{B}}\left(\sqrt{\mathbf{p}^2 + \alpha_2^{js} k^2}\right) \right] \theta\left(\sqrt{\mathbf{p}^2 + \text{Re } \alpha_2^{js} k^2} - \sqrt{\mathbf{p}^2 + \text{Re } \alpha_1^{ir} k^2} - q_0\right) \\ &\quad \left. + \left[n_{\text{B}}\left(\sqrt{\mathbf{p}^2 + \alpha_2^{js} k^2}\right) - n_{\text{B}}\left(\sqrt{\mathbf{p}^2 + \alpha_1^{ir} k^2}\right) \right] \theta\left(\sqrt{\mathbf{p}^2 + \text{Re } \alpha_1^{ir} k^2} - \sqrt{\mathbf{p}^2 + \text{Re } \alpha_2^{js} k^2} - q_0\right) \right], \end{aligned} \quad (257)$$

which is to be evaluated at \mathbf{p}^2 as given in (253). If $\alpha_1^{ir} \approx \text{Re } \alpha_1^{ir}$ the square root fractions in front are approximately one. Also, at $T = 0$ all terms $\propto n_{\text{B}} \propto e^{-p_0/T}$ drop out and (257) simplifies to

$$\begin{aligned} \text{disc } J|_{T=0} &= -\frac{1}{4} \sum_{i,j,r,s} \frac{\pi^{\frac{d}{2}}}{\Gamma(\frac{d}{2})} \frac{\pi \beta_1^{ir} \beta_2^{js}}{2(2\pi)^d q_0} \theta\left(q_0 - \sqrt{\mathbf{p}^2 + \text{Re } \alpha_1^{ir} k^2} - \sqrt{\mathbf{p}^2 + \text{Re } \alpha_2^{js} k^2}\right) \\ &\quad \times \left(\frac{q_0^4 - 2q_0^2(\text{Re } \alpha_1^{ir} \text{Re } \alpha_2^{js}) + (\text{Re } \alpha_1^{ir} - \text{Re } \alpha_2^{js})k^4}{4q_0^2} \right)^{\frac{d-2}{2}}. \end{aligned} \quad (258)$$

7. Numerical Results

Equations (120) to (122) and (156) to (158) constitute a closed set of integro-differential equations. After inserting our results of secs. 5 and 6 for the Matsubara summation and momentum integration of the threshold functions, the system reduces to a coupled set of non-linear ordinary differential equations which can be solved numerically once we specify initial values for the parameters of our truncation at the ultraviolet cutoff scale $k = \Lambda$. For our calculations we choose

$$\tilde{\rho}_0(\Lambda) = \frac{1}{50}, \quad \lambda(\Lambda) = \frac{1}{2}, \quad \tilde{\gamma}_1^2(\Lambda) = 0, \quad Z_1(\Lambda) = 1, \quad N = 2, \quad (259)$$

where $\tilde{\rho}_0(\Lambda) = \rho_0(\Lambda)/\Lambda^2$ and $\tilde{\gamma}_1^2(\Lambda) = \gamma_1^2(\Lambda)/\Lambda^2$. The resulting real-time flow of the propagator and the effective potential in the truncation (98) of the scalar $O(N)$ -model at zero temperature in $3 + 1$ -dimensional spacetime is shown in fig. 12.

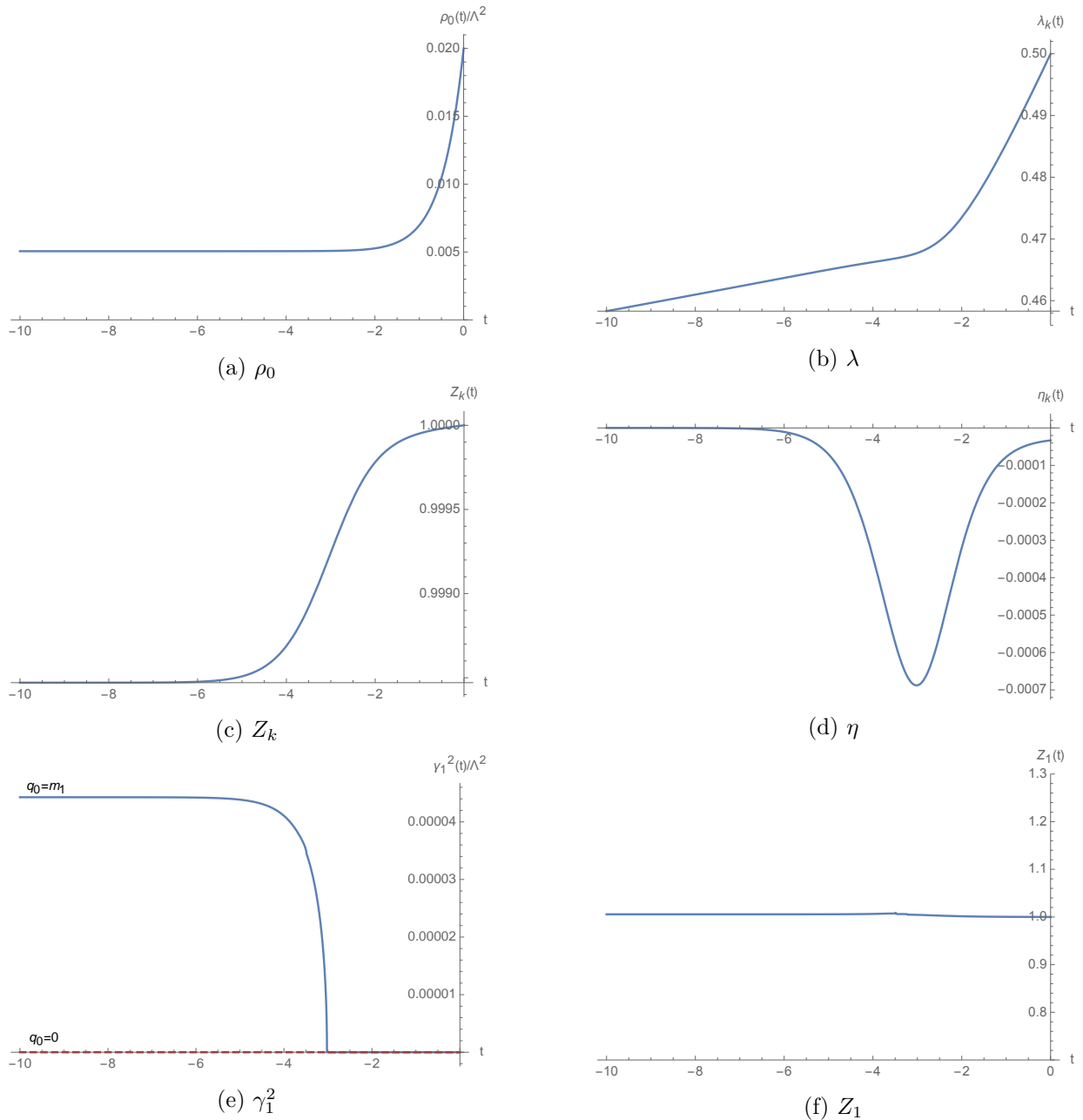


Figure 12: Flow of the $O(2)$ model at $T = 0$ in $3 + 1$ spacetime dimensions

Fig. 12a displays the scale dependence of the effective potential's minimum location $\rho_0(k)$. Near the ultraviolet cutoff Λ it exhibits a sharp fall-off to about a fourth of its initial value and then becomes scale independent for $k \lesssim \Lambda/e^2$.

Fig. 12b reveals a weak logarithmic flow of the quartic coupling λ from large values at microscopic distances to smaller values at $k \ll \Lambda$. The logarithmic running implies $\lambda(k) \rightarrow 0$ for $k \rightarrow 0$ which indicates that a field theory involving only scalars must be free in four spacetime dimensions. The underlying effect of charge screening forces the quartic coupling to zero at $k = 0$, a feature known as “triviality”.

We also point out that the flow behavior of λ separates into two regimes. Above the transition region $k^2 \approx m_1^2$, the logarithmic running is significantly stronger since fluctuations of both the radial and Goldstone modes contribute to the scale dependence. Below $k^2 \approx m_1^2$ contributions from the radial mode diminish since its fluctuations are suppressed by the non-zero mass $m_1^2 = 2\lambda\rho_0/Z_1$.

Figs. 12c and 12d show the flow of the overall wave function renormalization Z_k and its derivative,

the anomalous dimension $\eta = -1/Z_k \partial_t Z_k$. The latter exhibits a drop to small negative values with a minimum at $k \approx \Lambda/e^3$ after which it smoothly returns to zero for larger scales.

Of particular importance to our investigation is the flow of the discontinuity γ_1^2 shown in fig. 12e, both for external energies that correspond to on-shell ($q_0 = m_1$) and virtual ($q_0 = 0$) radial excitations. As we would expect, the on-shell discontinuity adheres to its initial value of zero until $k < q_0 = m_1 = \sqrt{2\lambda\rho_0/Z_1}$ at which point it abruptly rises to non-zero values before again becoming scale independent for $k \lesssim \Lambda/e^5$. The physical origin of the discontinuity γ_1^2 in the radial mode's propagator is its decay channel into two massless Goldstone bosons via the non-zero $\Gamma_{k,1aa}^{(3)}$, $a \in \{2, \dots, N\}$. The flow 12e signals that on-shell radial excitations are unstable at energies below the mass m_1 but become stable once $k > m_1$. On the other hand, for virtual $q_0 = 0$, the discontinuity γ_1^2 is zero on all scales, suggesting that zero-momentum radial fluctuations do not decay. We emphasize that our computation took this non-zero real-time decay width into account in a self-consistent manner.

Fig. 12f shows the scale dependence of the radial wave function renormalization Z_1 . The fact that Z_1 never strays far from unity shows that at zero temperature on-shell radial excitations renormalize just like the Goldstone bosons.

All results in fig. 12 agree with those obtained in [1].

8. Conclusions and Outlook

We discussed a method to analytically continue functional renormalization group equations from discrete imaginary Matsubara frequencies to the continuous real frequency axis. This method has been developed in [1]. The present work contains further details on the derivation of the flow equations. We showcased how this method works in practice for the example of a theory of N relativistic scalar fields with $O(N)$ symmetry, putting particular emphasis on the propagator $G_r(p)$ of the massive radial mode φ_1 in the regime where spontaneous symmetry breaking reduces the $O(N)$ to $O(N-1)$. An important characteristic of such excitations – one that has received little attention up to this point – is the imaginary discontinuity γ_1^2 of the inverse propagator at on-shell external momenta $q^2 = m_1^2/Z_1 = 2\rho_0 \lambda/Z_1$. It is closely related to a non-zero particle decay width $\Gamma = \gamma_1^2/m_1$ describing the fission of a massive radial field into two massless Goldstone bosons.

To obtain a truncation able to account for this new type of singularity in the analytic structure of the propagator $G_k(p)$, we employed a Minkowski-space derivative expansion of the average action Γ_k around singular points of the propagator. This expansion scheme is very close to the actual dynamics [1] in the sense that loop integrals on the r.h.s. of flow equations are strongly dominated by the on-shell physical excitations corresponding to these poles and branch cuts. Such an expansion may therefore exhibit improved convergence behavior compared to a Euclidean space derivative expansion around vanishing frequency.

We exploited this convenient circumstance by regulating our flow equations with a class of algebraic regulators due to Flörchinger [1] that would otherwise have been inadequate. These regulators exhibit a much milder decay in the ultraviolet and consequently inferior separation of momentum modes compared to typical Euclidean-space (exponential or Litim-type) regulators. Besides being fully compatible with Lorentz invariance, choosing the simplest representative of this class of regulators also allowed us to resort to contour integration methods to perform the summation over Matsubara frequencies both in flow equations for parameters of the effective potential and the radial propagator analytically. The resulting flow equations proved to be both infrared and ultraviolet finite without the need for further regularization, supporting our claim of improved convergence of the derivative expansion in Minkowski space.

An interesting prospect for future applications of this method is the first-principles calculation of transport properties. Since our formalism is based on a linear response framework, quantities such as viscosities, conductivities, permittivities, relaxation times, etc. now lie within the scope of functional renormalization.

We were mainly concerned with the investigation of conceptual issues and therefore restricted our treatment to the simple case of relativistic scalar fields. However, the method can also be applied to more complicated theories mixing both bosonic and fermionic degrees of freedom of different spin. With increased effort, it allows the treatment of such systems at arbitrary temperature and chemical potential.

In summary, the analytic continuation of functional renormalization group equations brings the renormalization group closer to the physical dynamics in Minkowski space. It enables the computation of new observables previously inaccessible to the FRG. Thanks to the enhanced performance of the derivative expansion in Minkowski space we believe it will lead to more accurate results despite little computational effort.

A. Propagator

A.1. Analytic Structure

The Källén-Lehmann spectral representation can be written

$$G(p) = \int_0^\infty d\mu^2 \frac{\rho(\mu^2)}{p^2 + \mu^2}, \quad (260)$$

where $p^2 = -p_0^2 + \mathbf{p}^2$ decomposes into real and imaginary parts,

$$\begin{aligned} \operatorname{Re}(p^2) &= -\operatorname{Re}(p_0^2) + \mathbf{p}^2 = -\operatorname{Re}(p_0)^2 + \operatorname{Im}(p_0)^2 + \mathbf{p}^2, \\ \operatorname{Im}(p^2) &= -\operatorname{Im}(p_0^2) = -2\operatorname{Re}(p_0)\operatorname{Im}(p_0). \end{aligned} \quad (261)$$

For $\operatorname{Im}(p_0) \approx 0$ and non-vanishing $\operatorname{Re}(p_0)$ and/or \mathbf{p}^2 , we have $|\operatorname{Re}(p^2)| \gg |\operatorname{Im}(p^2)|$. Thus close to the real p_0 -axis, we recognize a form to which we can apply the Sokhotski–Plemelj theorem for the real line (\mathcal{P} is the Cauchy principal value)

$$\lim_{\epsilon \rightarrow 0} \int_a^b dx \frac{f(x)}{x + y \pm i\epsilon} = \mathcal{P} \int_a^b \frac{f(x)}{x + y} dx \mp i\pi f(-y), \quad (a < y < b) \quad (262)$$

by identifying

$$x = \mu^2, \quad a = 0, \quad b = \infty, \quad f(x) = \rho(\mu^2), \quad y = \operatorname{Re}(p^2), \quad i\epsilon = i\operatorname{Im}(p^2). \quad (263)$$

Thus the propagator can also be written

$$G(p) = \mathcal{P} \int_0^\infty d\mu^2 \frac{\rho(\mu^2)}{p^2 + \mu^2} + i\pi s(p_0) \rho(-p^2), \quad (264)$$

where $s(p_0) = \operatorname{sign}(\operatorname{Re} p_0 \operatorname{Im} p_0)$ and we approximated $\operatorname{Re}(p^2) \approx p^2$. (264) reveals that the propagator has a branch cut along the real axis for all values of $-\operatorname{Im}(p_0)^2 - \mathbf{p}^2$ for which $\rho(-\operatorname{Im}(p_0)^2 - \mathbf{p}^2) \neq 0$. (Of course, $s(p_0)$ also switches sign when moving across the real axis. However, we cannot infer from this that the propagator also has a branch cut along the imaginary axis. (264) is valid only close to the real axis and does not allow any insight into the analytic structure of $G(p)$ for $\operatorname{Im}(p_0) \not\approx 0$. In fact, we already know there can't be a cut on the imaginary axis. The Källén-Lehmann decomposition (260) clearly shows that the Minkowski-space propagator is completely regular throughout the complex plane except for $p_0 \in \mathbb{R}$.)

The propagator's analytic structure also exhibits poles. To see this, we perform a partial fraction decomposition,

$$\begin{aligned} \frac{1}{p^2 + \mu^2} &\stackrel{!}{=} \frac{a}{-p_0 + \sqrt{\mathbf{p}^2 + \mu^2}} + \frac{b}{-p_0 - \sqrt{\mathbf{p}^2 + \mu^2}} \\ &= \frac{a(-p_0 - \sqrt{\mathbf{p}^2 + \mu^2}) + b(-p_0 + \sqrt{\mathbf{p}^2 + \mu^2})}{p_0^2 - \mathbf{p}^2 - \mu^2}, \end{aligned} \quad (265)$$

i.e.

$$1 \stackrel{!}{=} a(p_0 + \sqrt{\mathbf{p}^2 + \mu^2}) + b(p_0 - \sqrt{\mathbf{p}^2 + \mu^2}). \quad (266)$$

Inserting $p_0 = \pm\sqrt{\mathbf{p}^2 + \mu^2}$, we find the coefficients

$$a = \frac{1}{2\sqrt{\mathbf{p}^2 + \mu^2}} = -b. \quad (267)$$

Plugging this back into (260), we can make the pole structure explicit,

$$G(p) = \int_0^\infty d\mu^2 \frac{\rho(\mu^2)}{2\sqrt{\mathbf{p}^2 + \mu^2}} \left[\frac{1}{-p_0 + \sqrt{\mathbf{p}^2 + \mu^2} \pm i\epsilon} - \frac{1}{-p_0 - \sqrt{\mathbf{p}^2 + \mu^2} \pm i\epsilon} \right]. \quad (268)$$

We added the infinitesimal $i\epsilon$ -terms in (268) by hand to move the singularities slightly away from the real p_0 -axis. Different combinations of signs for these terms correspond to differently time-ordered propagators. $(+, +)$ gives the advanced, $(-, -)$ the retarded, $(-, +)$ the time-ordered (Feynman) and $(+, -)$ the anti-time-ordered propagator.

To complete our discussion, we give a quick proof of the Sokhotski–Plemelj theorem on the real line where $a < y < b$. Consider

$$\lim_{\epsilon \rightarrow 0} \int_a^b \frac{f(x)}{x + y \pm i\epsilon} dx = \mp i\pi \lim_{\epsilon \rightarrow 0} \int_a^b \frac{\epsilon f(x) dx}{\pi[(x + y)^2 + \epsilon^2]} + \lim_{\epsilon \rightarrow 0} \int_a^b \frac{(x + y)^2}{(x + y)^2 + \epsilon^2} \frac{f(x)}{x + y} dx. \quad (269)$$

In the first term, $\lim_{\epsilon \rightarrow 0} \epsilon / \{\pi[(x + y)^2 + \epsilon^2]\} = \delta(x + y)$ is a nascent delta function, giving simply $\mp i\pi f(-y)$ in the limit $\lim_{\epsilon \rightarrow 0}$. In the second term, $\frac{(x+y)^2}{(x+y)^2 + \epsilon^2}$ approaches 1 for $|x + y| \gg \epsilon$, 0 for $|x + y| \ll \epsilon$ and is symmetric about 0. For $\lim_{\epsilon \rightarrow 0}$, it thus gives the Cauchy principal value.

A.2. Decomposition

The sum of P_k and R_k defined as in (100) and (102),

$$P_k = Z_k \left[z p^2 + m^2 - i s(p_0) \gamma^2 \right], \quad R_k(p) = \frac{Z_k k^2}{1 + c \frac{p^2}{k^2}}, \quad (270)$$

gives [1, 68]

$$P_k + R_k = Z_k \frac{z p^4 + p^2 [m^2 - i s(p_0) \gamma^2 + z \frac{k^2}{c}] + \frac{k^2}{c} [m^2 - i s(p_0) \gamma^2] + \frac{k^4}{c}}{p^2 + \frac{k^2}{c}}. \quad (271)$$

To obtain an expression that closely resembles a sum of free propagators, the idea is now to decompose the regularized propagator into

$$\frac{1}{P_k + R_k} = \frac{1}{Z_k} \left(\frac{\beta^+}{p^2 + \alpha^+ k^2} + \frac{\beta^-}{p^2 + \alpha^- k^2} \right), \quad (272)$$

(272) implies

$$P_k + R_k = Z_k \frac{p^4 + p^2 (\alpha^+ + \alpha^-) k^2 + \alpha^+ \alpha^- k^4}{(\beta^+ + \beta^-) p^2 + (\alpha^+ \beta^+ + \alpha^- \beta^-) k^2}. \quad (273)$$

Comparing (271) and (273), we can read off the relations

$$\alpha^+ + \alpha^- = \frac{\tilde{m}^2}{z} - i s(p_0) \frac{\tilde{\gamma}^2}{z} + \frac{1}{c}, \quad \beta^+ + \beta^- = \frac{1}{z}, \quad (274)$$

$$\alpha^+ \alpha^- = \frac{1}{cz} \left(\tilde{m}^2 - i s(p_0) \tilde{\gamma}^2 + 1 \right), \quad \alpha^+ \beta^- + \alpha^- \beta^+ = \frac{1}{cz}. \quad (275)$$

We have four equations and four unknowns. Solving for α^\pm, β^\pm yields

$$\alpha^\pm = \frac{1}{2} \left(\frac{1}{c} + \frac{\tilde{m}^2}{z} - i s(p_0) \frac{\tilde{\gamma}^2}{z} \right) \pm (A + i s(p_0) B), \quad (276)$$

$$\beta^\pm = \frac{1}{2z} \pm (C + i s(p_0) D), \quad (277)$$

where A, B, C, D are independent of p and in particular of $s(p_0)$. Furthermore, $B = D = 0$ for $\gamma^2 = 0$, i.e. for $p_0 \notin \mathbb{R}_+$, as we will see below. A and B are obtained by inserting α^\pm from (276) into the left equality in (275), yielding

$$\begin{aligned} \alpha^+ \alpha^- &= \frac{1}{4} \left(\frac{1}{c} + \frac{\tilde{m}^2}{z} - i s(p_0) \frac{\tilde{\gamma}^2}{z} \right)^2 - (A + i s(p_0) B)^2, \\ &= \frac{1}{4} \left(\frac{1}{c} + \frac{\tilde{m}^2}{z} \right)^2 - \frac{\tilde{\gamma}^4}{4z^2} - A^2 + B^2 - i s(p_0) \left[\frac{1}{2} \left(\frac{1}{c} + \frac{\tilde{m}^2}{z} \right) \frac{\tilde{\gamma}^2}{z} + 2AB \right]^2, \\ &\stackrel{!}{=} \frac{1}{cz} + \frac{m^2}{czk^2} - i s(p_0) \frac{\gamma^2}{czk^2}, \end{aligned} \quad (278)$$

Equating the real and imaginary parts on both sides of $\stackrel{!}{=}$ results in

$$\begin{aligned} -A^2 + B^2 &= \frac{1}{cz} + \frac{m^2}{czk^2} - \frac{1}{4} \left(\frac{1}{c} + \frac{\tilde{m}^2}{z} \right)^2 + \frac{\tilde{\gamma}^4}{4z^2} \\ &= \frac{1}{cz} - \frac{1}{4} \left(\frac{1}{c} - \frac{\tilde{m}^2}{z} \right)^2 + \frac{\tilde{\gamma}^4}{4z^2}, \end{aligned} \quad (279)$$

$$\begin{aligned} 2AB &= \frac{\gamma^2}{czk^2} - \frac{1}{2} \left(\frac{1}{c} + \frac{\tilde{m}^2}{z} \right) \frac{\tilde{\gamma}^2}{z} \\ &= \frac{1}{2} \left(\frac{1}{c} - \frac{\tilde{m}^2}{z} \right) \frac{\tilde{\gamma}^2}{z}. \end{aligned} \quad (280)$$

With these relations, we can express $(iA + B)^2$ and $(iA - B)^2$ as

$$\begin{aligned} (iA + B)^2 &= -A^2 + B^2 + 2iAB = \frac{1}{cz} - \frac{1}{4} \left(\frac{1}{c} - \frac{\tilde{m}^2}{z} \right)^2 + \frac{\tilde{\gamma}^4}{4z^2} + \frac{i}{2} \left(\frac{1}{c} - \frac{\tilde{m}^2}{z} \right) \frac{\tilde{\gamma}^2}{z} \\ &= \frac{1}{cz} - \frac{1}{4} \left(\frac{1}{c} - \frac{\tilde{m}^2}{z} - i \frac{\tilde{\gamma}^2}{z} \right)^2, \end{aligned} \quad (281)$$

$$(iA - B)^2 = -A^2 + B^2 - 2iAB = \frac{1}{cz} - \frac{1}{4} \left(\frac{1}{c} - \frac{\tilde{m}^2}{z} + i \frac{\tilde{\gamma}^2}{z} \right)^2. \quad (282)$$

Taking the square root gives

$$iA + B = \pm \sqrt{\frac{1}{cz} - \frac{1}{4} \left(\frac{1}{c} - \frac{\tilde{m}^2}{z} - i \frac{\tilde{\gamma}^2}{z} \right)^2}, \quad (283)$$

$$iA - B = \pm \sqrt{\frac{1}{cz} - \frac{1}{4} \left(\frac{1}{c} - \frac{\tilde{m}^2}{z} + i \frac{\tilde{\gamma}^2}{z} \right)^2}, \quad (284)$$

and so

$$A = \frac{r}{2i} \left[\sqrt{\frac{1}{cz} - \frac{1}{4} \left(\frac{1}{c} - \frac{\tilde{m}^2}{z} - i \frac{\tilde{\gamma}^2}{z} \right)^2} + s \sqrt{\frac{1}{cz} - \frac{1}{4} \left(\frac{1}{c} - \frac{\tilde{m}^2}{z} + i \frac{\tilde{\gamma}^2}{z} \right)^2} \right], \quad (285)$$

$$B = \frac{r}{2} \left[\sqrt{\frac{1}{cz} - \frac{1}{4} \left(\frac{1}{c} - \frac{\tilde{m}^2}{z} - i \frac{\tilde{\gamma}^2}{z} \right)^2} - s \sqrt{\frac{1}{cz} - \frac{1}{4} \left(\frac{1}{c} - \frac{\tilde{m}^2}{z} + i \frac{\tilde{\gamma}^2}{z} \right)^2} \right], \quad (286)$$

where the signs $r, s \in \{\pm 1\}$ can be chosen for convenience.

We choose the branch cut of the complex square root to lie on the negative real axis \mathbb{R}_- . In this case, the two square roots in A and B are equal in the limit $\gamma^2 \rightarrow 0$ if

$$\frac{1}{cz} - \frac{1}{4} \left(\frac{1}{c} - \frac{\tilde{m}^2}{z} \right)^2 \geq 0. \quad (287)$$

Otherwise, they differ by a factor of -1 . Enforcing $B \rightarrow 0$ for $\gamma^2 \rightarrow 0$ is therefore equivalent to the choice

$$s = \text{sign} \left[\frac{1}{cz} - \frac{1}{4} \left(\frac{1}{c} - \frac{\tilde{m}^2}{z} \right)^2 \right]. \quad (288)$$

Note that with the definition (288) A and B are real for $s = -1$ and imaginary for $s = 1$.

The choice for r is irrelevant since sending $r \rightarrow -r$ simply switches $\alpha^+ \leftrightarrow \alpha^-$. For definiteness, we choose $r = 1$ and s as in (288).

Conditions for C and D derive from $\alpha^+ \beta^- + \alpha^- \beta^+ = \frac{1}{cz}$ (see (275)) by inserting (276) and (277),

$$\begin{aligned} & \left[\frac{1}{2} \left(\frac{1}{c} + \frac{\tilde{m}^2}{z} - i s(p_0) \frac{\tilde{\gamma}^2}{z} \right) + (A + i s(p_0) B) \right] \left[\frac{1}{2z} - (C + i s(p_0) D) \right] \\ & + \left[\frac{1}{2} \left(\frac{1}{c} + \frac{\tilde{m}^2}{z} - i s(p_0) \frac{\tilde{\gamma}^2}{z} \right) - (A + i s(p_0) B) \right] \left[\frac{1}{2z} + (C + i s(p_0) D) \right] \\ & = \frac{1}{2z} \left(\frac{1}{c} + \frac{\tilde{m}^2}{z} - i s(p_0) \frac{\tilde{\gamma}^2}{z} \right) - 2AC + 2BD - i s(p_0) [2BC + 2AD] \stackrel{!}{=} \frac{1}{cz}. \end{aligned} \quad (289)$$

Equating again real and imaginary parts on both sides of $\stackrel{!}{=}$ we find

$$\frac{1}{2z} \left(\frac{1}{c} + \frac{\tilde{m}^2}{z} \right) - 2AC + 2BD = \frac{1}{cz}, \quad (290)$$

$$\frac{\gamma^2}{2z^2 k^2} + 2BC + 2AD = 0. \quad (291)$$

or in matrix form,

$$\begin{pmatrix} A & -B \\ B & A \end{pmatrix} \begin{pmatrix} C \\ D \end{pmatrix} = -\frac{1}{4z} \begin{pmatrix} \frac{1}{c} - \frac{\tilde{m}^2}{z} \\ \frac{\tilde{\gamma}^2}{z} \end{pmatrix}. \quad (292)$$

Inverting $\begin{pmatrix} A & -B \\ B & A \end{pmatrix}^{-1} = \frac{1}{A^2 + B^2} \begin{pmatrix} A & B \\ -B & A \end{pmatrix}$ yields

$$C = -\frac{A \left(\frac{1}{c} - \frac{\tilde{m}^2}{z} \right) + B \frac{\tilde{\gamma}^2}{z}}{4z(A^2 + B^2)}, \quad D = \frac{B \left(\frac{1}{c} - \frac{\tilde{m}^2}{z} \right) - A \frac{\tilde{\gamma}^2}{z}}{4z(A^2 + B^2)}. \quad (293)$$

For $\gamma^2 = 0$, we have $B = 0$ and thus also $D = 0$.

Explicit expressions Plugging (285), (286) and (293) into (276), we get the following expressions for α^\pm ,

$$\begin{aligned} \alpha^\pm &= \frac{1}{2} \left(\frac{1}{c} + \frac{\tilde{m}^2}{z} - i s(p_0) \frac{\tilde{\gamma}^2}{z} \right) \pm \frac{i}{2} [-1 + s(p_0)] \sqrt{\frac{1}{cz} - \frac{1}{4} \left(\frac{1}{c} - \frac{\tilde{m}^2}{z} - \frac{i\tilde{\gamma}^2}{z} \right)^2} \\ & \mp \frac{i}{2} [1 + s(p_0)] \text{sign} \left[\frac{1}{cz} - \frac{1}{4} \left(\frac{1}{c} - \frac{\tilde{m}^2}{z} \right)^2 \right] \sqrt{\frac{1}{cz} - \frac{1}{4} \left(\frac{1}{c} - \frac{\tilde{m}^2}{z} + \frac{i\tilde{\gamma}^2}{z} \right)^2}. \end{aligned} \quad (294)$$

If instead we choose $s = -1$ we get

$$\begin{aligned} \alpha^\pm &= \frac{1}{2} \left(\frac{1}{c} + \frac{\tilde{m}^2}{z} - i s(p_0) \frac{\tilde{\gamma}^2}{z} \right) \pm \frac{i}{2} [-1 + s(p_0)] \sqrt{\frac{1}{cz} - \frac{1}{4} \left(\frac{1}{c} - \frac{\tilde{m}^2}{z} - \frac{i\tilde{\gamma}^2}{z} \right)^2} \\ & \pm \frac{i}{2} [1 + s(p_0)] \sqrt{\frac{1}{cz} - \frac{1}{4} \left(\frac{1}{c} - \frac{\tilde{m}^2}{z} + \frac{i\tilde{\gamma}^2}{z} \right)^2}. \end{aligned} \quad (295)$$

which gives rise to the convenient relation

$$\alpha^\pm(s(p_0) = 1) = \alpha^{\pm*}(s(p_0) = -1), \quad (296)$$

or $\alpha^{\pm\pm} = (\alpha^{\pm-})^*$ using the notation introduced in (177). Similarly, we can insert (293) into (277) to get,

$$\beta^\pm = \frac{1}{2z} \pm \frac{(-A + is(p_0)B)\left(\frac{1}{c} - \frac{\tilde{m}^2}{z} + is(p_0)\frac{\tilde{\gamma}^2}{z}\right)}{4z(A^2 + B^2)} \quad (297)$$

which using (285) and (286) yields the following explicit expressions for β^\pm ,

$$\begin{aligned} \beta^\pm = \frac{1}{2z} \pm \frac{1}{4z} \left(\frac{1}{c} + \frac{\tilde{m}^2}{z} - is(p_0)\frac{\tilde{\gamma}^2}{z} \right) & \left[\frac{i}{2} [1 + s(p_0)] \sqrt{\frac{1}{cz} - \frac{1}{4} \left(\frac{1}{c} - \frac{\tilde{m}^2}{z} + \frac{i\tilde{\gamma}^2}{z} \right)^2}^{-1} \right. \\ & \left. + \frac{i}{2} [1 - s(p_0)] \operatorname{sign} \left[\frac{1}{cz} - \frac{1}{4} \left(\frac{1}{c} - \frac{\tilde{m}^2}{z} \right)^2 \right] \sqrt{\frac{1}{cz} - \frac{1}{4} \left(\frac{1}{c} - \frac{\tilde{m}^2}{z} - \frac{i\tilde{\gamma}^2}{z} \right)^2}^{-1} \right], \end{aligned} \quad (298)$$

whereas for $s = -1$ we have

$$\begin{aligned} \beta^\pm = \frac{1}{2z} \pm \frac{1}{4z} \left(\frac{1}{c} + \frac{\tilde{m}^2}{z} - is(p_0)\frac{\tilde{\gamma}^2}{z} \right) & \left[\frac{i}{2} [1 + s(p_0)] \sqrt{\frac{1}{cz} - \frac{1}{4} \left(\frac{1}{c} - \frac{\tilde{m}^2}{z} + \frac{i\tilde{\gamma}^2}{z} \right)^2}^{-1} \right. \\ & \left. \pm \frac{i}{2} [1 - s(p_0)] \sqrt{\frac{1}{cz} - \frac{1}{4} \left(\frac{1}{c} - \frac{\tilde{m}^2}{z} - \frac{i\tilde{\gamma}^2}{z} \right)^2}^{-1} \right]. \end{aligned} \quad (299)$$

B. Numerical Implementation

All numerical operations were carried out in *Mathematica*. To implement the closed set of flow equations (120) to (122) and (156) to (158) numerically, we defined several auxiliary functions.

B.1. Auxiliary functions

A complex square root with branch cut along the negative real axis.

```
In[1]:= sqrt[(x_)?NumericQ,(y_)?NumericQ] = Piecewise[{{I*Sqrt[-x],Re[x] < 0
&& Re[y] >= 0},{(-I)*Sqrt[-x],Re[x] < 0 && Re[y] < 0}},Sqrt[x]]
```

```
Out[1]= i sqrt[-x]      Re[x]<0 && Re[y]>=0
        -i sqrt[-x]     Re[x]<0 && Re[y]<0
        sqrt[x]         True
```

The second argument y decides which branch to take (upper branch if $\operatorname{Re}(y) \geq 0$, lower if $\operatorname{Re}(y) < 0$). To allow *Mathematica* to perform symbolic simplifications on `sqrt`, we supply

```
In[2]:= Derivative[1,0][sqrt][x_,y_] = 1/(2*sqrt[x,y]);
        Derivative[0,1][sqrt][x_,y_] = 0;
```

The numerator coefficients $\alpha^{\pm\pm}$ of the propagator decomposition (272) are defined as

```
In[3]:= alpha[1,1][m2_,g2_,z_,c_] := 1/2 (1/c + m2/z - i g2/z)
        + i sqrt[1/cz - 1/4 (1/c - m2/z + i g2/z)^2, -(1/c - m2/z)];
        alpha[1,2][m2_,g2_,z_,c_] := 1/2 (1/c + m2/z + i g2/z)
        - i sqrt[1/cz - 1/4 (1/c - m2/z - i g2/z)^2, 1/c - m2/z];
```

$$\begin{aligned}
\alpha_k[2,1][m2_,g2_,z_,c_] &:= \frac{1}{2} \left(\frac{1}{c} + \frac{m2}{z} - \frac{i g2}{z} \right) \\
&\quad - i \operatorname{sqrt} \left[\frac{1}{c z} - \frac{1}{4} \left(\frac{1}{c} - \frac{m2}{z} + \frac{i g2}{z} \right)^2, - \left(\frac{1}{c} - \frac{m2}{z} \right) \right]; \\
\alpha_k[2,2][m2_,g2_,z_,c_] &:= \frac{1}{2} \left(\frac{1}{c} + \frac{m2}{z} + \frac{i g2}{z} \right) \\
&\quad + i \operatorname{sqrt} \left[\frac{1}{c z} - \frac{1}{4} \left(\frac{1}{c} - \frac{m2}{z} - \frac{i g2}{z} \right)^2, \frac{1}{c} - \frac{m2}{z} \right]; \\
\alpha_k[1,0][m2_,g2_,z_,c_] &:= \frac{1}{2} \left(\frac{1}{c} + \frac{m2}{z} \right) + \frac{1}{2} \left(i \operatorname{sqrt} \left[\frac{1}{c z} - \frac{1}{4} \left(\frac{1}{c} - \frac{m2}{z} + \frac{i g2}{z} \right)^2, - \left(\frac{1}{c} - \frac{m2}{z} \right) \right] \right. \\
&\quad \left. - \left(\frac{1}{c} - \frac{m2}{z} \right) \right) - i \operatorname{sqrt} \left[\frac{1}{c z} - \frac{1}{4} \left(\frac{1}{c} - \frac{m2}{z} - \frac{i g2}{z} \right)^2, \frac{1}{c} - \frac{m2}{z} \right]; \\
\alpha_k[2,0][m2_,g2_,z_,c_] &:= \frac{1}{2} \left(\frac{1}{c} + \frac{m2}{z} \right) - \frac{1}{2} \left(i \operatorname{sqrt} \left[\frac{1}{c z} - \frac{1}{4} \left(\frac{1}{c} - \frac{m2}{z} + \frac{i g2}{z} \right)^2, - \left(\frac{1}{c} - \frac{m2}{z} \right) \right] \right. \\
&\quad \left. - \left(\frac{1}{c} - \frac{m2}{z} \right) \right) - i \operatorname{sqrt} \left[\frac{1}{c z} - \frac{1}{4} \left(\frac{1}{c} - \frac{m2}{z} - \frac{i g2}{z} \right)^2, \frac{1}{c} - \frac{m2}{z} \right];
\end{aligned}$$

where $m2 = \tilde{m}^2 = m^2/k^2$, $g2 = \tilde{\gamma}^2 = \gamma^2/k^2$. Similarly, the numerator $\beta^{\pm\pm}$ coefficients read

$$\begin{aligned}
\ln[4] := \beta_k[1,1][m2_,g2_,z_,c_] &:= \frac{1}{2 z} + \frac{i \left(\frac{1}{c} - \frac{m2}{z} + \frac{i g2}{z} \right)}{(4 z) \operatorname{sqrt} \left[\frac{1}{c z} - \frac{1}{4} \left(\frac{1}{c} - \frac{m2}{z} + \frac{i g2}{z} \right)^2, - \left(\frac{1}{c} - \frac{m2}{z} \right) \right]}; \\
\beta_k[1,2][m2_,g2_,z_,c_] &:= \frac{1}{2 z} - \frac{i \left(\frac{1}{c} - \frac{m2}{z} - \frac{i g2}{z} \right)}{(4 z) \operatorname{sqrt} \left[\frac{1}{c z} - \frac{1}{4} \left(\frac{1}{c} - \frac{m2}{z} - \frac{i g2}{z} \right)^2, \frac{1}{c} - \frac{m2}{z} \right]}; \\
\beta_k[2,1][m2_,g2_,z_,c_] &:= \frac{1}{2 z} - \frac{i \left(\frac{1}{c} - \frac{m2}{z} + \frac{i g2}{z} \right)}{(4 z) \operatorname{sqrt} \left[\frac{1}{c z} - \frac{1}{4} \left(\frac{1}{c} - \frac{m2}{z} + \frac{i g2}{z} \right)^2, - \left(\frac{1}{c} - \frac{m2}{z} \right) \right]}; \\
\beta_k[2,2][m2_,g2_,z_,c_] &:= \frac{1}{2 z} + \frac{i \left(\frac{1}{c} - \frac{m2}{z} - \frac{i g2}{z} \right)}{(4 z) \operatorname{sqrt} \left[\frac{1}{c z} - \frac{1}{4} \left(\frac{1}{c} - \frac{m2}{z} - \frac{i g2}{z} \right)^2, \frac{1}{c} - \frac{m2}{z} \right]}; \\
\beta_k[1,0][m2_,g2_,z_,c_] &:= \frac{1}{2 z} + \frac{i \left(\frac{1}{c} - \frac{m2}{z} + \frac{i g2}{z} \right)}{(8 z) \operatorname{sqrt} \left[\frac{1}{c z} - \frac{1}{4} \left(\frac{1}{c} - \frac{m2}{z} + \frac{i g2}{z} \right)^2, - \left(\frac{1}{c} - \frac{m2}{z} \right) \right]} \\
&\quad - \frac{i \left(\frac{1}{c} - \frac{m2}{z} - \frac{i g2}{z} \right)}{(8 z) \operatorname{sqrt} \left[\frac{1}{c z} - \frac{1}{4} \left(\frac{1}{c} - \frac{m2}{z} - \frac{i g2}{z} \right)^2, \frac{1}{c} - \frac{m2}{z} \right]}; \\
\beta_k[2,0][m2_,g2_,z_,c_] &:= \frac{1}{2 z} - \frac{i \left(\frac{1}{c} - \frac{m2}{z} + \frac{i g2}{z} \right)}{(8 z) \operatorname{sqrt} \left[\frac{1}{c z} - \frac{1}{4} \left(\frac{1}{c} - \frac{m2}{z} + \frac{i g2}{z} \right)^2, - \left(\frac{1}{c} - \frac{m2}{z} \right) \right]} \\
&\quad + \frac{i \left(\frac{1}{c} - \frac{m2}{z} - \frac{i g2}{z} \right)}{(8 z) \operatorname{sqrt} \left[\frac{1}{c z} - \frac{1}{4} \left(\frac{1}{c} - \frac{m2}{z} - \frac{i g2}{z} \right)^2, \frac{1}{c} - \frac{m2}{z} \right]};
\end{aligned}$$

B.2. Threshold Functions

The $T = 0$ -part of the threshold functions I_j in $d + 1 = 4$ spacetime dimensions can be defined as

$$\begin{aligned}
\ln[5] := \operatorname{tfI}[0][m2_,g2_,z_,0,c_,4] &= \frac{m2^2 - g2^2}{16\pi^2 z^2} + (4 \#1 - 2 m2 \partial_{m2} \#1 - 2 g2 \partial_{g2} \#1 \&)[\operatorname{ker}[4]]; \\
\operatorname{tfI}[1][m2_,g2_,z_,0,c_,4] &= -\frac{m2}{8\pi^2 z^2} - (2 \partial_{m2} \#1 - 2 m2 \partial_{\{m2,2\}} \#1 - 2 g2 \partial_{m2,g2} \#1 \&)[\operatorname{ker}[4]]; \\
\operatorname{tfI}[2][m2_,g2_,z_,0,c_,4] &= \frac{1}{8\pi^2 z^2} - (2 m2 \partial_{\{m2,3\}} \#1 + 2 g2 \partial_{\{m2,2\},g2} \#1 \&)[\operatorname{ker}[4]]; \\
\operatorname{tfI}[3][m2_,g2_,z_,0,c_,4] &= (2 \partial_{\{m2,3\}} \#1 + 2 m2 \partial_{\{m2,4\}} \#1 + 2 g2 \partial_{\{m2,3\},g2} \#1 \&)[\operatorname{ker}[4]]; \\
\operatorname{tfI}[4][m2_,g2_,z_,0,c_,4] &= -(4 \partial_{\{m2,4\}} \#1 + 2 m2 \partial_{\{m2,5\}} \#1 + 2 g2 \partial_{\{m2,4\},g2} \#1 \&)[\operatorname{ker}[4]];
\end{aligned}$$

where the derivatives act on the kernel

$$\ln[6]:= \text{ker}[4]=\frac{1}{64\pi^2}\sum_{i,j}^2\alpha_k[i,j][m_2,g_2,z,c]^2\text{Log}[\alpha_k[i,j][m_2,g_2,z,c]];$$

The temperature-independent part of $\partial_{q^2}J$ in $d+1=4$ we implemented as

$$\begin{aligned} \ln[7]:= & \text{dqTfJ}[q_0,m_1,m_2,g_1,g_2,z_1,z_2,0,c,4]=\frac{1}{2(2\pi^2)}\text{Re}[(-2\#1-q_0\partial_{q_0}\#1-2m_1 \\ & \partial_{m_1}\#1-2m_2\partial_{m_2}\#1-2g_1\partial_{g_1}\#1-2g_2\partial_{g_2}\#1\&)[\text{Module}[\{a_1,a_2,b_1,b_2\},\frac{1}{4}\sum_{i,j}^2\sum_{\text{sig1}}^2\sum_{\text{sig2}}^2(a_1=\alpha_k[i, \\ & \text{sig1}][m_1,g_1,z_1,c];a_2=\alpha_k[j,\text{sig2}][m_2,g_2,z_2,c];b_1=\beta_k[i,\text{sig1}][m_1,g_1,z_1,c];b_2=\beta_k[\\ & j,\text{sig2}][m_2,g_2,z_2,c];b_1b_2(\text{Piecewise}[\{\frac{(a_1-a_2)^2-(a_1+a_2)q_0^2}{4q_0^4\sqrt{-(a_1-a_2)^2+2(a_1+a_2)q_0^2-q_0^4}}(\text{ArcTan}[\\ & \frac{q_0^2+a_1-a_2}{\sqrt{-q_0^4-(a_1-a_2)^2+2q_0^2(a_1+a_2)}}] \\ & +\text{ArcTan}[\frac{q_0^2-a_1+a_2}{\sqrt{-q_0^4-(a_1-a_2)^2+2q_0^2(a_1+a_2)}}])+\frac{1}{4q_0^2}-\frac{(a_1-a_2)(\text{Log}[a_1]-\text{Log}[a_2])}{8q_0^4}, \\ & a_1-a_2\neq 0\},\{\frac{1}{4q_0^2}-\frac{a_1\text{ArcTan}[\frac{q_0^2}{\sqrt{4a_1q_0^2-q_0^4}}]}{q_0^2\sqrt{4a_1q_0^2-q_0^4}},a_1-a_2=0\})]]]; \end{aligned}$$

and for $q_0=0$ as appropriate for Goldstone bosons and the flow equation of Z_k as

$$\begin{aligned} \ln[8]:= & \text{dqTfJ}[0,m_1,m_2,g_1,g_2,z_1,z_2,0,c,4]=\frac{1}{2(2\pi^2)}\text{Re}[(-2\#1-2m_1\partial_{m_1}\#1-2m_2 \\ & \partial_{m_2}\#1-2g_1\partial_{g_1}\#1-2g_2\partial_{g_2}\#1\&)[\text{Module}[\{a_1,a_2,b_1,b_2\},\frac{1}{4}\sum_{i,j}^2\sum_{\text{sig1}}^2\sum_{\text{sig2}}^2(a_1=\alpha_k[i,\text{sig1}][m_1, \\ & g_1,z_1,c];a_2=\alpha_k[j,\text{sig2}][m_2,g_2,z_2,c];b_1=\beta_k[i,\text{sig1}][m_1,g_1,z_1,c];b_2=\beta_k[j,\text{sig2}][\\ & m_2,g_2,z_2,c];b_1b_2\text{Piecewise}[\{\frac{-a_1^2+a_2^2+2a_1a_2(\text{Log}[a_1]-\text{Log}[a_2])}{8(a_1-a_2)^3},a_1-a_2\neq 0\},\{- \\ & \frac{1}{24a_1},a_1-a_2=0\})]]]; \end{aligned}$$

The discontinuous part $\text{disc}_{q_0}J$ is given by

$$\begin{aligned} \ln[9]:= & \text{discTfJ}[q_0,m_1,m_2,g_1,g_2,z_1,z_2,0,c,4]=(q_0\partial_{q_0}\#1+2m_1\partial_{m_1}\#1+2m_2\partial_{m_2}\#1 \\ & +2g_1\partial_{g_1}\#1+2g_2\partial_{g_2}\#1\&)[\text{Module}[\{a_1,a_2,b_1,b_2\},\sum_{i,j}^2(a_1=\alpha_k[i,0][m_1,g_1,z_1,c];a_2=\alpha_k[\\ & j,0][m_2,g_2,z_2,c];b_1=\beta_k[i,0][m_1,g_1,z_1,c];b_2=\beta_k[j,0][m_2,g_2,z_2,c];\frac{1}{16\pi q_0}(b_1b_2) \\ & \sqrt{(q_0^4-2q_0^2(a_1+a_2)+(a_1-a_2)^2)/q_0^2}\text{UnitStep}[\text{Re}[q_0]-\text{Re}[\sqrt{a_1}+\sqrt{a_2}]])]]; \end{aligned}$$

B.3. Flow equations

With the above definitions, the flow equations for ρ_0 , λ , Z_k , γ_1^2 and Z_1 read

$$\begin{aligned} \ln[10]:= & \rho_0\text{Flow}[\rho_0,\lambda_k,\eta_k,g_2,Z_1,c,d,N]:=-(2+\eta_k)\rho_0 \\ & +(\frac{3}{2}\text{tfI}[1][2\rho_0\lambda_k,g_2,Z_1,0,c,d]+\frac{1}{2}(N-1)\text{tfI}[1][0,0,1,0,c,d]) \\ & \lambda_k\text{Flow}[\rho_0,\lambda_k,\eta_k,g_2,Z_1,c,d,N]:=2\eta_k\lambda_k \\ & +\lambda_k^2(\frac{9}{2}\text{tfI}[2][2\rho_0\lambda_k,g_2,Z_1,0,c,d]+\frac{1}{2}(N-1)\text{tfI}[2][0,0,1,0,c,d]) \\ & g_2\text{Flow}[q_0,\rho_0,\lambda_k,\eta_k,g_2,Z_1,c,d,N]:=(\eta_k-2)g_2 \\ & -2\rho_0\lambda_k^2(9\text{discTfJ}[q_0,2\rho_0\lambda_k,2\rho_0\lambda_k,g_2,Z_1,Z_1,0,c,d]) \end{aligned}$$

```

+(N-1)discTfJ[q0,0,0,0,0,1,1,0,c,d])
Z1Flow[q0_,rho_,lambda_,eta_,g2_,Z1_,c_,d_,N_]:=eta Z1
-2rho lambda^2(9dqTfJ[q0,2rho lambda,g2,g2,Z1,Z1,0,c,d]
-(N-1)dqTfJ[q0,0,0,0,0,1,1,0,c,d])
ZkFlow[Zk_,rho_,lambda_,g2_,Z1_,c_,d_]:=2Zk rho lambda^2 dqTfJ[0,2rho lambda,0,g2,0,Z1
,1,0,c,d]

```

and can be solved with

```

In[11]:= AbsoluteTiming@Module[{runner=0,counter=0,domain={t,-10,0},sol=run[5]},
With[{eta=-Zk'[t]/Zk[t],c=1,d=4,N=2},
run[5]=NDSolve[{rho'[t]==rhoFlow[rho[t],lambda[t],eta,g2[t],Z1[t],c,d,N],
lambda'[t]==lambdaFlow[rho[t],lambda[t],eta,g2[t],Z1[t],c,d,N],
Zk'[t]==ZkFlow[Zk[t],rho[t],lambda[t],g2[t],Z1[t],c,d],
g2'[t]==g2Flow[Sqrt[2 rho[t] lambda[t]/Z1[t],rho[t],lambda[t],eta,g2[t],Z1[t],c,d,N],
Z1'[t]==Z1Flow[Sqrt[2 rho[t] lambda[t]/Z1[t],rho[t],lambda[t],eta,g2[t],Z1[t],c,d,N],
WhenEvent[-Z1[t]+lambda[t] rho[t]>0,"CrossDiscontinuity"],
rho[0]==0.02',lambda[0]==0.5',Zk[0]==1,g2[0]==0,Z1[0]==1},{rho,lambda,Zk,g2,Z1},
domain,
StepMonitor:→counter++ If[Abs[t]>runner,Print[Chop[{counter,Round[t,1],-
Z1[t]+lambda[t] rho[t],e^t rho[t],lambda[t],Zk[t],e^t g2[t],Z1[t]}]];runner++]];
Plot[e^t rho[t]/.sol,domain,PlotRange→{0,All},AxesLabel→{"t",rho(t)/Lambda^2}]
Plot[lambda[t]/.sol,domain,AxesLabel→{"t",lambda(t)}]
Plot[-Zk'[t]/Zk[t]/.sol,domain,AxesLabel→{"t",eta_k(t)}]
Plot[e^t g2[t]/.sol,domain,AxesLabel→{"t",gamma_1^2(t)/Lambda^2}]
Plot[Z1[t]/.sol,domain,AxesLabel→{"t",Z1(t)}]]]

```

The plot commands contain $e^{2t} \rho[t]$ and $e^{2t} g2[t]$ because we performed the internal calculations using dimensionless variables $\tilde{\rho}_0(k) = \rho_0(k)/k^2 = \rho_0(k)/(\Lambda^2 e^{2t})$, $\tilde{\gamma}_1^2 = \gamma_1^2/k^2 = \gamma_1^2/(\Lambda^2 e^{2t})$. We use the event handler `WhenEvent[Re[Sqrt[-Z1[t]+lambda[t] rho[t]]]==0,"CrossDiscontinuity"]` here to take care of a singularity of `g2Flow` that is due to the term $\sqrt{-Z1[t]+lambda[t] rho[t]}$ in the denominator of `discTfJ[Sqrt[2 rho[t] lambda[t]],0,0,0,0,1,1,0,1,4]` which incorporates fluctuations of the Goldstone bosons. $\sqrt{-Z1[t]+lambda[t] rho[t]}$ vanishes near $t = -3$. The singularity leads to a divergent derivative `g2'[t]` of the discontinuity γ_1^2 of the radial propagator which abruptly becomes zero (cf. fig. 12e) above a certain renormalization scale $k^2 > m_1^2$ because the radial mode can exist as an on-shell stable particle above those energies.

References

- [1] S. Floerchinger. “Analytic continuation of functional renormalization group equations”. *Journal of High Energy Physics* 5, 21 (2012), 21. 1112.4374 (cit. on pp. 1–3, 7, 8, 11, 15–17, 19–23, 25, 27, 32, 45, 48, 50).
- [2] H. A. Lorentz. *The Theory of Electrons and its Applications to the Phenomena of*
- [3] K. G. Wilson. “Renormalization group and critical phenomena. I. Renormalization group and the Kadanoff scaling picture”. *Physical review B* 4.9 (1971), 3174 (cit. on pp. 2, 8).
- [4] C. Wetterich. “The average action for scalar fields near phase transitions”.

- Zeitschrift für Physik C Particles and Fields* 57.3 (1993), 451 (cit. on pp. 2, 15, 16).
- [5] S. Diehl, S. Floerchinger, H. Gies, J. Pawłowski, C. Wetterich. “Functional renormalization group approach to the BCS-BEC crossover”. *Annalen der Physik* 522.9 (2010), 615. [0907.2193](#) (cit. on p. 2).
- [6] S. Floerchinger. *Functional renormalization and ultracold quantum gases*. Springer Science & Business Media, 2010. [0909.0416](#) (cit. on p. 2).
- [7] I. Boettcher, J. M. Pawłowski, S. Diehl. “Ultracold atoms and the functional renormalization group”. *Nuclear Physics B-Proceedings Supplements* 228 (2012), 63. [1204.4394](#) (cit. on p. 2).
- [8] P. Strack, R. Gersch, W. Metzner. “Renormalization group flow for fermionic superfluids at zero temperature”. *Physical Review B* 78.1 (2008), 014522. [0804.3994](#) (cit. on p. 2).
- [9] S. Floerchinger, C. Wetterich. “Superfluid Bose gas in two dimensions”. *Physical Review A* 79.1 (2009), 013601. [0805.2571](#) (cit. on p. 2).
- [10] S. Floerchinger, M. Scherer, C. Wetterich. “Modified Fermi sphere, pairing gap, and critical temperature for the BCS-BEC crossover”. *Physical Review A* 81.6 (2010), 063619. [0912.4050](#) (cit. on p. 2).
- [11] S. Floerchinger, S. Moroz, R. Schmidt. “Efimov physics from the functional renormalization group”. *Few-Body Systems* 51.2-4 (2011), 153. [1102.0896](#) (cit. on p. 2).
- [12] C. Wetterich. “Effective Average Action in Statistical Physics and Quantum Field Theory”. *International Journal of Modern Physics A* 16 (2001), 1951. [hep-ph/0101178](#) (cit. on pp. 2, 4, 6–8, 10–12, 14, 15).
- [13] J. Berges, N. Tetradis, C. Wetterich. “Non-perturbative renormalization flow in quantum field theory and statistical physics”. *Physics Reports* 363.4 (2002), 223. [hep-ph/0005122](#) (cit. on pp. 2, 6–8, 10, 11, 15, 27, 33).
- [14] C. Honerkamp, M. Salmhofer. “Magnetic and superconducting instabilities of the Hubbard model at the van Hove filling”. *Physical Review Letters* 87.18 (2001), 187004. [cond-mat/0109392](#) (cit. on p. 2).
- [15] J. Zinn-Justin. *Quantum field theory and critical phenomena*. Clarendon Press, 1996 (cit. on p. 2).
- [16] D. J. Amit, V. Martin-Mayor. *Field theory, the renormalization group, and critical phenomena: graphs to computers*. World Scientific Publishing Co Inc, 2005 (cit. on p. 2).
- [17] K. G. Wilson. “The renormalization group and critical phenomena”. *Reviews of Modern Physics* 55.3 (1983), 583 (cit. on p. 2).
- [18] A. Pelissetto, E. Vicari. “Critical phenomena and renormalization-group theory” (2000). [cond-mat/0012164](#) (cit. on p. 2).
- [19] M. E. Fisher. “The renormalization group in the theory of critical behavior”. *Reviews of Modern Physics* 46.4 (1974), 597 (cit. on p. 2).
- [20] J. Berges, N. Tetradis, C. Wetterich. “Critical equation of state from the average action”. *Physical review letters* 77.5 (1996), 873. [hep-th/9507159](#) (cit. on p. 2).
- [21] C. Bagnuls, C. Bervillier. “Exact renormalization group equations: an introductory review”. *Physics Reports* 348.1 (2001), 91. [hep-th/0002034](#) (cit. on p. 2).
- [22] G. v. Gersdorff, C. Wetterich. “Nonperturbative renormalization flow and essential scaling for the Kosterlitz-Thouless transition”. *Physical Review B* 64.5 (2001), 054513. [hep-th/0008114](#) (cit. on p. 2).
- [23] B.-J. Schaefer, J. Wambach. “Renormalization group approach towards the QCD phase diagram”. *Physics of Particles and Nuclei* 39.7 (2008), 1025. [hep-ph/0611191](#) (cit. on p. 2).
- [24] J. M. Pawłowski. “Functional RG methods in QCD” (2006) (cit. on p. 2).
- [25] D. J. Gross, R. D. Pisarski, L. G. Yaffe. “QCD and instantons at finite temperature”. *Reviews of Modern Physics* 53.1 (1981), 43 (cit. on pp. 2, 18).

- [26] J. Braun, H. Gies. “Chiral phase boundary of QCD at finite temperature”. *Journal of High Energy Physics* 2006.06 (2006), 024. [hep-ph/0602226](#) (cit. on p. 2).
- [27] J. Braun, L. M. Haas, F. Marhauser, J. M. Pawłowski. “Phase structure of two-flavor QCD at finite chemical potential”. *Physical review letters* 106.2 (2011), 022002 (cit. on p. 2).
- [28] M. Reuter. “Nonperturbative evolution equation for quantum gravity”. *Physical Review D* 57.2 (1998), 971. [hep-th/9605030](#) (cit. on p. 2).
- [29] M. Reuter, F. Saueressig. “Functional renormalization group equations, asymptotic safety, and quantum Einstein gravity” (2007). [0708.1317](#) (cit. on p. 2).
- [30] D. F. Litim, J. M. Pawłowski. “On gauge invariant Wilsonian flows” (1999). [hep-th/9901063](#) (cit. on p. 2).
- [31] H. Gies. “Introduction to the functional RG and applications to gauge theories”. *Renormalization Group and Effective Field Theory Approaches to Many-Body Systems*. Springer, 2012, 287. [hep-ph/0611146](#) (cit. on p. 2).
- [32] S. Weinberg, S. Hawking, W. Israel. “General Relativity: An Einstein Centenary Survey”. *Cambridge University Press, Cambridge* (1979) (cit. on p. 2).
- [33] M. Niedermaier. “The asymptotic safety scenario in quantum gravity: an introduction”. *Classical and Quantum Gravity* 24.18 (2007), R171. [gr-qc/0610018](#) (cit. on p. 2).
- [34] D. Oriti. *Approaches to quantum gravity: Toward a new understanding of space, time and matter*. Cambridge University Press, 2009 (cit. on p. 2).
- [35] D. F. Litim. “Fixed points of quantum gravity and the renormalisation group” (2008). [0810.3675](#) (cit. on p. 2).
- [36] N. Christiansen, D. F. Litim, J. M. Pawłowski, A. Rodigast. “Fixed points and infrared completion of quantum gravity”. *Physics Letters B* 728 (2014), 114. [1102.4624](#) (cit. on p. 2).
- [37] R. Percacci. “A short introduction to asymptotic safety” (2011). [1110.6389](#) (cit. on p. 2).
- [38] M. Reuter, F. Saueressig. “Quantum Einstein Gravity”. *New Journal of Physics* 14.5 (2012), 055022. [1202.2274](#) (cit. on p. 2).
- [39] M. Reuter, F. Saueressig. “Asymptotic safety, fractals, and cosmology”. *Quantum Gravity and Quantum Cosmology*. Springer, 2013, 185. [1205.5431](#) (cit. on p. 2).
- [40] S. Nagy. “Lectures on renormalization and asymptotic safety”. *Annals of Physics* 350 (2014), 310. [1211.4151](#) (cit. on p. 2).
- [41] R. Percacci. “Asymptotic safety”. *Approaches to quantum gravity: towards a new understanding of space, time and matter* (2009), 111. [0709.3851](#) (cit. on p. 2).
- [42] J. M. Pawłowski, N. Strodthoff. “Real time correlation functions and the functional renormalization group”. *Physical Review D* 92.9 (2015), 094009. [1508.01160](#) (cit. on pp. 2, 17).
- [43] F. J. Wegner, A. Houghton. “Renormalization group equation for critical phenomena”. *Physical Review A* 8.1 (1973), 401 (cit. on p. 3).
- [44] J. Polchinski. “Renormalization and effective Lagrangians”. *Nuclear Physics B* 231.2 (1984), 269 (cit. on pp. 3, 5).
- [45] C. Wetterich. “Exact evolution equation for the effective potential”. *Physics Letters B* 301.1 (1993), 90 (cit. on pp. 3, 4, 14).
- [46] N. Tetradis, C. Wetterich. “Critical exponents from the effective average action”. *Nuclear Physics B* 422.3 (1994), 541 (cit. on pp. 4, 5, 7, 8, 10, 14).
- [47] B. Delamotte. “An introduction to the non-perturbative renormalization group”. Springer, 2012, 49. [cond-mat/0702365](#) (cit. on pp. 6, 12).
- [48] J. Adams et al. “Solving non-perturbative flow equations”. *Modern Physics Letters A* 10.31 (1995), 2367. [hep-th/9507093](#) (cit. on p. 7).

- [49] J. M. Pawłowski, N. Strodthoff, N. Wink. “Finite temperature spectral functions in the $O(N)$ model” (2017). [1711.07444](#) (cit. on p. 17).
- [50] K. Kamikado, N. Strodthoff, L. von Smekal, J. Wambach. “Real-time correlation functions in the $O(N)$ model from the functional renormalization group”. *The European Physical Journal C* 74.3 (2014), 2806. [1302.6199](#) (cit. on p. 17).
- [51] T. Gasenzer, S. Keßler, J. M. Pawłowski. “Far-from-equilibrium quantum many-body dynamics”. *The European Physical Journal C-Particles and Fields* 70.1 (2010), 423. [1003.4163](#) (cit. on p. 17).
- [52] H. Schoeller. “A perturbative nonequilibrium renormalization group method for dissipative quantum mechanics”. *The European Physical Journal-Special Topics* 168.1 (2009), 179. [0902.1449](#) (cit. on p. 17).
- [53] M. Keil, H. Schoeller. “Real-time renormalization-group analysis of the dynamics of the spin-boson model”. *Physical Review B* 63.18 (2001), 180302. [cond-mat/0011051](#) (cit. on p. 17).
- [54] T. Korb, F. Reininghaus, H. Schoeller, J. König. “Real-time renormalization group and cutoff scales in nonequilibrium applied to an arbitrary quantum dot in the Coulomb blockade regime”. *Physical Review B* 76.16 (2007), 165316. [0705.3200](#) (cit. on p. 17).
- [55] R.-A. Tripolt, N. Strodthoff, L. von Smekal, J. Wambach. “Spectral functions for the quark-meson model phase diagram from the functional renormalization group”. *Physical Review D* 89.3 (2014), 034010. [1311.0630](#) (cit. on p. 17).
- [56] R.-A. Tripolt, N. Strodthoff, L. von Smekal, J. Wambach. “Spectral functions from the functional renormalization group”. *Nuclear Physics A* 931 (2014), 790. [1407.8387](#) (cit. on p. 17).
- [57] R.-A. Tripolt, N. Strodthoff, L. von Smekal, J. Wambach. “Finite-Temperature Spectral Functions from the Functional Renormalization Group” (2013). [1311.4304](#) (cit. on p. 17).
- [58] N. Strodthoff. “Self-consistent spectral functions in the $O(N)$ model from the functional renormalization group”. *Physical Review D* 95.7 (2017), 076002. [1611.05036](#) (cit. on p. 17).
- [59] N. Dupuis. “Infrared behavior and spectral function of a Bose superfluid at zero temperature”. *Physical Review A* 80.4 (2009), 043627. [0907.2779](#) (cit. on p. 17).
- [60] A. Sinner, N. Hasselmann, P. Kopietz. “Spectral function and quasiparticle damping of interacting bosons in two dimensions”. *Physical review letters* 102.12 (2009), 120601. [0811.0624](#) (cit. on p. 17).
- [61] M. Haas, L. Fister, J. M. Pawłowski. “Gluon spectral functions and transport coefficients in Yang-Mills theory”. *Physical Review D* 90.9 (2014), 091501. [1308.4960](#) (cit. on p. 17).
- [62] S. Floerchinger. “Variational principle for theories with dissipation from analytic continuation”. *Journal of High Energy Physics* 2016.9 (2016), 99. [1603.07148](#) (cit. on p. 18).
- [63] A. Das. “Topics in finite temperature field theory” (2000). [hep-ph/0004125](#) (cit. on p. 18).
- [64] F. Bloch, F. Bloch. *Zur Theorie des Austauschproblems und der Remanenzerscheinung der Ferromagnetika*. Springer, 1932 (cit. on p. 18).
- [65] T. Matsubara. “A new approach to quantum-statistical mechanics”. *Progress of theoretical physics* 14.4 (1955), 351 (cit. on p. 18).
- [66] S. Weinberg. “Gauge and global symmetries at high temperature”. *Physical Review D* 9.12 (1974), 3357 (cit. on p. 18).
- [67] S. Weinberg. *The quantum theory of fields*. Vol. 2. Cambridge university press, 1995, 457 (cit. on p. 19).
- [68] S. Floerchinger. Unpublished notes. 2017 (cit. on pp. 25, 33, 38, 42, 44, 45, 50).
- [69] M. Q. Huber, J. Braun. “Algorithmic derivation of functional renormalization group equations and Dyson–Schwinger equations”. *Computer Physics Communications* 183.6 (2012), 1290. [1102.5307](#) (cit. on p. 28).

Acknowledgments

I would like to thank Stefan Flörchinger for providing me with this exciting research topic and for continued guidance during the preparation of this thesis. I also extend my gratitude to my other advisors Christof Wetterich and Michael Scherer for helpful feedback and thoughtful counsel. I thank Fabian Rennecke, Nicolas Wink, Manuel Scherzer, Sebastian Wetzel and Daniel Rosenblüh for many interesting discussions, patient explanations and enjoyable company. My sincerest appreciation goes to Thomas Mikhail and Lukas Barth for proofreading this thesis and providing me with valuable feedback, coming up with many critical questions and following through with enlightening discussions! For wonderful memories and many special moments during my studies in Heidelberg I thank my friends Friederike Erbe, Florian Kleinicke, Lars Hansen, Daniel Rosenblüh, Lukas Barth, Thomas Mikhail, Benjamin Freist, Adrian van Kan, Clara Miralles Vila, Clara Murgui Galvez and my sister Kaja Riebesell. Lastly, the biggest thank-you goes out to my parents Mona Botros and Ulf Riebesell, who supported me in every way possible and without whom I would not be who and where I am today!

Declaration of Authorship

I hereby certify that this thesis has been composed by me and is based on my own work, except where stated otherwise.

Heidelberg, _____